

MIT Joint Program on the Science and Policy of Global Change



Characterization of Wind Power Resource in the United States and its Intermittency

Udaya Bhaskar Gunturu and C. Adam Schlosser

**Report No. 209
December 2011**

The MIT Joint Program on the Science and Policy of Global Change is an organization for research, independent policy analysis, and public education in global environmental change. It seeks to provide leadership in understanding scientific, economic, and ecological aspects of this difficult issue, and combining them into policy assessments that serve the needs of ongoing national and international discussions. To this end, the Program brings together an interdisciplinary group from two established research centers at MIT: the Center for Global Change Science (CGCS) and the Center for Energy and Environmental Policy Research (CEEPR). These two centers bridge many key areas of the needed intellectual work, and additional essential areas are covered by other MIT departments, by collaboration with the Ecosystems Center of the Marine Biology Laboratory (MBL) at Woods Hole, and by short- and long-term visitors to the Program. The Program involves sponsorship and active participation by industry, government, and non-profit organizations.

To inform processes of policy development and implementation, climate change research needs to focus on improving the prediction of those variables that are most relevant to economic, social, and environmental effects. In turn, the greenhouse gas and atmospheric aerosol assumptions underlying climate analysis need to be related to the economic, technological, and political forces that drive emissions, and to the results of international agreements and mitigation. Further, assessments of possible societal and ecosystem impacts, and analysis of mitigation strategies, need to be based on realistic evaluation of the uncertainties of climate science.

This report is one of a series intended to communicate research results and improve public understanding of climate issues, thereby contributing to informed debate about the climate issue, the uncertainties, and the economic and social implications of policy alternatives. Titles in the Report Series to date are listed on the inside back cover.


Ronald G. Prinn and John M. Reilly
Program Co-Directors

For more information, please contact the Joint Program Office

Postal Address: Joint Program on the Science and Policy of Global Change
77 Massachusetts Avenue
MIT E19-411
Cambridge MA 02139-4307 (USA)

Location: 400 Main Street, Cambridge
Building E19, Room 411
Massachusetts Institute of Technology

Access: Phone: +1(617) 253-7492
Fax: +1(617) 253-9845
E-mail: globalchange@mit.edu
Web site: <http://globalchange.mit.edu/>

 Printed on recycled paper

Characterization of Wind Power Resource in the United States and its Intermittency

Gunturu Udaya Bhaskar^{*†} and C. Adam Schlosser^{*}

Abstract

Wind resource in the continental and offshore United States has been reconstructed and characterized using metrics that describe, apart from abundance, its availability, persistence and intermittency. The Modern Era Retrospective-Analysis for Research and Applications (MERRA) boundary layer flux data has been used to construct wind profile at 50 m, 80 m, 100 m and 120 m turbine hub heights. The wind power density estimates at 50 m are qualitatively similar to those in the U.S. wind atlas developed by the National Renewable Energy Laboratory (NREL), but quantitatively a class less in some regions, but are within the limits of uncertainty. The wind speeds at 80 m were quantitatively and qualitatively close to the NREL wind map. The possible reasons for overestimation by NREL have been discussed. For long tailed distributions like those of the wind power density, the mean is an overestimation and the median is suggested for summary representation of the wind resource. The impact of raising the wind turbine hub height on metrics of abundance, persistence, variability and intermittency is analyzed. There is a general increase in availability and abundance of wind resource but there is an increase in intermittency in terms of level crossing rate in low resource regions. The key aspect of geographical diversification of wind farms to mitigate intermittency - that the wind power generators are statistically independent - is also tested. This condition is found in low resource regions like the east and west coasts. However, in the central U.S. region which has rich resource the condition fails as widespread coherent intermittence in wind power density is found. Thus, large regions are synchronized in having wind power or lack thereof. Thus, geographical diversification in this region needs to be planned strategically. The annual distribution of hourly wind power density shows considerable variability and suggests wind floods and droughts that roughly correspond with La-Nina and El-Nino years, respectively. The collective behavior of wind farms in seven Independent System Operator (ISO) areas has also been studied. The generation duration curves for each ISO show that there is no aggregated power for some fraction of the time. Aggregation of wind turbines mitigates intermittency to some extent, but each ISO has considerable fraction of time with less than 5% capacity. The hourly wind power time series show benefit of aggregation but the high and low wind events are lumped in time, thus corroborating the result that the intermittency is synchronized. The time series show that there are instances when there is no wind power in most ISOs because of large-scale high pressure systems. An analytical consideration of the collective behavior of aggregated wind turbines shows that the benefit of aggregation saturates beyond ten units. Also, the benefit of aggregation falls rapidly with temporal correlation between the generating units.

^{*} The Joint Program on the Science and Policy of Global Change, Massachusetts Institute of Technology, Cambridge, MA USA.

[†] Corresponding author (Email: bhaskar@mit.edu)

Contents

1. INTRODUCTION	2
1.1 Characterization of Wind Resource	2
1.1.1 Implications of Weibull Distribution	3
1.1.2 Shape Factor	3
1.1.3 Length of the Record	4
1.1.4 Wind Droughts	4
1.1.5 Characterizations or Variables Used to Describe the Wind Resource	4
1.2 Intermittency	5
1.2.1 Mitigating Intermittency	6
2. METHODOLOGY	7
2.1 MERRA Data	7
2.1.1 Wind Resource at Different Heights	8
2.2 Resource Metrics	8
2.2.1 Fluctuations	9
2.3 Intermittency Metrics	9
3. RESULTS & DISCUSSION	11
3.1 Descriptive Statistics of Wind Power from MERRA Wind	11
3.1.1 Mean Wind Power Density	11
3.1.2 Coefficient of Variation (CoV) of Wind Power	12
3.1.3 Inter-Quartile Range	13
3.1.4 Availability of Power	13
3.1.5 Wind Episode Lengths	14
4. WIND POWER DENSITY AT DIFFERENT ALTITUDES	15
4.1 Comparison with NREL Map at 50 m	15
4.2 Comparison of Wind Speed at 80 m with the NREL Map	16
4.3 Wind Power Density at Different Hub Heights	19
5. INTERMITTENCY	28
5.1 Experiments	29
5.1.1 Null Anti-Coincidence	32
5.2 Interannual Variability of Wind Resource	36
5.3 Analysis Without Cut-in WPD	37
5.3.1 Turbine Size and Power Curve	39
5.3.2 Number of Turbines	39
5.4 Generation Duration Curves	40
5.5 Power Time Series	44
6. CONCLUSIONS	50
6.1 Limitations and Key Assumptions	50
6.2 Wind Power Density at the surface	53
6.3 Altitude Dependence of Wind Power Density	54
6.4 Intermittency	55
6.5 Future Research	57
7. REFERENCES	58
APPENDIX A: Statistics of Intermittency	62
APPENDIX B: WPD Distribution	63
APPENDIX C: Wind Power Classes	64
Abbreviations	64

1. INTRODUCTION

1.1 Characterization of Wind Resource

The U.S. national wind energy resource estimates were developed by the National Renewable Energy Laboratory (NREL) (Elliott *et al.*, 1987, 1991) and the wind resource was remapped at a

higher resolution for the midwestern U.S. (Schwartz and Elliot, 2001). Several data sources were used to collect the wind data. Most importantly, National Climate Data Center (NCDC) archives constituted the major proportion of the data. The atlas preferred to use wind power density and not wind speed as a measure of the resource because the former combines the effect of changes in air density. The air density was estimated using measured temperature and station pressure and the equation of state. When temperature and pressure were not available, air density at the surface was assumed to be 1.225 kg/m^3 and extrapolated to the height of the wind speed record. The wind speed at the surface or 10 m was adjusted to 50 m using an exponential law with an exponent of $1/7$. Because the seasonal and geographical variation of density is not taken into consideration, the wind resource has been overestimated in the wind atlas. Further, the wind atlas depicts the mean wind power density. Below, we discuss some of the key caveats when using such distributions to estimate wind power resources.

1.1.1 Implications of Weibull Distribution

Several researchers used the two-parameter Weibull distribution to fit wind speed frequency distributions (Elliott *et al.*, 1987; Schwartz and Elliot, 2001; Dorvlo, 2002; Lun and Lam, 2000; Pavia and O'Brien, 1986; Chang *et al.*, 2003; Ucar and Balo, 2009; Pryor and Barthelmie, 2010; Zaharim *et al.*, 2009; Eskin *et al.*, 2008). Some of the merits cited are the flexibility and ease of use as only two parameters need to be determined to fit the distribution. Tuller and Brett (1984) describe the conditions under which wind speeds approximately follow Weibull distribution. He *et al.* (2010) pointed out that buoyancy fluxes force the distribution away from Weibull behavior. They reported that the daytime winds are near-Weibull but the nighttime winds showed greater positive skewness than the Weibull distribution. Thus the use of Weibull distribution overestimates the frequencies of the higher wind speeds. As argued by Morrissey *et al.* (2010), the first step in computing a WPD distribution is to study the WPD distribution rather than the wind speed distribution. Jaramillo and Borja (2004) found that the two-parameter Weibull distribution can not be generalized since it is not accurate in the case of some wind regimes. Morrissey *et al.* (2010) give an example of wind speed distribution for Boise city, Oklahoma and point out that the two-parameter Weibull distribution does not fit the wind speed distribution well. When the Weibull distribution is used for that wind speed data, the frequencies of lower speeds are underestimated and those of the higher speeds are overestimated which results in an overestimation of the resource.

1.1.2 Shape Factor

The shape factor of the Weibull distribution has a great impact on the fit of wind speeds because as shape factor increases, the tail of the Weibull distribution decreases. Thus, the extreme wind speeds decrease and the distribution transforms towards a normal one. Usually, the measured wind speeds are fit to the Weibull distribution and the mean wind power density is computed using the Weibull distribution. This is done because the wind speed record is usually small. In doing so, the wind power density is not estimated accurately because the Weibull is only an approximate fit for the wind speeds and also because the wind power density involves cube of the wind speed, any error in wind speed gets amplified in wind power density. Also, sometimes, as in the U.S. wind

energy atlas (Elliott *et al.*, 1987), a constant shape factor of 2 is assumed for using the Weibull distribution. The implication is that if the actual shape factor is less than 2, the frequencies of very high wind speeds are lowered and the mean wind power density is underestimated. Similarly, if the actual shape factor is greater than 2, the frequencies of very high wind speeds are increased and the mean wind power density is overestimated.

The skewness of a Weibull distribution is only a function of its shape parameter c . Hennessey (1977) studied the statistical behavior of wind speeds and wind power density and inferred that the locations that have the highest mean wind speeds have the lowest shape parameters for the wind distributions and hence greatest skewness. Thus, using a constant shape parameter of $c = 2$ increases the wind power density in the distribution. Because of the cubic relationship between the wind power density and the wind speed, small changes in wind speed can mean large increases in the wind power density.

1.1.3 Length of the Record

To compute the wind resource in a geographical region, most researchers used measurements using dedicated meteorological towers, airport measurements or the observational data from the NCDC (Elliott *et al.*, 1987; Archer and Jacobson, 2003, 2007; Brower, 2008). Since the data size in most of these records is small, the data is fit to the Weibull distribution. Also, such small records fail to capture the longer term variations in wind speeds. For example, Atkinson *et al.* (2006) has studied the correlation between the North Atlantic Oscillation (NAO) and wind speeds in Europe and found that there is a wind flood during the early 1990s followed by a return to the long term average after 1995. Thus, if the measurements taken during this high wind period are used to construct the wind resource maps, the wind resource is overestimated.

1.1.4 Wind Droughts

Boccard (2009) pointed out that the average wind capacity factors in several countries in Europe have been estimated to be in the range 30-35% while the realized values are very low, averaging at 21%. For the U.S., they report 25.7% for the whole U.S. and 22.45% for California while that claimed by AWEA (2005) is 35%. He argues that one of the reason for the overestimation of wind energy potential is the short record of observations used to estimate. He reasons that atmospheric oscillations like NAO need to be taken into account (Atkinson *et al.*, 2006).

1.1.5 Characterizations or Variables Used to Describe the Wind Resource

In many of the studies preceding this, a mean value was used as a measure of the central tendency of the WPD. A cursory plot of the histogram of WPD at a site or for a region shows that it is a highly skewed and long-tailed distribution. Thus, the mean may not faithfully represent the distribution's central tendency of the WPD accurately. Thus, estimates of backup or power produced tend not to be estimated accurately. Further, Hennessey (1977) showed that wind power studies based only on the total mean wind power density do not give an accurate picture of the wind power potential of a site and omit valuable information in terms of intermittency and variability.

Many researchers used data from meteorological towers or observations from airports. Most of

these observations that are at different heights and different schemes have been used to extrapolate the wind speeds to the wind turbine hub heights. Kiss and Jánosi (2008) used the ECMWF's ERA-40 reanalysis eastward and northward winds at 10 m to study wind field statistics over Europe. Larsen and Mann (2009) also used reanalysis data from NCEP/NCAR to estimate the geostrophic wind and extrapolated the geostrophic wind to 10 m height. Elliott *et al.* (1987) used a power law with the exponent $1/7$ as mentioned above. Archer and Jacobson (2007) used the upper air measurements from balloons and rawinsondes at the nearest meteorological stations to extrapolate the wind speeds at 10 m to the hub height at 50 m or 80 m. Similarly, many researchers used a power or logarithmic law assuming roughness length and friction velocity in the boundary layer that did not vary with seasons, terrain and stability of the atmosphere.

To overcome these shortcomings, we chose to use the Modern Era Retrospective-Analysis for Research and Applications (MERRA) reanalysis data (Rienecker *et al.*, 2011) that has a resolution of $1/2^\circ \times 2/3^\circ$ and a long record of hourly data for 31 years to reconstruct the wind field at 50 m, 80 m, 100 m and 120 m. The details of the methodology adapted for this reconstruction of the wind power density field across the U.S. are described in the section Methodology on page 7. Instead of using the wind speeds, we computed the wind speed at different heights using boundary layer flux data and boundary layer similarity theory.

While trying to look at the wind resource as a system, we tried to characterize the reliability using some metrics from reliability theory. Most of the wind atlases of many countries describe the wind resource in terms of only the mean wind power density and only some atlases show maps of the variability in terms of the standard deviation. In this attempt, we studied the statistics of the episode lengths of the wind power density runs using a reasonable threshold of 200 W/m^2 (Gustavson, 1979). Although these statistics have not been looked at earlier, these metrics that describe the persistence of wind power density are important considerations considering the enormous impact variability of wind power has on the power grid, electricity prices and the resource itself. Further, the level crossing statistics of the wind power density are presented, as these raise important considerations in the maintenance of backup for the times of lulls.

1.2 Intermittency

One of the most important discussions in renewable energy studies - mostly wind and solar energies - is the variation of the energy resource in time and space and the consequent effects on energy economics, technical feasibility and reliability. Most of the studies used standard deviation to measure the variation (Holttinen, 2005a,b; Holttinen *et al.*, 2008; Estanqueiro, 2008). Holttinen *et al.* (2008) studied the use of standard deviation as a measure of variability of wind power output. Largely, the standard deviation of wind resource has been used to estimate the required reserves of the power system. Thus, $\pm 4\sigma$ as the range of variability covers most of the variation, where σ is the standard deviation. Thus, 6σ has been used to estimate the regulation reserves and $2 - 3\sigma$ for load following reserves (Holttinen *et al.*, 2008). Estanqueiro (2008) used standard deviation to study the reduction of variability of wind power when several wind farms are aggregated.

Cox (2009) found that the wind power between 2000-2007 in the United Kingdom was below 5% of its maximum capacity for 209 single hours and one long period of almost three days. And for the Irish market, the wind generation was that low for 542 single hours. The British and Irish markets had frequency distributions of low wind distributions up to several hours. He found that the intermittent nature of wind power makes the power prices very volatile. When the wind generation is high, the market prices are slightly depressed, but there are sharp jumps when the high or low wind persists. In some cases, when the wind is very high, the prices are negative too. This was recently the case in the U.S. where the Bonneville Power Authority (BPA) gave hydro-power free to wind farms to sell in the market when wind power was curtailed. Intermittent and variable nature of wind power connected to a grid affects the power quality. Power quality is usually expressed in terms of the physical characteristics and electrical properties. The usual characteristics used to describe power quality are: voltage, frequency and interruptions (Ackermann, 2005). Lund (2005) reiterates the fact that wind intermittency limits its applicability as a power source and affects the temporal stability of the frequency and voltage of power generation, thus altering the quality of power. Integration of large amounts of intermittent wind power results in reduced conventional generation like thermal and hydro-power plants as their efficiency decreases when operated below their optimum. On a longer time scale, the variability of wind power affects the adequacy of power capacity. Ackermann (2005) infers that the essential reliability of the system is usually 'in the order of a larger blackout in 10-15 years'. On the other hand, the time scale of intermittency of wind power can range from micro and millisecond to minutes and also to hours, days and longer durations. The consequences of the intermittency depend on the duration. At smaller scales, the intermittency appears as a spike and impacts the voltage and frequency stability of the grid. At longer scales, the capacity adequacy, resource stability and the price of the power are affected.

1.2.1 Mitigating Intermittency

While intermittency is one of the key limitations to large-scale installation of wind power, several solutions have been suggested to overcome this impediment and achieve a larger penetration of wind power. Archer and Jacobson (2007) report that interconnecting the wind turbines reduces the intermittency such that wind can provide base-load supply of electric power. Some other solutions suggested are: using complimentary non-variable energy sources like hydro-power, using smart demand-response management, storage mechanisms, installation of excess wind farms to minimize non-availability of wind power and forecasting the weather better for better planning for power traffic. Of these, aggregation of wind turbines located in geographically diverse locations has been studied extensively and is being looked upon as the most suitable solution to mitigate intermittency and variability in wind power output. Several studies have studied the viability of this option (Sinden, 2007; Archer and Jacobson, 2007; Degeilh and Singh, 2011; Katzenstein *et al.*, 2010; Kempton *et al.*, 2010). A recent study by Katzenstein *et al.* (2010) showed that a substantial reduction in the small scale variability of wind power can be achieved by interconnecting wind plants. The most important assumption in choosing this mitigation option is that the wind power from the different aggregated farms is anti-correlated. Many researchers studied the presence of such anti-correlation (Apt, 2007; Archer and Jacobson, 2007; Kempton *et al.*, 2010; Katzenstein

et al., 2010; Degeilh and Singh, 2011). Another important inherent assumption in integrating wind farms is that of availability of wind power.

In light of this, the present study looks at the character of intermittency in wind resource and the implications thereof. Most importantly, the presence of anti-correlation in the wind resource among different regions of the U.S. will be considered. Given all these considerations, we assess wind power density over the contiguous U.S. using the multi-decade MERRA data set. Our analysis will first consider how to faithfully characterize the central tendency of wind power density, and how our quantifications compare with previous estimates. Further, we define metrics to evaluate intermittency and variability of wind power density. The data processing and metrics are considered in the next section.

2. METHODOLOGY

The domain considered for the study spans the contiguous states of the U.S. bound between 20°N and 50°N latitudes and 130°W and 60°W longitudes. This domain also takes into account the offshore regions on the east and west side of the U.S..

2.1 MERRA Data

The data needed for this study has been taken from the MERRA, which is a reconstruction of the atmospheric state by assimilating observational data from different platforms into a global model (Rienecker *et al.*, 2011). The data assimilation included conventional data from many sources and also data from several trains of satellites. MERRA was conducted at the NASA Center for Climate Simulation as three separate analysis streams. The initial key goal of MERRA was to improve upon the water cycle analysis in previous generation reanalyses like NCEP Reanalysis 1 and 2 and, ERA-40. Overall, MERRA aims to provide a more accurate dataset using the comprehensive suite of satellite based information for climate and atmospheric research. The present data set has been constructed with GEOS-5 Atmospheric Data Assimilation System (version 5.2.0) (ADAS). The system consists of the GEOS-5 model and the Grid-point Statistical Interpolation (GSI) analysis. GSI is a system developed by GMAO and NOAA's National Centers for Environmental Prediction jointly. The data set has a spatial resolution of $1/2^\circ \times 2/3^\circ$ and a time resolution of an hour. The data spans the time from 0030 Hrs on 1st January, 1979 to 2330 Hrs on 31st December, 2009. Thus, the dataset provides an opportunity to look at the variation of the winds over several scales up to the decadal scale. The dataset is averaged in time. So, if there are any jumps in any of the quantities at scales lower than 1 hour, they will be represented in the average.

Wind power density is used to describe wind resource as it is independent of the wind turbine characteristics and also because it will ease comparison with other estimates like that by NREL. It indicates how much wind energy can be harvested at a location by a wind turbine and has the units W/m². The wind power density at each time step is calculated using the expression:

$$P = \frac{1}{2}\rho V^3 \quad (1)$$

where P , ρ and V are the wind power density, density of the atmosphere and the wind speed at the point. MERRA dataset has hourly density ρ and wind speed V values. The MERRA 2D surface

turbulent flux diagnostics data set provides these values at a single level corresponding to the center of the lowest model layer. The height of this center varies between 60 m and 66 m across the domain considered.

2.1.1 Wind Resource at Different Heights

During the 1990s the general wind turbine height was 50 m. With the advancement of technology, the hub height of the turbine could be raised to 80 m, 100 m and 120 m although turbines of 80 m hub height are more common now. Thus, the estimation of wind resource and its variability at these different heights is imperative to study the behavior of wind power over the U.S..

The similarity theory in boundary layer dynamics is used to estimate the wind speed at the different heights.

The atmospheric boundary layer is controlled most importantly by (Stull, 1991)

- aerodynamic roughness length of the surface
- surface heat flux

Further, the stability of the atmosphere also plays a key role in the maintenance of winds in the boundary layer. The shear-stress in the boundary layer is estimated by the friction velocity u_* .

Using these variables, the wind speed at a height z in the boundary layer is expressed as

$$V_z = \left(\frac{u_*}{k}\right) \log \left[\frac{(z-d)}{z_0} - \psi \right] \quad (2)$$

where d is the displacement height, z_0 is the roughness length and k is the von Karman constant. z is the height at which the wind speed is estimated.

ψ depends on the stability of the boundary layer. For this study, the boundary layer is assumed to be neutrally stable. This assumption is reasonable because at the high wind speeds at which wind power is generated, the boundary layer has large wind shear and so, the boundary layer is approximately neutrally stable. Thus, equation 2 becomes:

$$V_z = \left(\frac{u_*}{k}\right) \log \left[\frac{(z-d)}{z_0} \right]. \quad (3)$$

2.2 Resource Metrics

Taking the instantaneous values of u_* , d , z_0 , the wind speed at height z is determined. Using this relationship, the wind speed at the heights 50 m, 80 m, 100 m and 120 m was computed. Thus, a dataset of hourly wind speed from 0030 Hrs on January 1st, 1979 to 2330 Hrs on 31st December, 2009 has been constructed for each of the heights. It is assumed that the air density does not differ appreciably at these heights through the well-mixed boundary layer. Thus, using the air density at the center of the lowest model layer ρ and the wind speed computed using the logarithmic wind profile above, the wind power density at these heights is estimated using:

$$P_z = \frac{1}{2} \rho V_z^3 \quad (4)$$

The U.S. wind atlas developed by NREL (Elliott *et al.*, 1987, 1991) used a power law for wind speed or wind power density of the form:

$$\left(\frac{\bar{V}_r}{\bar{V}_a}\right) = \left(\frac{z_r}{z_a}\right)^\alpha \text{ or } \left(\frac{\bar{P}_r}{\bar{P}_a}\right) = \left(\frac{z_r}{z_a}\right)^{S\alpha} \quad (5)$$

where $\bar{V}_{a,z}$ and $\bar{P}_{a,z}$ are the mean wind speed and wind power density at heights a and z (the anemometer height and the reference level respectively) and α is the power law exponent. Based on empirical fits of the anemometer measurements at some airport locations, the value of $1/7$ was used for the exponent α to adjust the mean wind speed to 50 m height. But Schwartz and Elliot (2005), using anemometers mounted at higher hub heights, found that the shear exponent α is significantly higher than $1/7$ used in making the wind atlas.

As described above, our estimates take into account the effects of surface heat flux on the friction velocity, the time variation in displacement height and roughness length. As such, our estimates are more explicit and comprehensive in the analytic formalism. Conventionally, wind power density is used as the physical quantity to describe the wind energy potential or the wind resource at a place. The U.S. wind atlas (Elliott *et al.*, 1987, 1991), for instance, maps the mean wind power density over the contiguous states of the U.S. To describe the quality of wind resource, it is proposed that more metrics of location and dispersion be taken into account. So, the median as another measure of location has been computed.

2.2.1 Fluctuations

Most of the studies on the wind resource in the U.S. looked at the mean wind power density. Since a key objective of this study is the investigation of the fluctuations in wind power density, fluctuations of two kinds are distinguished. **Figure 1** shows the wind power density for two hundred consecutive hours at a grid point in the central U.S. This figure is used to define and differentiate two kinds of fluctuations.

According to the classification of wind power density (WPD) into different classes (Table C1), 200 W/m² is the upper bound for the class 1, defined as the poor class. That is, if a location has WPD less than 200 W/m², usable power cannot be produced. In the plot, the red line marks this lower limit of 200 W/m².

For the initial 22 hours, there is usable WPD (above 200 W/m²) at this location but the value fluctuates from ~ 200 W/m² to ~ 650 W/m², then dips to ~ 400 W/m², rises to slightly above 700 W/m² and falls to less than 100 W/m². So, although during this time, the turbine can produce useful power, the power produced fluctuates very much. For the sake of differentiation, this kind of fluctuation, herein, is termed variability.

Since power density less than 200 W/m² is equivalent to no power, during the 200 hours shown, there is power initially for 22 hours, then there is no power for 10 hours, then there is power for ~ 7 hours and then, there is no power for ~ 110 hours and so on. This phenomenon of switching between power and no-power states is, herein, termed intermittency.

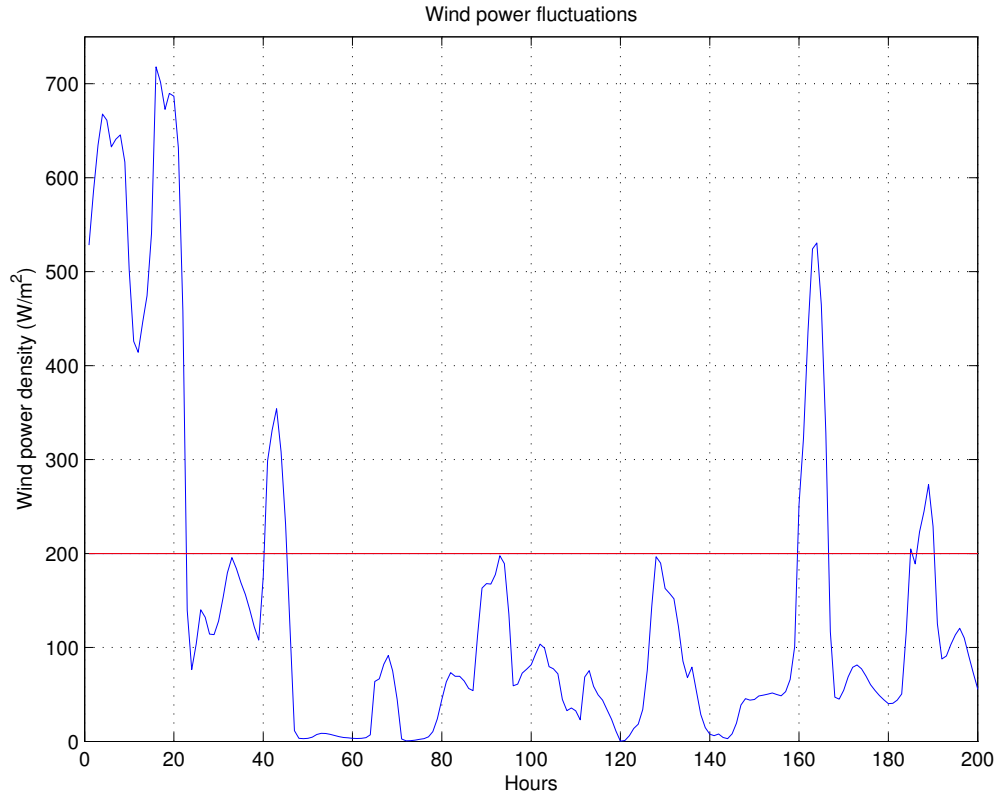


Figure 1. Illustrative wind power density profile showing the fluctuations in wind.

2.3 Intermittency Metrics

As mentioned, our analyses not only focus on characterizing the extent of wind power resource, but also its intermittent and variable behavior. As such, the following metrics are considered to investigate the intermittency of wind power density.

1. Statistics of wind power episode lengths.
2. Statistics of no-wind power episode lengths.
3. Availability/unavailability of power density.
4. Probability distribution of wind episode lengths.
5. Probability distributions of no-wind episode lengths.

These metrics measure the persistence of wind power, or lack thereof, and it is generally acknowledged that persistence of wind power density is important for reliability of power generation. Sigl *et al.* (1979) investigated the episode length distributions and developed a model for the episode length distributions based on a simple composite distribution. They showed that the shorter episode lengths obeyed a power law and the longer ones followed an exponential law. Following Sigl *et al.* (1979), the episode lengths in this study are modeled according to a composite

distribution which is a mixture of a power law and an exponential law. The probability density function of this composite distribution is described by:

$$u(x) = \begin{cases} at^{-b} & \text{if } t_0 \leq t \leq t_1 \\ A\lambda e^{-\lambda t} & \text{if } t_1 \leq t \leq \infty \end{cases}$$

where the first equation describes power law for episode lengths t less than the partition parameter t_1 and the second equation is the exponential law for longer durations than t_1 .

The episode lengths in hours are fitted to these distributions using the maximum likelihood estimation method. The parameters a , b , A , λ are found for each location.

Run duration analysis is mostly used for estimating or predicting the performance of a future wind energy installation at the location. For greater persistence of wind power, the probability of the shorter runs should decrease and that of the longer ones should increase. In terms of the equation above, the power law factor should decrease and the exponential factor should increase.

The scaling factor, a , is the scaling factor in the power law that is applicable for the short duration run lengths. For the wind power to persist for longer durations, the probability of the short runs should fall very fast. So, for the locations that have this scaling factor a low, the probability of shorter runs is low. The exponent, b , is the exponent in the power law. So, if the b is larger, because of the negativity in the exponent, the probability of the short runs is rendered small. Thus the median run length is longer. Similar to a , if A is large, the probability of the longer runs increases. So, A should be greater. For small values of λ , the probability curve described by exponential part of the above equation has a shallower tail and hence the longer episodes have greater probability compared to the cases when the λ is greater. As λ increases, the probability of the shorter run lengths increases drastically.

3. RESULTS & DISCUSSION

3.1 Descriptive Statistics of Wind Power from MERRA Wind

3.1.1 Mean Wind Power Density

Figure 2 shows the mean wind power density at the center of the lowest model layer across the U.S. The Midwest region has power density in the range of 300 W/m² to 600 W/m² whereas most of the regions flanking the Midwest on the east and west sides have wind power density less than 200 W/m² which is classified as poor. The offshore regions in the east and west have wind power densities in excess of 800 W/m². Texas, Oklahoma, Kansas, Nebraska, Indiana, Minnesota, North Dakota and South Dakota – have wind power density classified at least as fair and some pockets have 'good' and 'excellent' quality wind power densities corresponding to 400 W/m² to 500 W/m² and 500 W/m² to 600 W/m². The eastern half of Wyoming has the greatest onshore wind power density of 500 W/m² to 800 W/m². The offshore regions on the east and west coasts which are closer to the coastline have power densities of ~700 W/m² whereas the offshore region near northern California falls into the 'outstanding' class with ~1000 W/m².

Figure 3 shows the median wind power density at the center of the lowest model layer in W/m² across the U.S. Comparing with the mean wind power density in Figure 2, the median values are

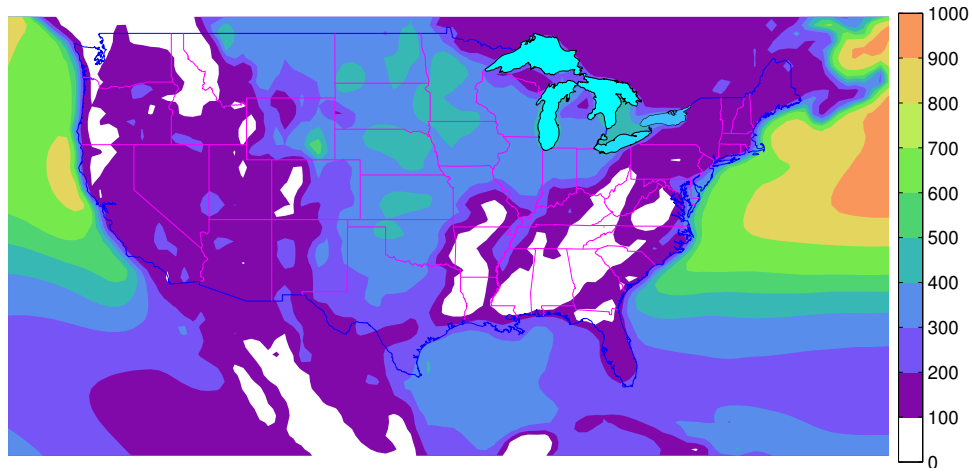


Figure 2. Geographical variation of mean wind power density (W/m^2) across the U.S.

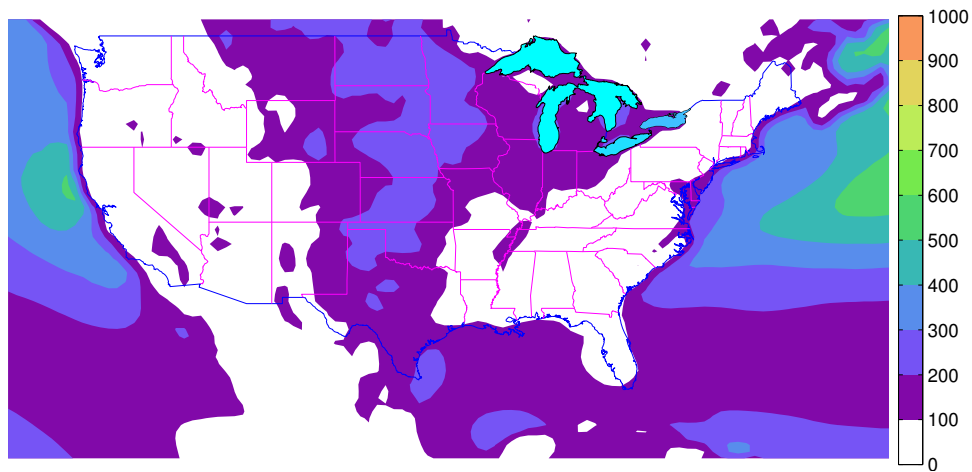


Figure 3. Geographical variation of median wind power density (W/m^2) across the U.S.

almost half of the mean values. For any distribution, 50% of the values are below the median and 50% of the values are above the median. So, this figure implies that for at least 50% of the time, the mean wind power density is less than half of the mean wind power density. Thus, we should regard the mean wind power density as an overestimate to the true central tendency of this resource.

Figure B1 shows the histogram of the wind power density at an illustrative point from the domain. Since the distribution is very skewed, the mean is not a robust measure of the center of this distribution. Given this long-tailed distribution, the very extreme values cause the deviation of the mean from the actual center of this distribution. We therefore view the median to be a more robust indicator of central tendency and a more appropriate metric to represent wind power density.

3.1.2 Coefficient of Variation (CoV) of Wind Power

The variability of a quantity is best captured in terms of coefficient of variation because it is desirable that the wind power is constant as much as possible. For two regions with the same mean power density, the one with a lower standard deviation will have lower CoV and is preferable (i.e.

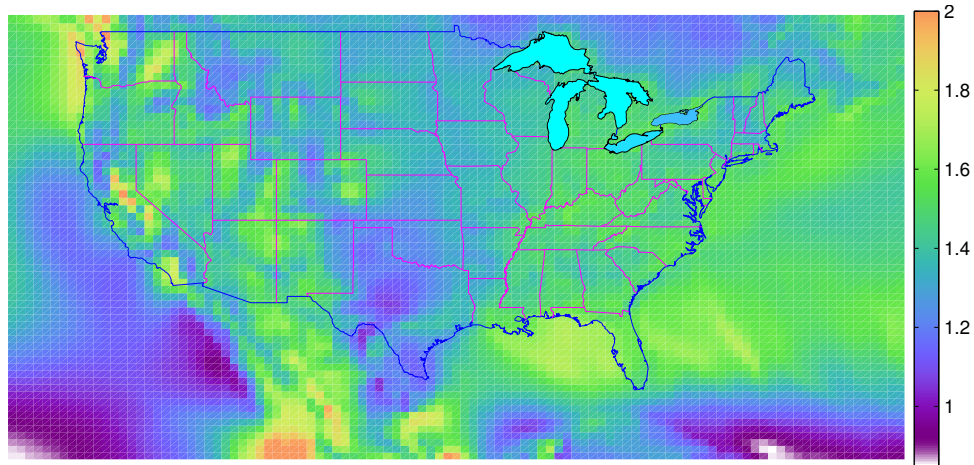


Figure 4. Geographical variation of coefficient of variation (CoV) of wind power density across the U.S.

less variable power quality). Similarly, for two regions with the same standard deviation, the one with greater mean power density is preferable and this has lower CoV. Given the impact of variability in wind power on the electric grid and the economics of power generation and distribution, it is desirable to lay wind farms in regions of low CoV of wind power. **Figure 4** shows the coefficient of variation of wind power density over the U.S. Central, south and northeast Texas have the lowest coefficient of variation. This region also has class 4 and class 5 mean wind power density. By this measure, this region would have the best onshore region for wind power generation. Similarly, Oklahoma, southern Kansas, southern Wyoming have appreciable wind power with less variability. Although southwest Montana and northeast Idaho has low coefficient of variation, the region has class 1 wind power. The offshore region near California has low variability as measured by the CoV whereas the offshore region north of California in the west and all the offshore region in the east have very high variability.

3.1.3 Inter-Quartile Range

Inter-quartile range (IQR) is a robust measure of statistical dispersion. The IQR shows the possible 'swings' of the wind power density at a location. Thus it is a measure of the backup power that needs to be maintained. The central U.S. region has an IQR of 300 W/m^2 to 600 W/m^2 whereas for the rest of the continental U.S., the values are very low – below 200 W/m^2 . The non-central U.S. has a median WPD of 100 W/m^2 and also the 75th percentile is 200 W/m^2 or less. Thus, this region has very low IQR. The offshore regions along the east and west coast have IQR $\sim 700 \text{ W/m}^2$ except the offshore region near northern California which has an IQR of $\sim 1000 \text{ W/m}^2$. It should be noted that this region also has greater mean WPD of about $\sim 1000 \text{ W/m}^2$. The far offshore Atlantic region on the east also has very large IQR – $\sim 1000 \text{ W/m}^2$.

3.1.4 Availability of Power

In reliability theory, *availability* is a measure of the reliability of a system. Extending the concept to wind power, the availability of wind power at a location has been estimated as:

$$\text{Availability} = \frac{\text{No. of hours with WPD} \geq 200 \text{ W/m}^2}{\text{Total number of hours}} \quad (6)$$

Figure 5 shows the unavailability, which is $1 - \text{availability}$, of wind power in the U.S. The central U.S. has the lowest unavailability onshore whereas most of the offshore region has the lowest unavailability of 40% or lower. The non-central U.S. region has the greatest unavailability of 70% or more. This representation of wind resource is very important because it provides the temporal distribution of the resource.

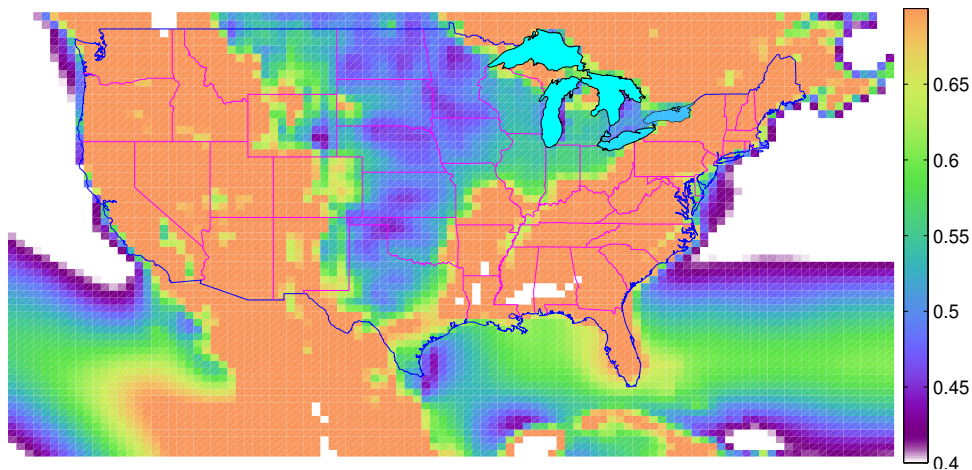


Figure 5. Unavailability (dimensionless) of wind power density across the U.S.

3.1.5 Wind Episode Lengths

Episode lengths of wind power density above 200 W/m^2 are an important facet in understanding the persistence of the wind power density and the nature of intermittency.

Figure 6 shows the median wind power episode lengths across the U.S. The central U.S. region has median episode lengths that range from 10 to 15 hours. Oklahoma, Kansas, eastern Nebraska, Iowa and North Dakota have median episode lengths close to 15 hours whereas the offshore regions on both sides of the U.S. have long median episodes of 20 hours or more. The non-central U.S. states have very short median episodes of 10 hours or less.

Figure 7 shows the geographical variation of the mean wind episode lengths across the U.S. Comparing the median and mean values of episode lengths, while the central U.S. has greater median episode lengths than some regions in West Virginia, Virginia, Louisiana, Mississippi, Alabama, Georgia, Tennessee, the latter regions have greater mean episode length. These states in the east and southeast have mean episode lengths as large as 120 hours. The consistency between mean and median values indicates that the wind episodes in the central U.S. region are evenly

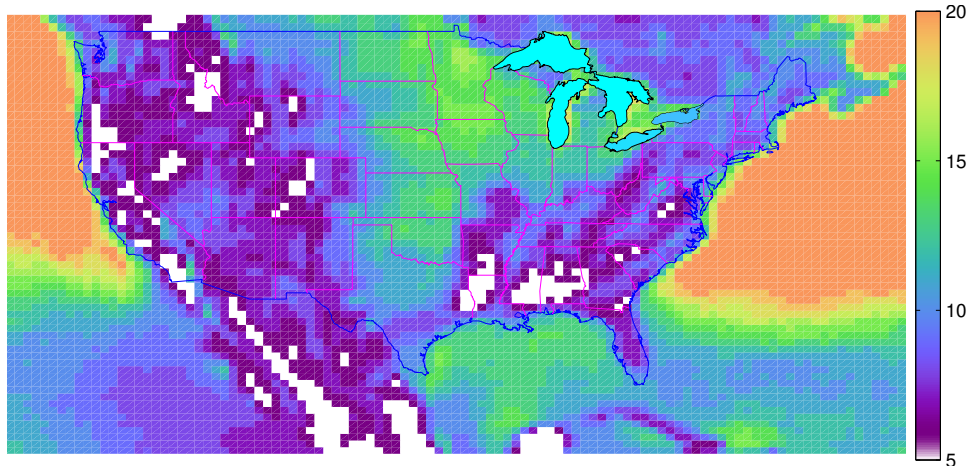


Figure 6. Geographical variation of the median wind power episode length (h) across the U.S.

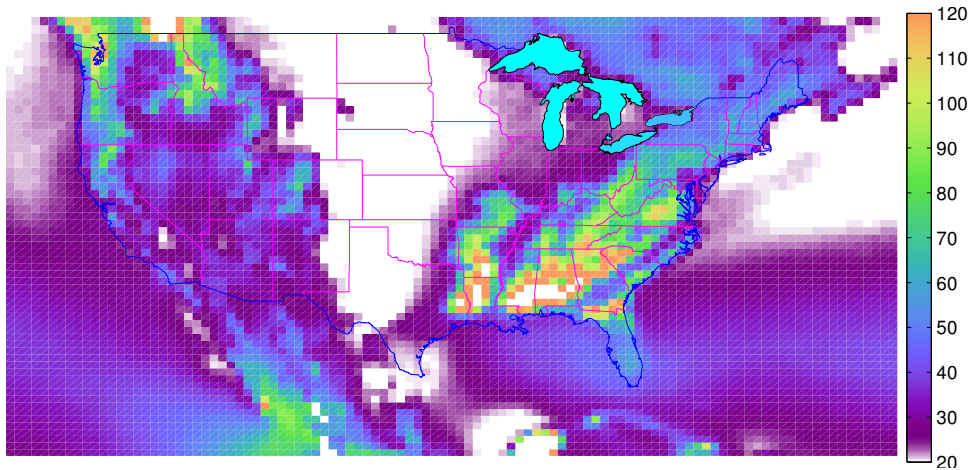


Figure 7. Geographical variation of the mean wind power episode length (h) across the U.S.

distributed whereas in the southeastern states, the wind power is very steady only for isolated periods.

According to the reliability theory, the 'time to repair' is an important metric of the reliability of a system. In wind power, it corresponds to the no-wind episode length, that is, the time for which the wind power is below the critical lower limit (200 W/m^2) between two wind power episodes. The geographical variation of no-wind episode lengths is consistent with the mean and median episode length variation shown in Figures 7 and 6.

This knowledge of persistence of wind power density should prove valuable in planning and developing a robust deployment strategy for harvesting wind power.

4. WIND POWER DENSITY AT DIFFERENT ALTITUDES

4.1 Comparison with NREL Map at 50 m

Comparison of the mean wind power density at 50 m height estimated in this study, **Figure 8a**, and the estimate developed by NREL, **Figure 8b**, shows that the regions with considerable wind

resource – most of the midwest region viz. eastern Montana, North Dakota, South Dakota, eastern Wyoming, Nebraska, eastern Colorado, Kansas, Iowa, western Minnesota, the Gulf of Mexico coast of Texas, the Great Lakes – are all common features in both the estimates. The remainder of the U.S. contains widespread areas of wind power density that corresponds to the 'poor' class (Class 1). Thus the wind resource estimation using the MERRA dataset is qualitatively similar to the wind resource at 50 m estimated by Elliott *et al.* (1987, 1991) for NREL.

Further, Elliott *et al.* (1987), based on the three criteria – abundance and quality of the observational data used to estimate the wind speed, the complexity of the terrain and the geographical variability of the resource – described the confidence in the wind resource estimate using certainty rating from 1 to 4, 1 being highly uncertain and 4 being very uncertain. In regions where the certainty rating is 1, the actual wind power density may vary by a few wind power classes. When these certainty ratings are taken into consideration, the wind power density estimated at 50 m is well within the bounds of uncertainty.

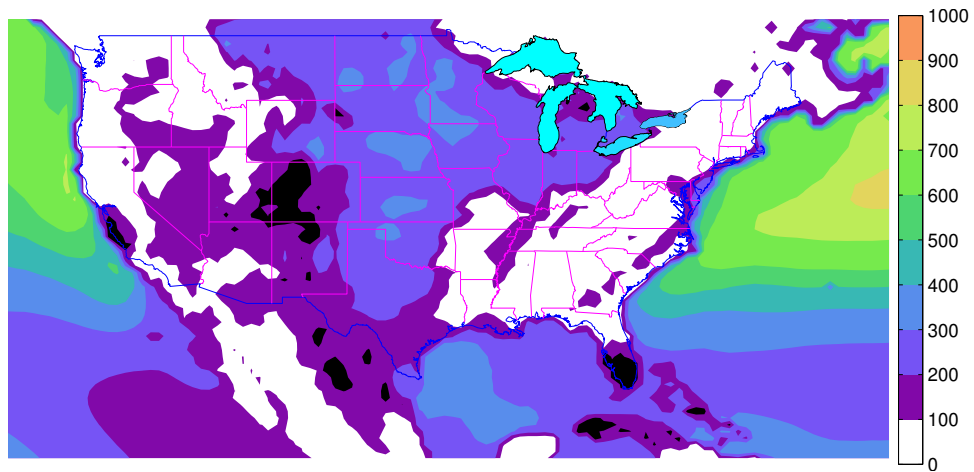
Justus *et al.* (1976) observed that across the U.S., the shape parameter for Weibull distribution of wind speeds varies between 1.1 and 2.7 and the mean value is 2.0. As discussed above, a larger shape parameter is used for larger wind speed regions. Note also that a unit of difference in wind speed corresponds to greater change in wind power density for the larger wind speed region than the lower wind speed regions. Thus, in addition to the uncertainty in the data, the Weibull-fitted estimate may be prone to systematic overestimations in regions of greater resource, for instance in the Midwest.

4.2 Comparison of Wind Speed at 80 m with the NREL Map

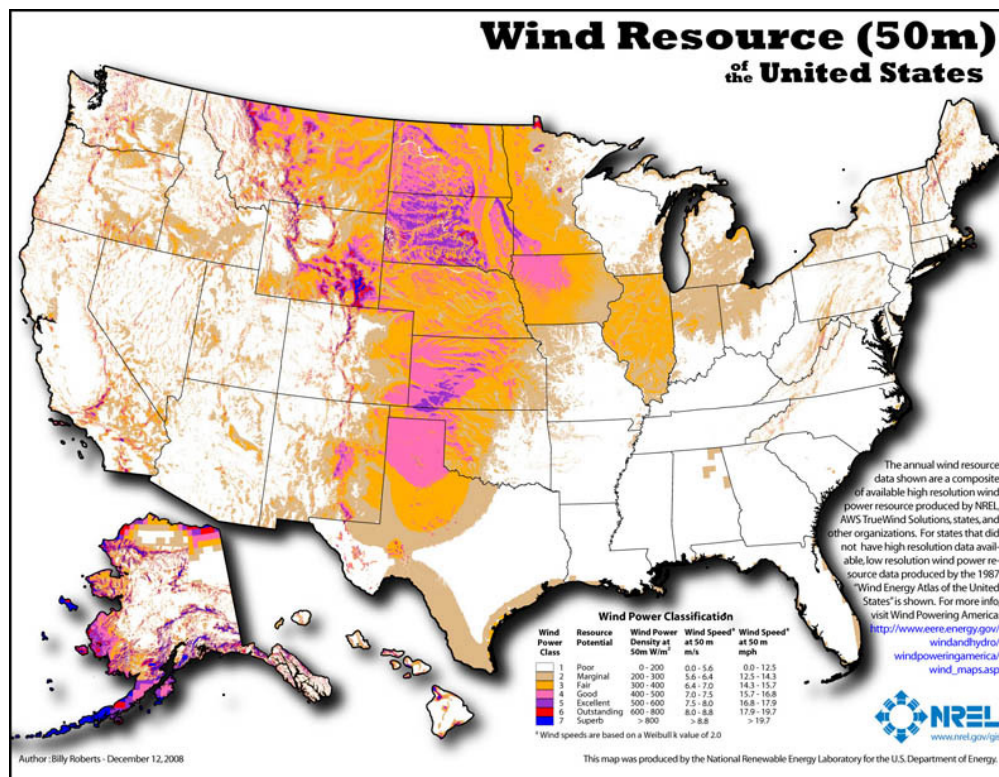
Figure 9b shows the estimates of annual mean wind speed at 80 m height developed by AWS Truepower NREL (2010). A mesoscale model, MASS, was run at a higher resolution with boundary conditions from NCEP Reanalysis. The simulated winds were downscaled using a statistical model to a resolution of $50\text{ m} \times 50\text{ m}$. The figure shows the mean wind speed from 4 m/s to 10.5 m/s with 0.5 m/s interval. **Figure 9a** shows the mean wind speed at 80 m developed in this study. The figure shows the wind speed from 4 m/s to 10 m/s.

Remarkably, the two figures match very well qualitatively and also are very close in their geographical variation. For example, the central U.S. region consisting approximately of eastern New Mexico, northern Texas, western Oklahoma, Kansas, Nebraska, South Dakota, North Dakota, western Iowa, southwestern Minnesota, eastern Montana, eastern and southeastern Wyoming have wind speeds between 7 m/s and 8.5 m/s. Wisconsin, eastern Minnesota, eastern Iowa, Illinois, northern Indiana and Ohio, large parts of Texas and Missouri and Michigan have wind speeds roughly between 5.5 m/s and 7.0 m/s.

The eastern region of Florida has a mean wind speed of 5 m/s, whereas a large tract of land covering northern Florida, Georgia, South Carolina, North Carolina, Alabama, a large part of Mississippi, Kentucky, Tennessee, Virginia, West Virginia, southern Ohio, southeastern New York, New Jersey, Connecticut, non-coastal Massachusetts, New Hampshire, Vermont and western Maine have wind speeds in the lower end of the spectrum below 5.5 m/s.

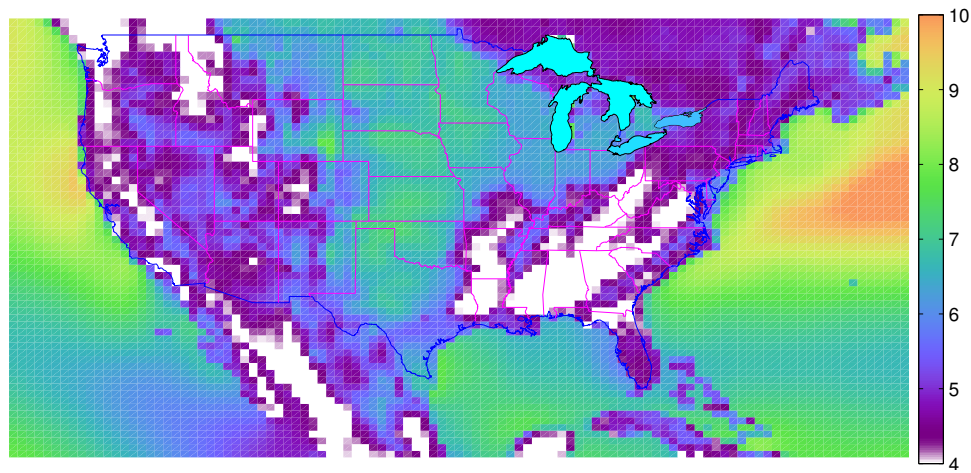


(a)

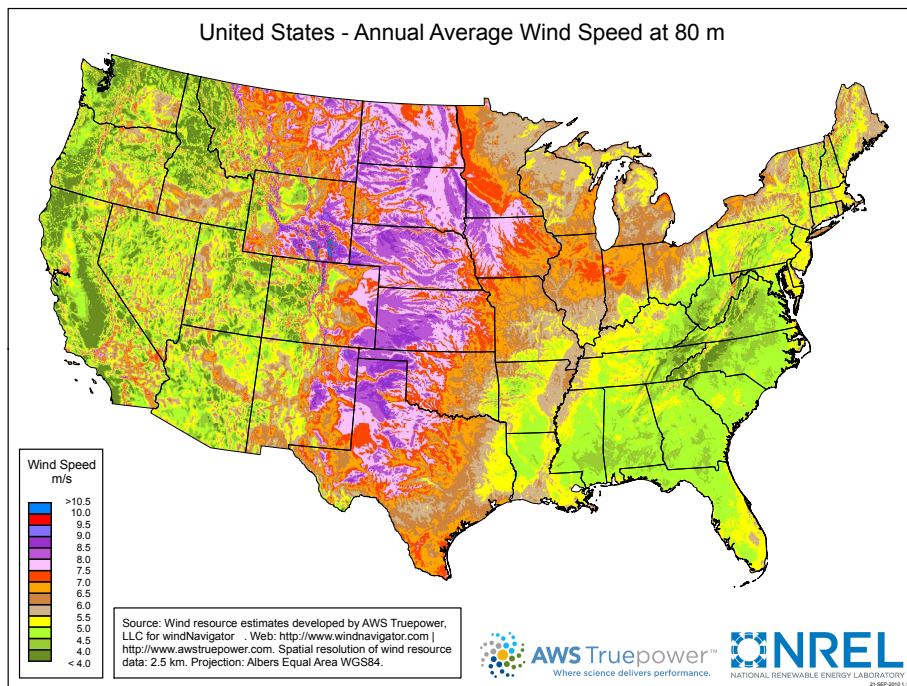


(b)

Figure 8. Wind power density (W/m^2) at 50 m hub height. Subfigure (a) shows the geographical variation of the mean WPD at 50 m computed in this study and subfigure (b) shows that estimated by NREL.



(a)



(b)

Figure 9. Wind speed (m/s) at 80 m hub height. Subfigure (a) shows the mean wind speed computed in this study and subfigure (b) shows the mean wind speed estimated by NREL. The white-shaded regions have annual mean wind speeds that are less than or equal to 4 m/s.

On the west side, most of the regions have low wind speeds except the mountainous stretches. Some small patches of regions in southern California, western Utah, central Arizona, southwest New Mexico, southwest Wyoming, southeast Oregon, southwest Idaho, and southwest Washington have considerable wind speeds between 6.0 m/s and 7.5 m/s.

Although the NREL estimate is at a higher resolution of 2.5 km compared to $1/2^\circ$ in this estimate, this estimate compares very well with the NREL estimate in almost all regions. There are some small regions in the central U.S. where the NREL estimate shows wind speeds of 8.5 m/s and greater which this estimate misses because of the lower resolution.

Archer and Jacobson (2003, 2007) used measurements from surface stations and soundings and extrapolated winds at 10 m to 80 m assuming a power law profile. The measurement data was for the year 2000. The wind speed estimates at 80 m in this study are largely similar to the estimates by Archer and Jacobson (2003, 2007).

4.3 Wind Power Density at Different Hub Heights

With the confidence gained out of the close match of the two estimates as described above, we now look at the effect of raising the altitude on the different metrics and quality of the wind resource.

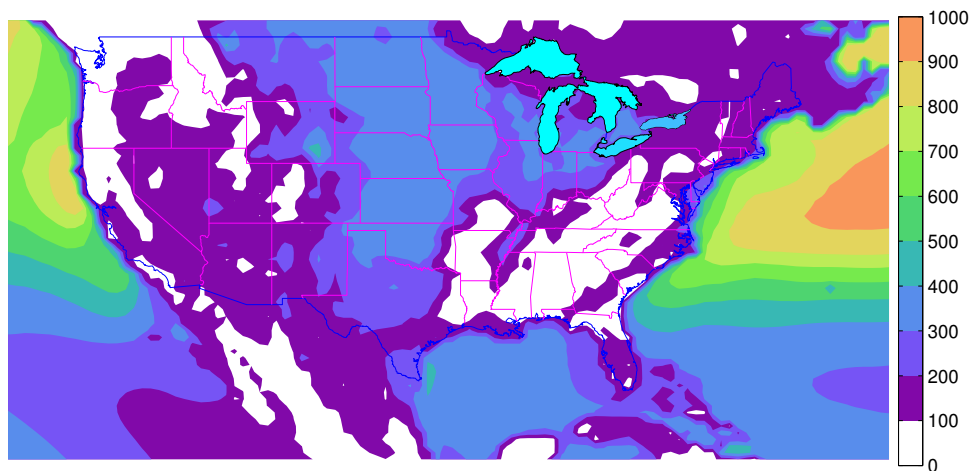


Figure 10. Geographical variation of the mean wind power density at 80 m (W/m^2).

To complete the picture of wind resource, in addition to the description of wind speeds, we discuss wind power density variation across the U.S. **Figure 10** shows the mean wind power density for an 80 m hub height in the contiguous U.S. and over the off-shore regions on both sides of the U.S.

The central U.S. consisting of the areas from north Texas in the south, Oklahoma, Kansas, Nebraska, South Dakota to North Dakota and the regions around the Great Lakes – northeastern Illinois, eastern Wisconsin, northern Indiana, southern Michigan, and northwest Ohio – are regions of high resource, generally in the range of $300 W/m^2$ to $400 W/m^2$. The southwest region of Wyoming has the greatest inland wind power density of $400 W/m^2$ to $500 W/m^2$.

Even though the mountainous regions on the west coast have high wind speeds, as can be seen in Figure 9a, those regions have low wind power density (Figure 10). Similarly, the wind speeds on the Appalachians are high but the wind power density is low. This is a result of the lower density of air on these high altitude regions. The air density and altitude of a location are related as:

$$\rho = 1.225 - (1.19 \times 10^{-4} \times z) \quad (7)$$

This equation 7 shows that a difference in altitude of 2000 m makes a difference of about 20% in the mean wind power density. Further, it also erroneously characterizes the mountainous regions as high wind resource locations. Thus, wind speed is not a suitable measure for the wind resource. If wind power density is used, it is more comprehensive as it covers the variation of air density.

Although the coastal states have very poor wind resource, the offshore regions abutting the coast have high wind resource. Particularly, the coasts of Connecticut, Rhode Island, Massachusetts and Maine have wind power density of 600 W/m² to 700 W/m². Similarly, the offshore region near the coast of northern California also has very high resource in the range of 700 W/m² to 800 W/m². The Gulf of Mexico region also has appreciable wind resource of 300 W/m² to 400 W/m² although it is in general less than the offshore wind power density on the east and west coasts.

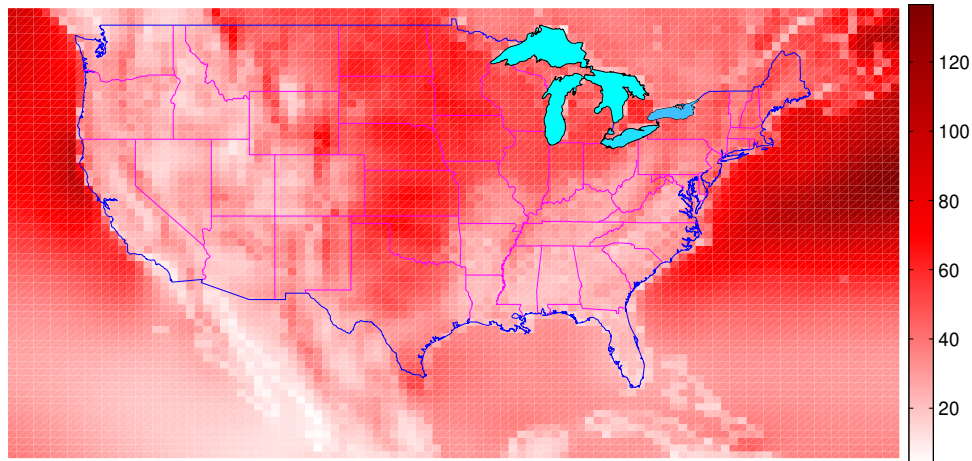


Figure 11. Difference mean wind power density between 80 m and 50 m(W/m²).

Figure 11 shows the difference in mean wind power density between 80 m and 50 m. Clearly, in general, there is an increase in the quantity as the height is raised. The increase is higher in the central U.S. region and in the New England region, along the Appalachian mountain region, New Jersey, New York and some regions of Pennsylvania.

Intuitively, the change is dependent on the wind resource at the lower level and the roughness length. In regions where the resource is high at the lower level, even a small gradient in the vertical profile would mean an appreciable increase at the upper level. Also, in regions which have high surface roughness length, the wind profile has a sharper gradient and so, even a smaller wind speed at the lower level may mean an appreciable increase in the wind speed at the upper level. Thus, the greatest advantage of raising the altitude is in regions that have higher surface roughness length, for instance due to vegetation, and also in regions that have higher resource at the lower level.

Another important reason for the large increase in the central U.S. is the presence of a strong nocturnal low level jet that has a maximum between 500 m and 800 m. This low level jet induces a gradient in the vertical wind profile that is considerable and is maximum at 6:00 in the morning. Schwartz and Elliot (2005) measured the wind speed using towers fitted with anemometers at several sites in the central U.S. as a part of wind resource assessment at higher altitudes. They reasoned that the nocturnal jet is an important cause of the increase in wind resource at night in these regions.

As discussed above, the hub height of most wind turbines installed in the last decade is 80 m. Therefore, in the subsequent sections, the wind resource, its variation and intermittent character is discussed accordingly.

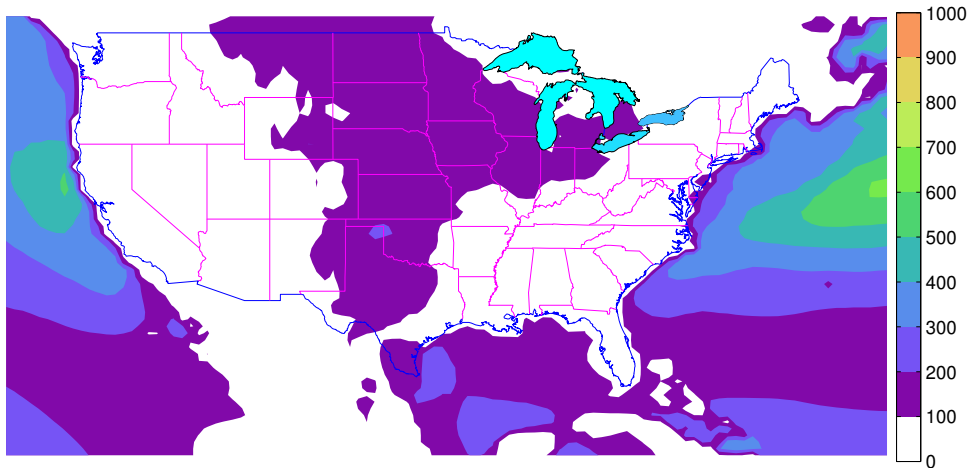
As discussed in page 20, there is a general increase in the resource as the altitude is increased. As the hub height is increased, the mean wind power density increases fast initially and with further rise in height, the increase in the mean resource is less. Although increase in the mean wind resource decreases, there does not seem to be a saturation in the benefit even with reasonable increase in hub heights beyond the present 100 m and 120 m.

It was argued that both mean and median should be used to describe the wind resource. **Figure 12a** shows the geographical distribution of median wind power density at 80 m. It shows that most of the central U.S. has median wind power density ranging between 100 W/m^2 and 200 W/m^2 . As the height is increased from 80 m to 120 m, the median increases (**Figures 12b** and **12c**). That is, frequencies of higher wind power densities than those of the median at 80 m increase. But similar to the mean resource, the increase in median wind power density decreases with altitude.

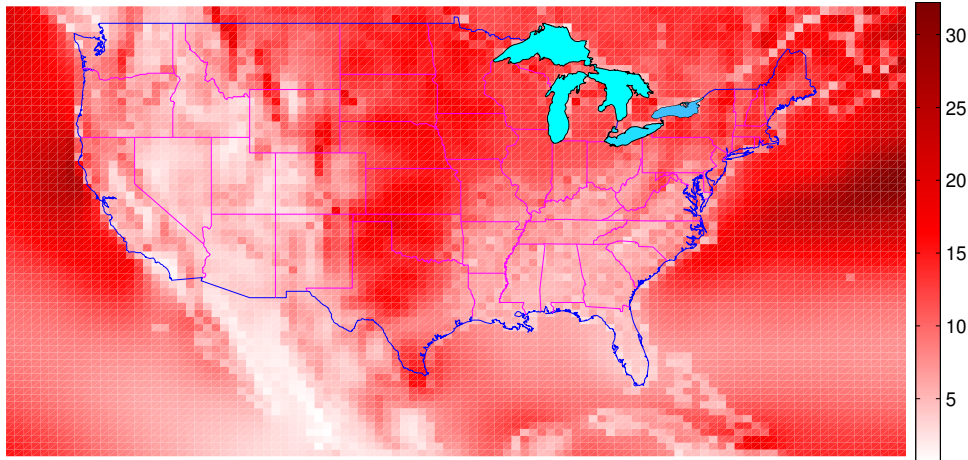
Schwartz and Elliot (2005) found that the shear exponent for vertical adjustment of wind speed is considerably greater than the conventionally used $1/7$. Also, they reported that the windy sites, for instance those in the central U.S., have lower α s than the less windy sites. Thus, the increase in the mean and median wind power density in the central U.S., and the less windy sites like the New England region, may be the same because of the higher shear exponent in the less windy regions. Thus the altitude variation shown in Figures 12b and 12c are consistent with the recent measurements and the patterns of vertical variation.

Because the mean wind resource increases with altitude, as seen in the previous subsection, it implies that the frequency distribution of the wind power density shifts to the right. Also, the frequency distribution is broadened. Thus, the inter-quartile range increases with height, but the increase diminishes with height. Going from 80 m to 100 m, the inter-quartile range increases by half a class in the central U.S., whereas in the offshore regions the increase is larger. Raising the turbine hub height from 80 m to 120 m results in more than a class of increase in the wind resource quality.

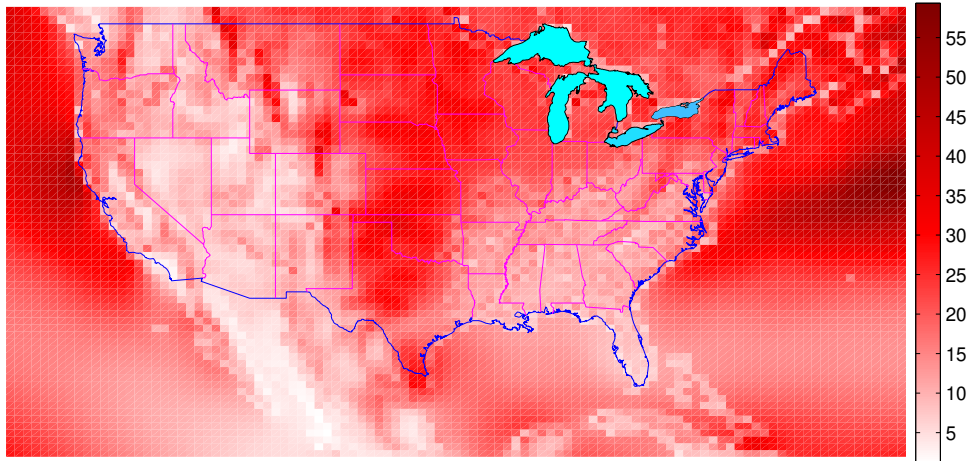
Coefficient of variation describes the variability of a quantity globally. **Figure 13a** shows the variation of CoV across the U.S. **Figures 13b** and **13c** are the differences in CoV at 100 m and 120 m from that at 80 m. It is interesting to note that while the CoV decreases over land, it increases slightly over the oceans. This is because the wind resource increases in general and by a large amount over the ocean. The CoV decreases with increasing mean for a steady standard deviation.



(a)

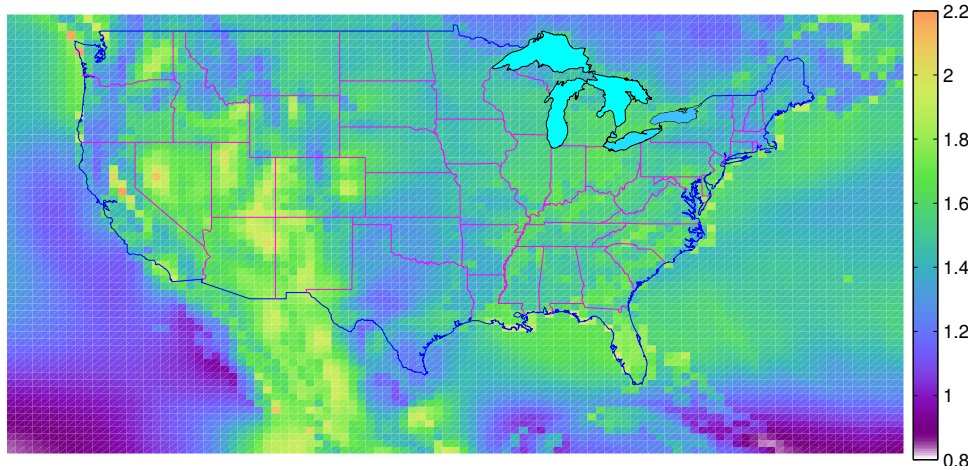


(b)

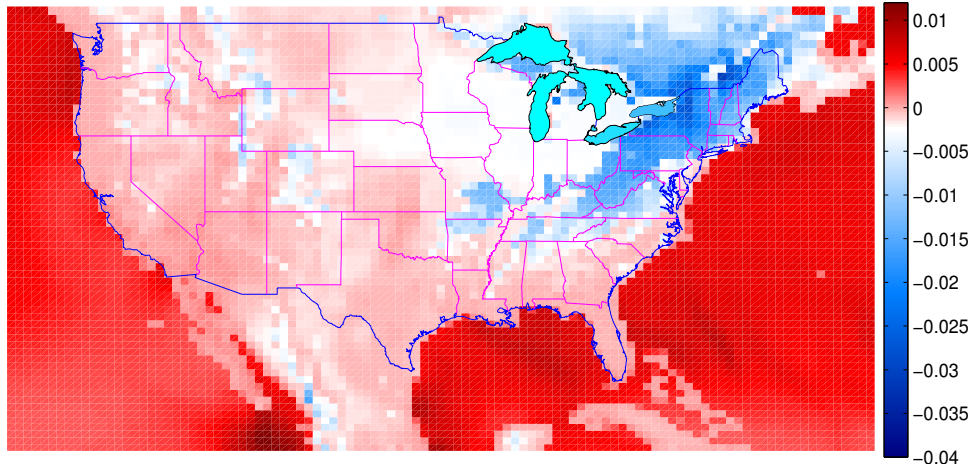


(c)

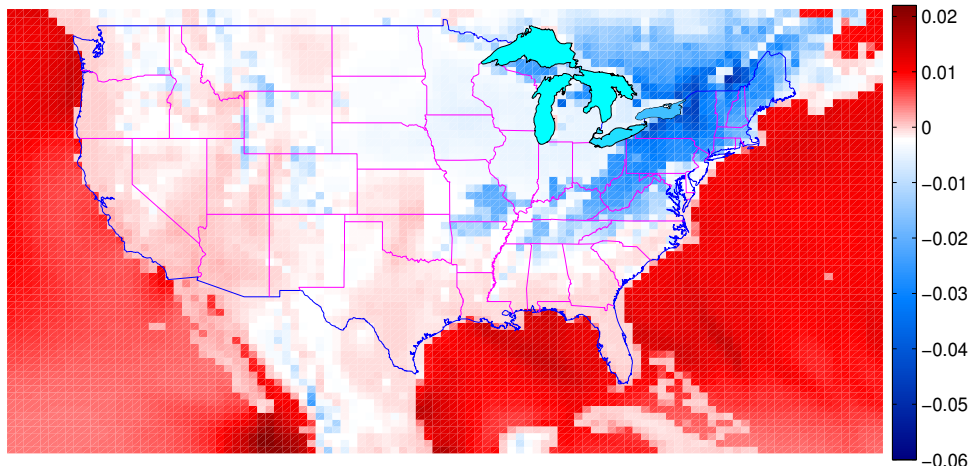
Figure 12. Variation of median wind power density (W/m^2) at different heights. Subfigure (a) shows the median wind power at 80 m and subfigures (b) and (c) show the difference median wind power density at 100 m and 120 m from that at 80 m.



(a)



(b)



(c)

Figure 13. Variation of the coefficient of variation of wind power density at different heights. Subfigure (a) shows the CoV of wind power density at 80 m and subfigures (b) and (c) show the difference CoV of wind power density at 100 m and 120 m from that at 80 m.

Thus, this phenomenon means that the variance in the offshore regions increases much more than the mean. An important implication of this phenomenon is that the back-up required to compensate the variability in the wind power is greater.

Another interesting feature of the difference plots is that the CoV decreased in the northeastern states of Maine, Vermont, New Hampshire, New York, New Jersey, Pennsylvania, West Virginia and southern Ohio. Thus, the largest increase in persistence of wind power with altitude is in these northeastern states. The distribution of the wind power episode lengths are important in estimating and planning the back-up requirements. Thus, the knowledge of the changes in the statistical behavior of episode lengths at different heights may help in planning the utilization of the wind resource at a location or the enhancement of existing deployment facilities with higher turbines.

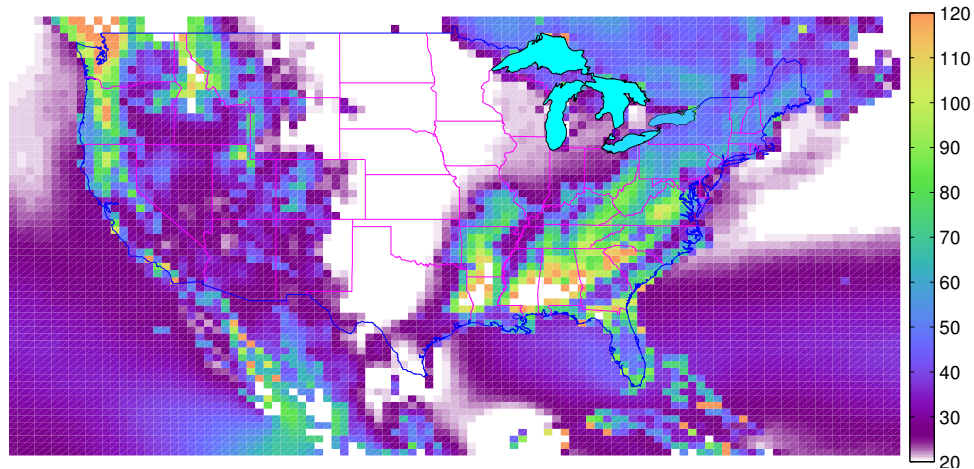
The geographical distribution of the mean wind episode length at 80 m shows great variation between 20 h to 120 h. The central U.S. and the offshore regions have very low episode lengths near 20 h whereas the other regions have episodes lasting longer. Central Virginia, northwest South Carolina, Georgia, southeast Alabama, northwest Mississippi, northwest Washington, western Oregon and northern Idaho have very long episode lengths near 120 h. The mean and median wind power density in these regions are very low. Thus, it is possible that these regions have very highly consistent wind resource due to cyclonic activity in the Pacific or in the Gulf of Mexico. The very low episode lengths of the central U.S. and the offshore regions is due to the strong diurnal cycle (24 h) in these regions. Thus, the episode length in these regions is very predictable compared to the regions where the episode length is very high but unpredictable.

A very different picture is shown by the variation of median episode lengths at 80 m, shown in **Figure 15a**. Not only are the median values very small (in the range 5 h to 20 h) compared to the mean episode lengths (which are in the range 20 h to 120 h), the central U.S. and the offshore regions have greater median values than the rest of the areas. But, the central U.S. and the offshore regions have lower mean values than the rest of the regions. These large differences in mean and median values of the distributions indicate that the frequency distributions of episode lengths in the non-central inland areas are very skewed and consist of a few episodes that are very long.

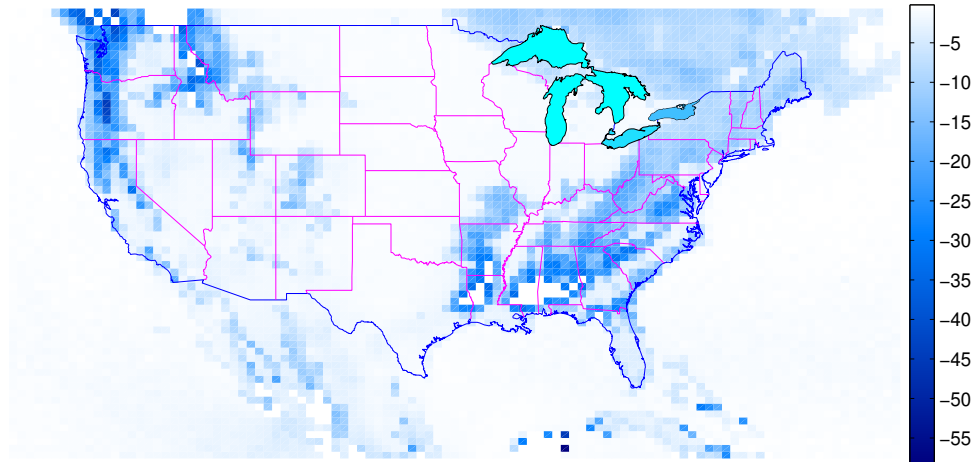
Figures 14b and **14c** show the geographical variation of the mean wind episodes at 100 m and 120 m compared to the mean wind episode lengths at 80 m. It is interesting to see that the mean wind episode length decreases everywhere - both inland and offshore - and the change is greater in low wind resource regions. Further, like in the case of the other measures, the change in mean wind episode length also slowed down with height. But for feasible turbine heights, the rate of change is steady.

Whereas the mean wind episode length changed by as much as 50 h between altitude levels, the median of wind episode length is almost steady and changed only by 3 h. Also, the median wind episode length changed in both direction - increase and decrease - although it increased or remained constant and there is no geographical patterns in the change (**Figures 15b** and **15c**).

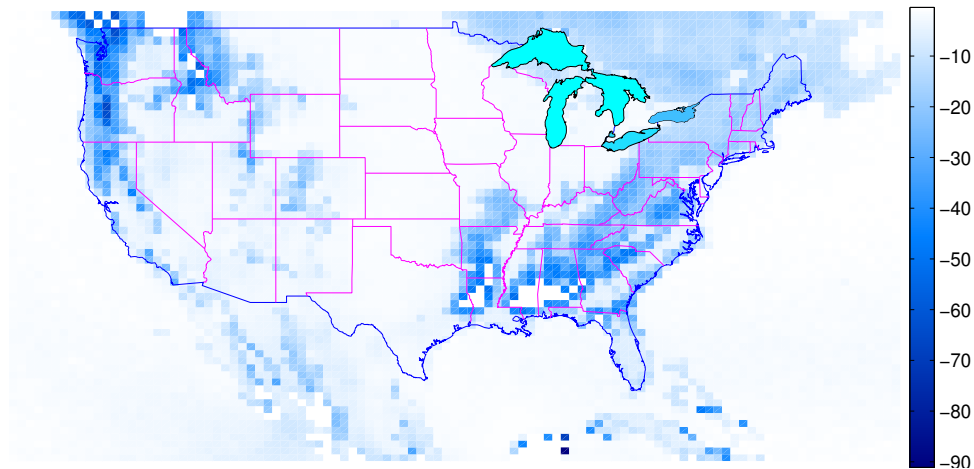
Coefficient of variation of wind power episode length at 80 m is shown in **Figure 16a**. It is interesting that some regions - northwest and south Montana, southeast Wyoming, central and southwest Texas, southern tip of Texas - have very high variability in episode length. The offshore



(a)

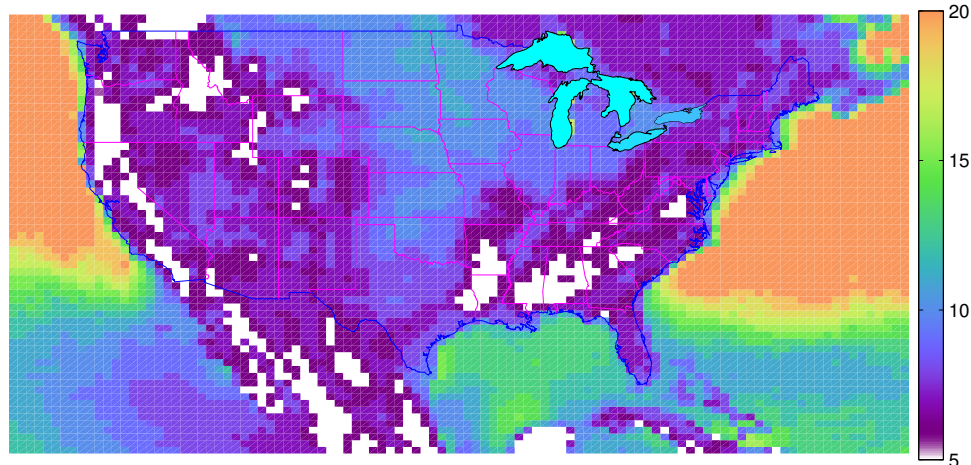


(b)

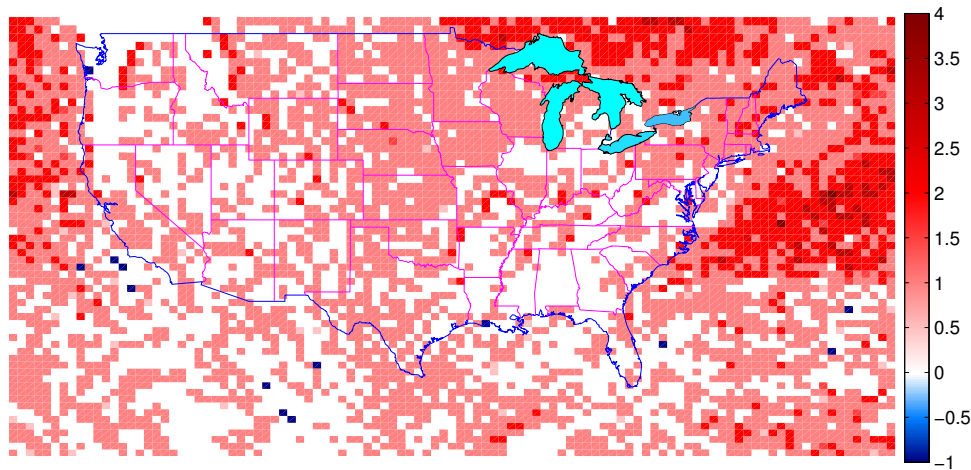


(c)

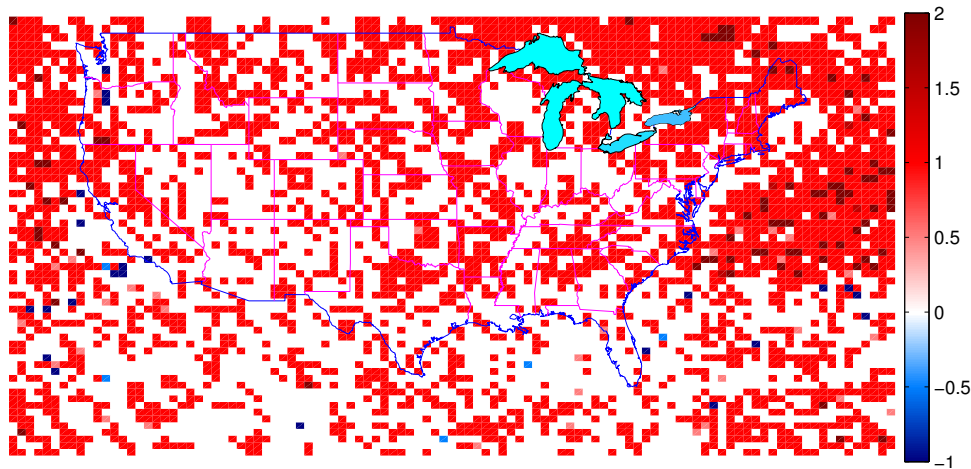
Figure 14. Variation of mean wind power density episode lengths (h) at different heights. Subfigure (a) shows mean wind power episode length at 80 m and subfigures (b) and (c) show the difference wind power density episode length at 100 m and 120 m from that at 80 m.



(a)

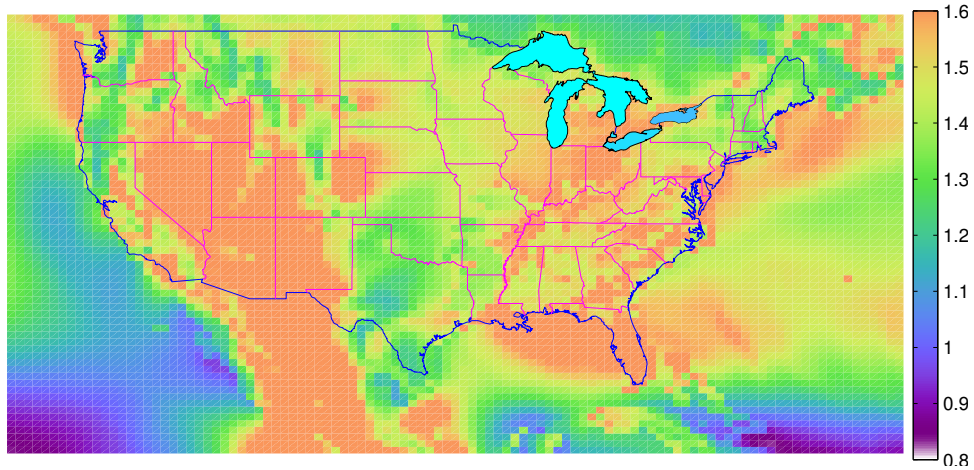


(b)

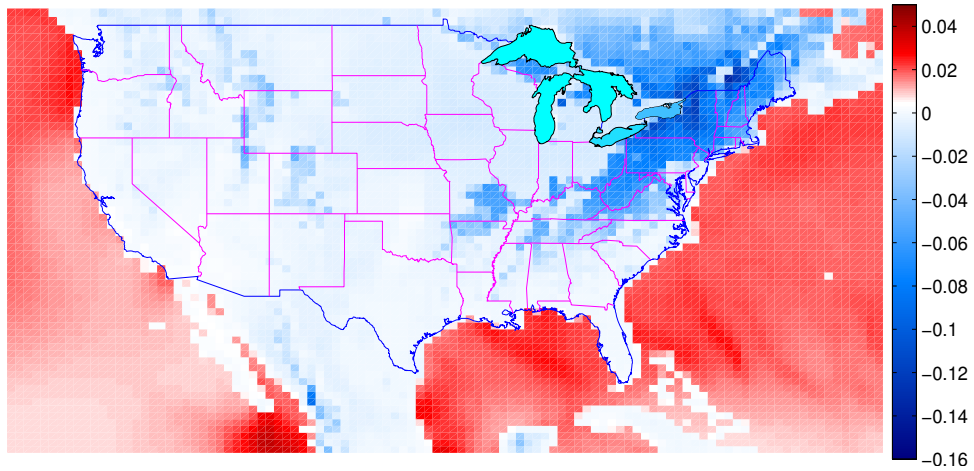


(c)

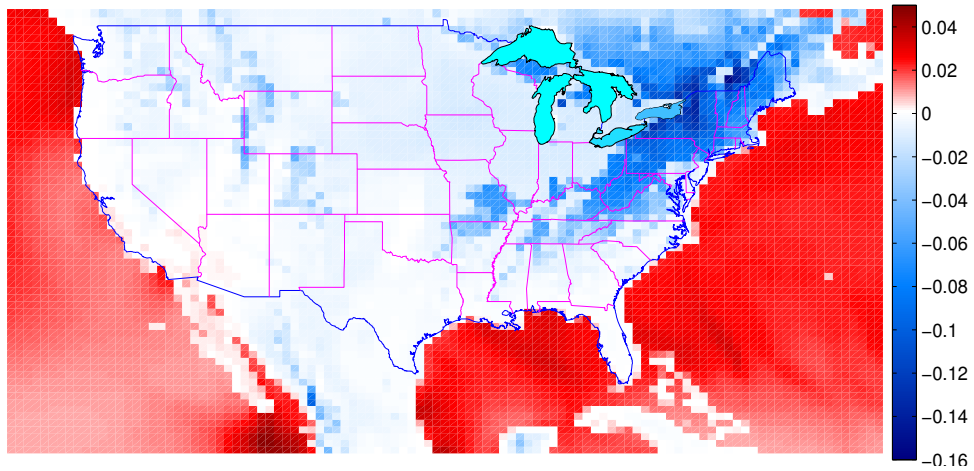
Figure 15. Geographical variation of the median wind power episode length (h) at different heights. Subfigure (a) shows median wind power episode length at (80 m) and subfigures (b) and (c) show the difference wind power density episode length at 100 m and 120 m from that at 80 m.



(a)



(b)



(c)

Figure 16. Variation of the coefficient of variation of wind power density episode lengths at different heights. Subfigure (a) shows the CoV of episode lengths at 80 m and subfigures (b) and (c) show the difference CoV of episode lengths at 100 m and 120 m from that at 80 m.

regions - south of San Francisco and south of Florida - also have very high variability in episode length. Some of the low resource regions on the leeward and windward sides of the Appalachian mountains on the east coast, and the mountainous regions in the west coast have steady episode lengths. The central U.S., western Oregon and the northeast states have moderately steady episode lengths.

Figures 16b and **16c** show the change in coefficient of variation in episode lengths as the hub height is raised to 100 m and 120 m respectively. These figures show that as height is increased, in most regions, the persistence of wind power episode length decreases. The increase is more pronounced in western Washington, west Oregon, northwestern California, western Montana, central Colorado, southern Texas, Arizona, north Mississippi, northern Alabama, northeast Georgia, Tennessee and western Virginia.

5. INTERMITTENCY

In the literature and previous studies, the word intermittency has been used to denote the variability of wind. In this study, we distinguish between two kinds of variations of wind. First, the wind turbine produces usable power, but the generated power changes over time. In this instance, the turbine produces always produces usable power. Second, the wind turbine either is still or the power generated is below the minimum usable power. Gustavson (1979) demonstrated that a minimum wind power density of 220 W/m^2 is needed for minimum usable wind power generation. To account for advances in technology, we consider 200 W/m^2 as the minimum wind power density for usable power production as used in the U.S. Wind Resource Atlas (Elliott *et al.*, 1987). Figure 1 shows the wind power density at a location in the central U.S. for 200 consecutive hours. The red horizontal line shows the 200 W/m^2 lower power density threshold. For the initial 21 h, the wind power density is above the minimum, but varies. Similarly, between 160th and 164th hour, it is more than the threshold value, but varies rapidly. In this study, this variation when the wind power density is at least sufficient is termed 'variability'. For some of the time, for instance from 43rd hour to 160th hour, the wind power density is less than the threshold and a turbine placed here would presumably not produce usable power. This is termed intermittency for the sake of the ensuing discussion.

In reliability theory, *availability* is one of the measures of the reliability of a system. Extending the concept to wind power, the availability of wind power at a location has been estimated as:

$$\text{Availability} = \frac{\text{No. of hours with WPD} \geq 200 \text{ W m}^{-1}}{\text{Total number of hours}} \quad (8)$$

Figure 17 shows the availability of wind power in the U.S. The central U.S. has the greatest availability onshore whereas most of the offshore region has the largest availability of 40% or higher. Large areas of the non-central U.S. region have an availability of 20% or less.

If we multiply the numerator and denominator in the ratio above by the peak capacity of the turbine and the area of the rotor blade of the turbine, the resulting ratio is the upper bound of the capacity factor of the turbine. Thus, availabilities as defined above are the upper bounds of the capacity factors of the turbines at the respective locations.

We then compare the availability of WPD to the capacity factors simulated in the Eastern Wind Integration Transmission Study (EWITS) (Corbus *et al.*, 2009, 2010). **Figure 18** shows the

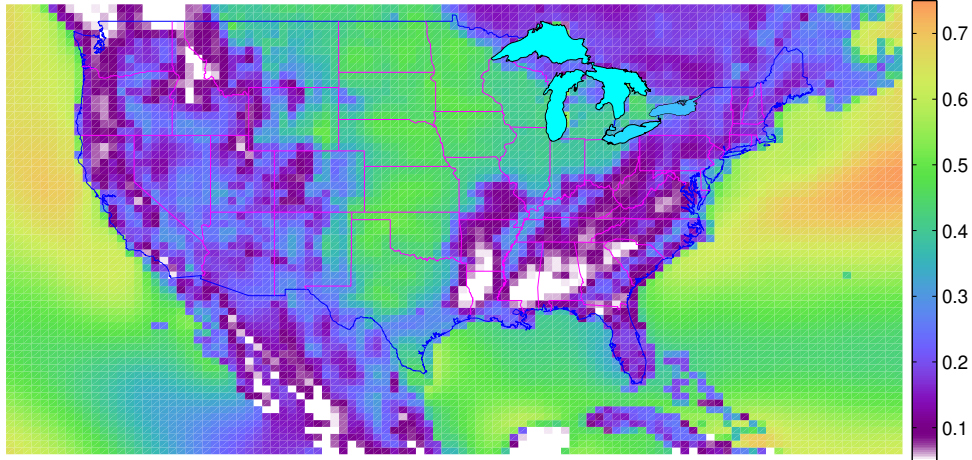


Figure 17. Availability (dimensionless) of wind power resource at 80 m.

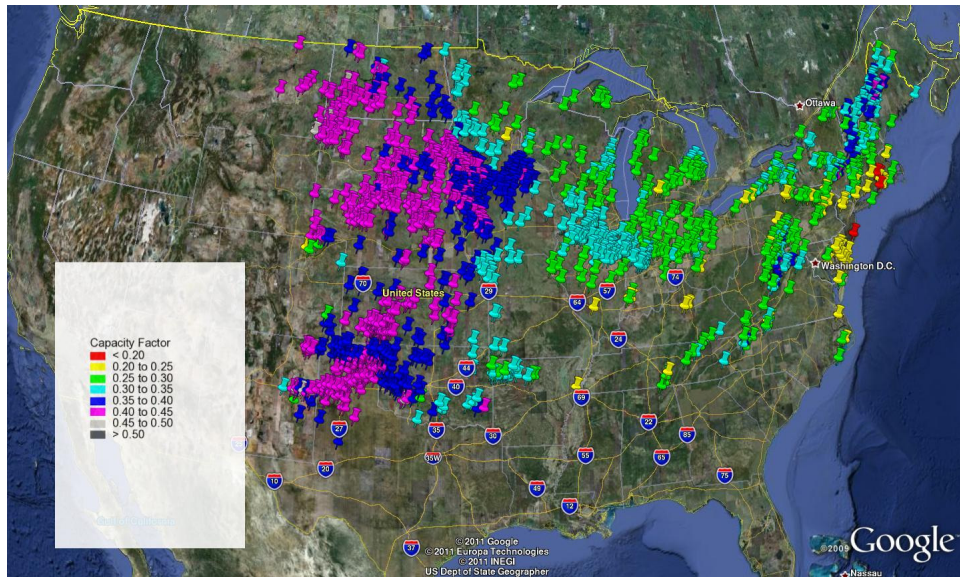


Figure 18. EWITS estimated capacity factors.

capacity factors simulated to study the feasibility of integration of large scale wind power into the grid in the eastern U.S. Comparison of the two figures shows that the availability data shown closely approximates the upper bounds of the capacity factors simulated in the EWITS.

5.1 Experiments

Following the assumption that the minimum wind power density needed for usable power generation is 200 W/m^2 , the time series of wind power density at each grid point is converted into a binary sequence of 1s and 0s depending on if the wind power density is greater or less than 200 W/m^2 . In the analyses that are described here, these binary sequences will be used.

To understand the spatial and temporal relationship between the wind resource at these grid

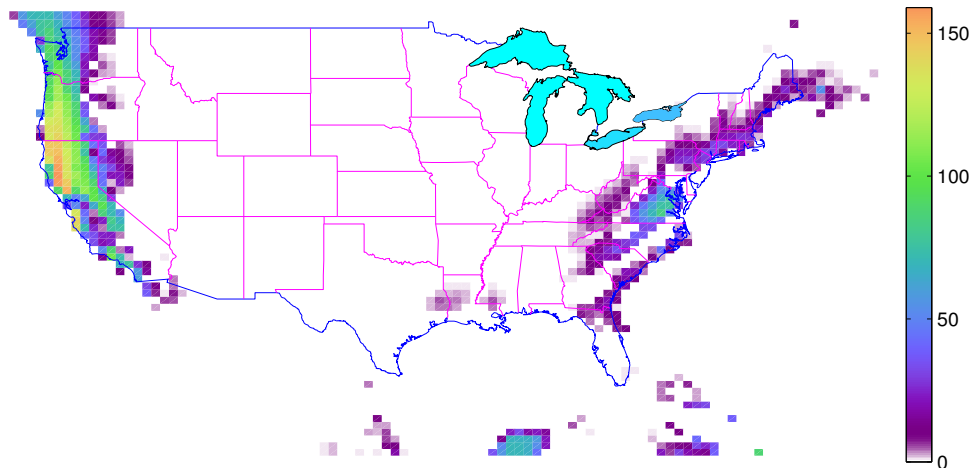


Figure 20. Geographical variation of anticoincidence of wind power density at 80 m height in the U.S. The color of each grid point shows the number of anticoincident points in a box of $\sim 1000 \text{ km} \times 1000 \text{ km}$ around it. The white region shows complete lack of anticoincidence or coincidence of intermittency.

the region along the northern Californian coast, in which some points have nearly half of the grid points in a region of $\sim 1000 \text{ km} \times 1000 \text{ km}$ around them. This inference conforms to an earlier conclusion by Kahn (1979) who looked at the reliability of an aggregated array of wind sites in California in a very comprehensive study. He found that most of the measures of reliability showed marked increase in performance. Later researchers also reported similar confidence in the ability of aggregated wind farms in ameliorating the fall in performance and reliability due to variability and intermittency of the wind resource. This conclusion is readily explained by the substantial spatial anti-coincidence of wind resource in the west coast. This inference is also supported by meteorology of the region. The topographic inhomogeneities and the presence of mountains are likely to contribute anti-coincidence of wind resource in this region. The east coast region in the figure shows marginal anti-coincidence. Here too, the topographic differences and proximity to sea contribute to the anti-coincidence. Although this region has some amenability for interconnecting wind farms, the quantity and quality of wind resource are low. Still, in different times and spatial scales, this region provides marginal benefit in interconnecting. It is very interesting that in the central U.S. region, there are no sites that have at least 50% anti-coincidence with any nearby sites in every region of $\sim 1000 \text{ km} \times 1000 \text{ km}$. It is also interesting that this region has the largest inland wind resource in the whole U.S. This region has low surface roughness, and is characterized by semi-arid climate and even terrain. Meteorologically, this region is largely impacted by the anti-cyclones due to the subtropical high pressure systems. As high pressure systems tend to spread over large areas, there is large coincidence of low wind state across the whole high pressure system.

The cyclones and low pressure systems due to the baroclinic instabilities, being mesoscale phenomena, are spread over very large areas. The even plain terrain also aids to the homogeneity of the wind resource in this spatial scale. Thus, the high wind instances are also highly correlated.

It may be noted that some earlier researchers (Archer and Jacobson, 2007) have shown that in a square box of $850 \text{ km} \times 850 \text{ km}$, the interconnection of wind turbines resulted in reduction of

variability of wind power.

5.1.1 Null Anti-Coincidence

With the surprising result in the central U.S. above, we wanted to see if a relaxed criterion shows any feasibility of interconnecting wind turbines in the central U.S. to mitigate variability and intermittency in wind power. So, the instances when the other point P has wind when R does not have power are counted and if the count is at least 50% of the number of instances of no-wind at R , they are termed null-anti-coincident. The number of such null-anti-coincident points around R in a box of 19×19 grid points is the score of R . **Figure 21** shows an illustration of the instances.

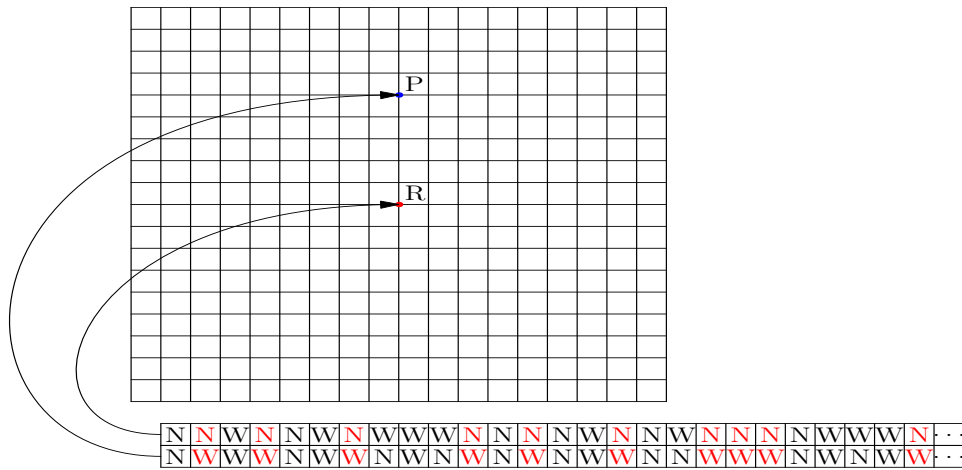


Figure 21. Schematic showing the criterion for null-anti-coincidence.

The geographical variation of null-anti-coincidence across the U.S. is shown in **Figure 22**. This

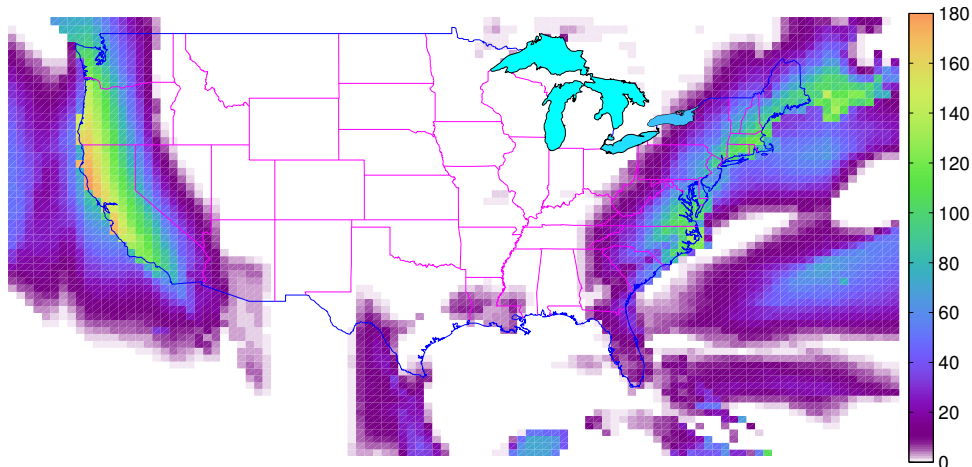


Figure 22. Null-anti-coincidence of wind power density at 80 m across the U.S.

figure shows that in the west coast, there is large null-anti-coincidence. That is, if there is no sufficient wind at any point, there are many sites around the point that have sufficient wind and

interconnecting the sites can provide a steady wind power. Similarly, on the east coast, there is considerable number of grid points around every point that can compensate for the lack of sufficient wind at the point.

It is also interesting to note that in the case of anti-coincidence, the offshore regions do not have sufficient anti-coincidence, whereas they satisfy the relaxed null-anti-coincidence.

The most significant lack of null-anti-coincidence occurs in the central U.S. This result is also very significant due to the fact that this is the region that has the greatest wind resource inland.

Apart from the perspective of interconnecting to mitigate the intermittency in wind resource, this result has another significant consequence that due to the high coincidence, the intermittency in the central U.S. is highly synchronized. That is, large regions of the central U.S. have synchronized high wind and synchronized low wind. Thus, if these regions are interconnected, then the synchronized high wind instances will result in very large wind power in the grid and the synchronized low wind situations will result in very low wind power output. This region with no anti-coincidence or null-anti-coincidence, effectively is characterized by a high correlation of greater than 0.5 between neighboring grid points.

There have been several studies that looked at intermittency in a smaller scale - millisecond, second and minutes (Parsons *et al.*, 2004, 2006; Smith *et al.*, 2007; Makarov *et al.*, 2009). The reported implications of intermittency at the smaller scales is the impact on grid stability. It was pointed out that sudden rise or fall of wind power does not occur and fall in wind power at a site is gradual. But the impact of intermittency at the scales of an hour and longer is different. The result is a rise or fall in the wind power in the grid. If the aggregated power from interconnected turbines falls in the scale of hours the grid will be driven into instability.

Since the results of this experiment depend on the cut-in WPD chosen, although the value of 200 W/m^2 is justified, we wanted to repeat the experiment for a cut-in WPD of 140 W/m^2 and the anti-coincidence scenario in the central U.S. does not change much.

To study the collective variation of the fraction of the grid points that have UWPD in the highly correlated wind resource region, the time series of the points with UWPD as a fraction of the total grid points in that region are plotted. **Figures 23** and **24** show the time series for the years 1979 and 2009 respectively. **Figure 25** shows the mean annual fraction of the points with UWPD averaged over the thirty one years.

The initial 2000 hours in these figures correspond to the first three winter months of the year, 2000-7000 hours to the next six warm summer months and the remaining hours to the last three cool/cold winter months. The most important inferences from these figures are discussed below.

1. The no-wind fraction is greater in summer than in the winter. As has been reported by some earlier researchers (Elliott *et al.*, 1987), this is a result of the lower density of air and lower frequency of the baroclinic instabilities that result in the large-scale storm systems. As discussed earlier, a large fraction of the wind resource in the central U.S. region is due to these storms, and so, the increase in wind power density due to these storms appears as the huge swings in power density in winter.
2. Rapid fluctuations of the no-wind fraction are large and frequent in the winter months.

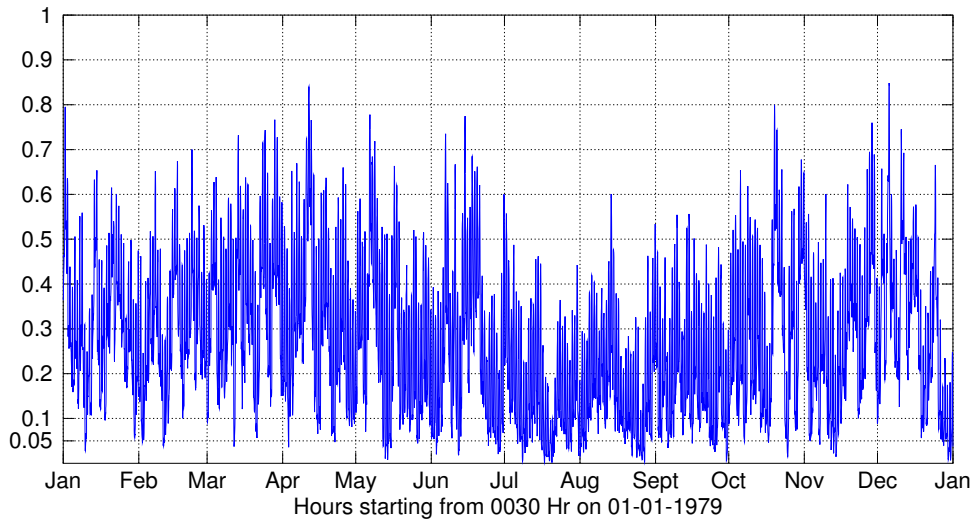


Figure 23. Time series of hourly fraction (dimensionless) of grid points that have usable WPD in the coincident U.S. region in 1979.

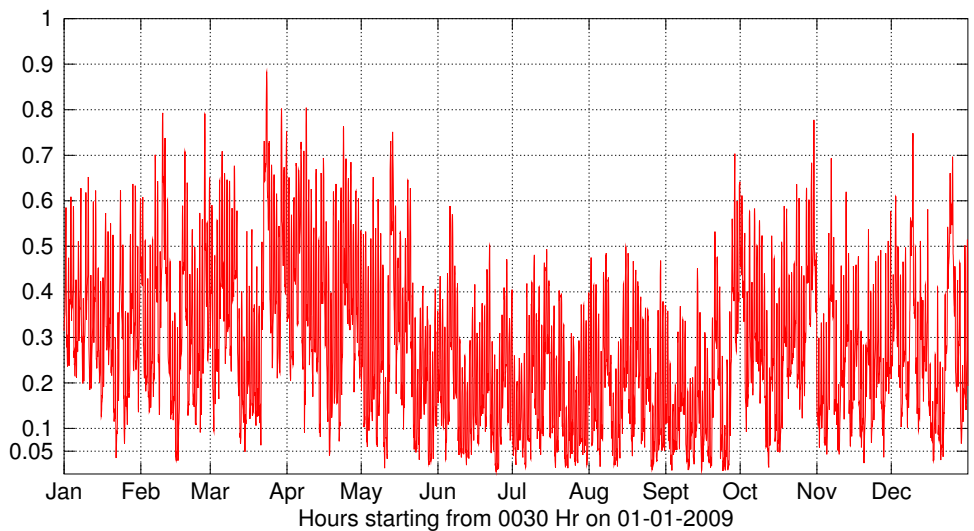


Figure 24. Time series of hourly fraction (dimensionless) of grid points that have usable WPD in the coincident U.S. region in 2009.

3. The curve lies most of the time below 0.5, and so, the likelihood of most of the grid points having high wind resource is less likely. But if the whole time series for the 31 years of the data is seen, there are instances when 99% of the grid points have wind resource.
4. Because of the lower frequency of storms in summer, the season is clear of the large swings in wind power density and the wind resource is less variable than in winter. Thus, the aggregated resource in the central U.S. region is less intermittent in summer. But it is to be noted that the resource itself is very low and the portion of the time the

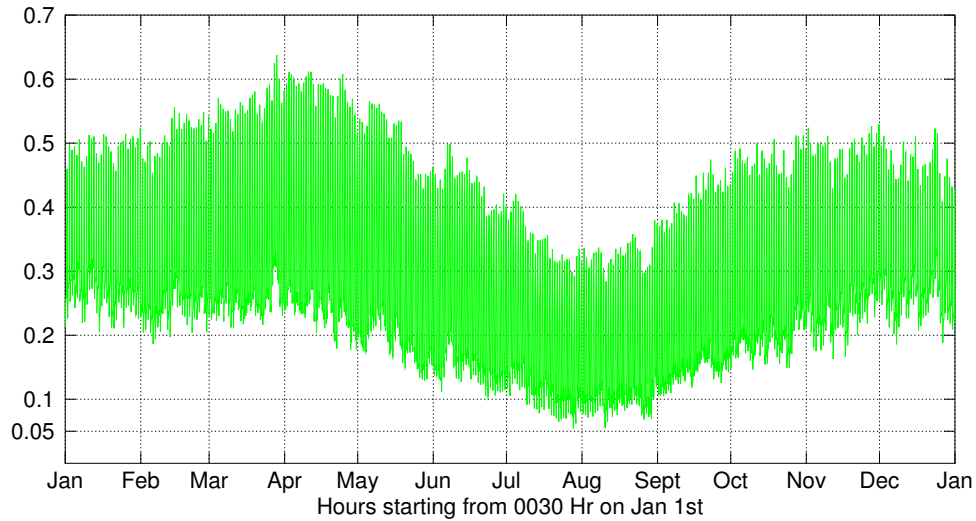


Figure 25. Time series of annual mean hourly fraction (dimensionless) of grid points that have usable WPD in the coincident U.S. region.

available wind resource exists below 0.1 is considerable, especially seen in 2009.

A cursory glance at Figure 10 points out that in the central U.S., most of the wind resource is concentrated in a north-south oriented salient from Texas to North Dakota. Thus, this region with availability greater than 25% is important for wind power generation. So, the variation of the fraction of the grid points in the central U.S. that have very high coincidence (Figure 20) and also have wind power density availability greater than 25% is shown in **Figure 26**. Shown are the results for 1979.

This plot shows that for this region with appreciable wind resource, the synchronization of the intermittency is exhibited to a greater extent. The number of hours for which less than 10% of the points have usable power density is considerable. For the 31 years of data, less than 10% of the points have power for approximately 8% of the time and less than 5% power for almost 3% of the time.

One of the most important assumptions of these experiments is that the wind resource at every grid point of any domain considered is utilized. It is reasonable to expect that with the development of present technology and expected advancement, the entire inland U.S. and the continental shelf region of the offshore region are at least marginally amenable for wind farming. So, to explore this area, the inland U.S. and the belt around the coasts for about ~ 100 km is considered. The collective behavior of the wind resource in this region is studied. **Figure 27** shows the fraction of grid points in this region, that have power as defined in the earlier sections, during 1979. Summer, in general, has the lowest power density and fluctuations. In addition, the summer months also have the largest number of hours for which less than 5% or 10% of the grid points have usable power density. Further, winter power density has large fluctuations. **Figure 28** shows the aggregated capacity factor, defined as the ratio of the total produced power in the region to the total name plate capacity in the region, of simulated wind power generated in the EWITS. It is clear from this figure that the

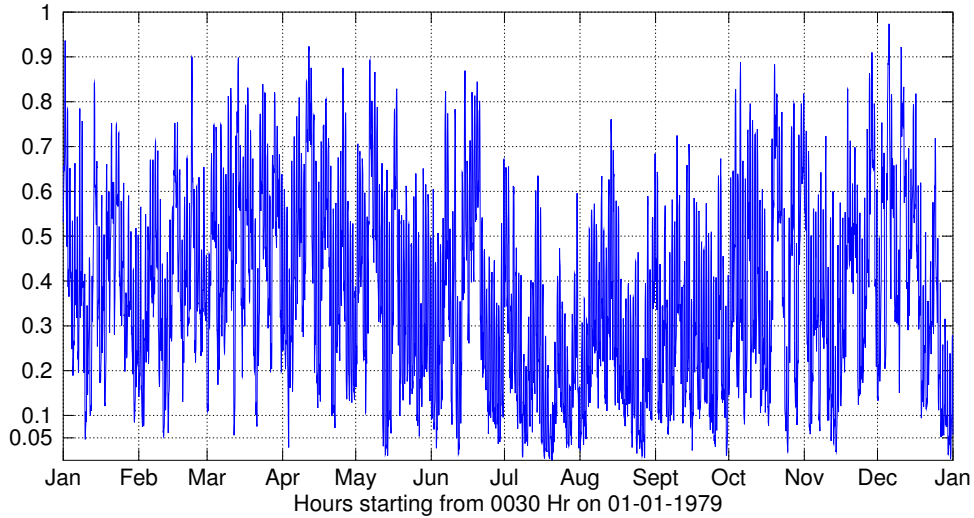


Figure 26. Time series of hourly fraction (dimensionless) of grid points that have usable WPD in the coincident central U.S. that have availability >25%.

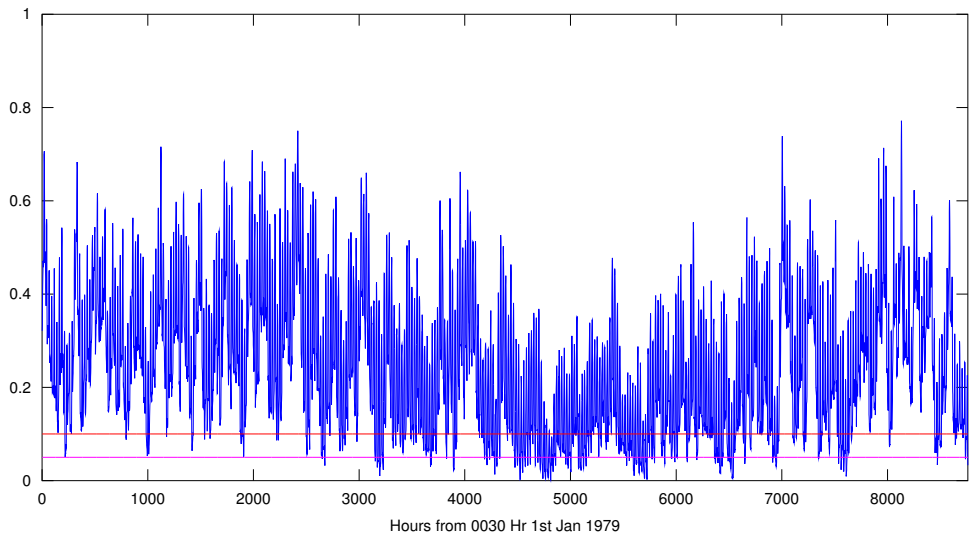


Figure 27. Fraction of points with UYPD in 1979 at each hour in the whole U.S. + off-shore region.

results of this experiment are very similar to those that are observable in the EWITS. It is to be noted that this plot shows the aggregated capacity factor and so, variations in the aggregated power generation will be large as this plot would be scaled by a large number. **Figure 29** shows, as boxplots, the annual distribution of the fraction grid points in the continental U.S. and ~100 km offshore that have usable wind power density from 1979-2009. This figure shows that there is a considerable fraction of time for which less than 20% of the area considered has usable wind power resource. Further, the situations in which a large fraction (i.e. >0.75) of the grid points have usable power can be characterized as outliers within these annual populations.

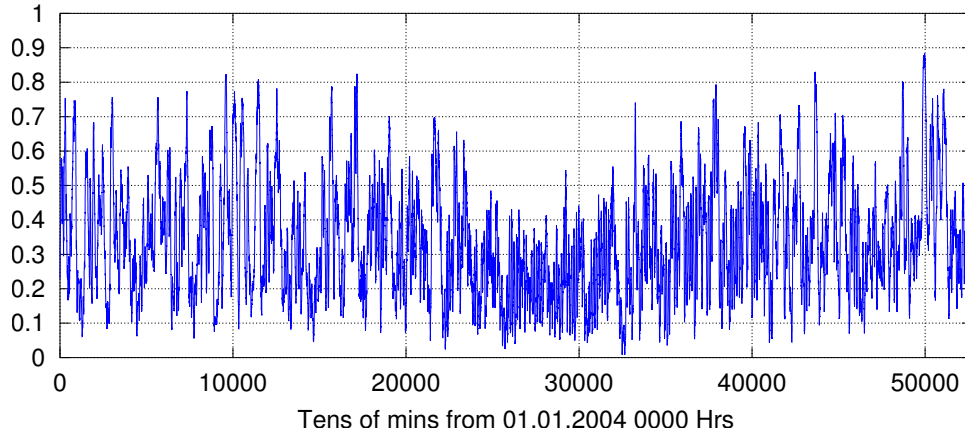


Figure 28. Aggregated capacity factor of 187 sites in EWITS for 2004.

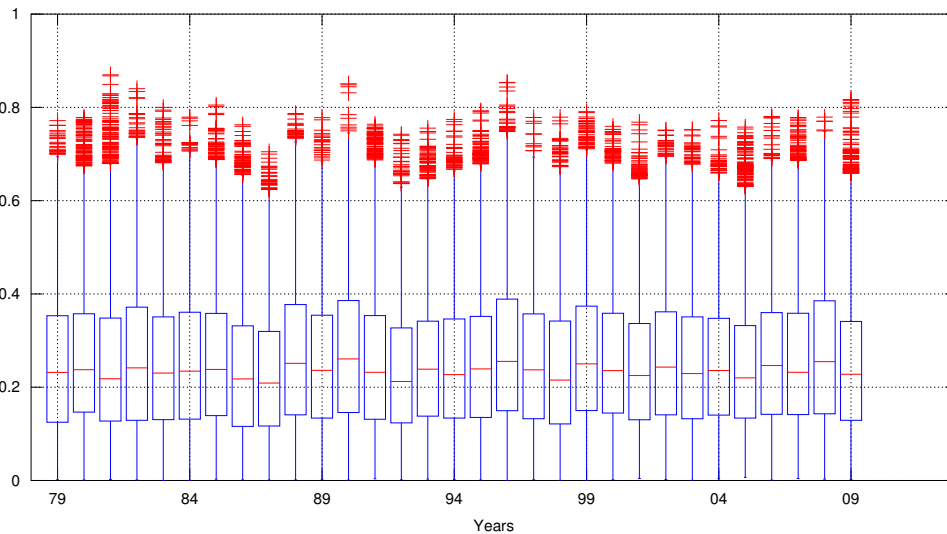


Figure 29. Annual distribution of fraction of highs in all the 31 years at each hour in continental U.S. + offshore.

5.2 Interannual Variability of Wind Resource

Figures 30 and 31 show the number of hours in the U.S. and the west coast for which almost 10% of the grid points have usable power density. The x-ticks of the plot are the El-Nino years. A very interesting feature of these plots is that during El-Nino years, in the entire U.S., for greater number of hours, almost 10% of the grid points have usable power whereas during the La-Nina years, less number of grid points have usable power for less number of hours. Interestingly, the opposite is true for the west coast. During El-Nino years, the increasing incidence of storms results in greater wind resource in the west coast. This points to an interesting differential variability of wind resource in the entire U.S. and the west coast and needs further in-depth study.

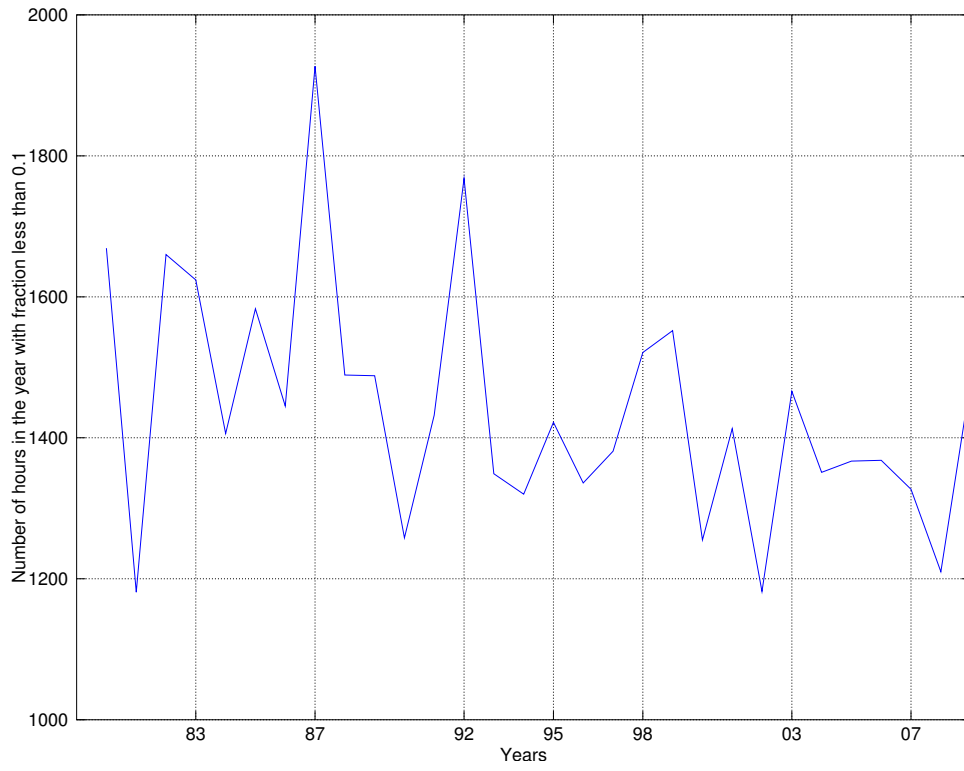


Figure 30. Number of hours in each year for which at most 10% of the grid points have UWPD.

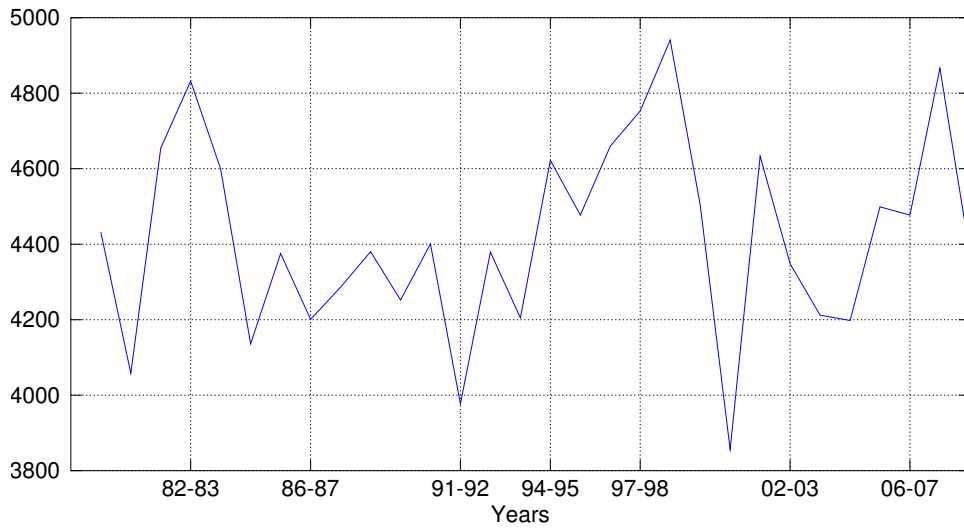


Figure 31. Number of hours in each year for which there is power at at most 10% of the grid points in the west coast of the U.S.

5.3 Analysis Without Cut-in WPD

The time series of hourly wind power density at each grid point has been used to estimate the hourly wind power generated at each grid point. To estimate the power generated, the following assumptions have been used:

5.3.1 Turbine Size and Power Curve

A number of GE 1.5SLE wind turbines are assumed to be installed at each grid point. This turbine has a hub height of 80 m and rotor diameter of 77 m. The nominal power of this turbine is rated at 1.5 MW at a wind speed of 14 m/s. The density of the atmosphere assumed by the technical specifications of the turbine is 1.225 kg/m^3 . The power curve of this turbine is shown in the **Figure 32**. This power curve is given as a function of wind speed. Using the reference air density, the power curve has been converted into a function of the wind power density. At each grid point, this power curve in terms of wind power density has been used to compute the power produced by this turbine each hour.

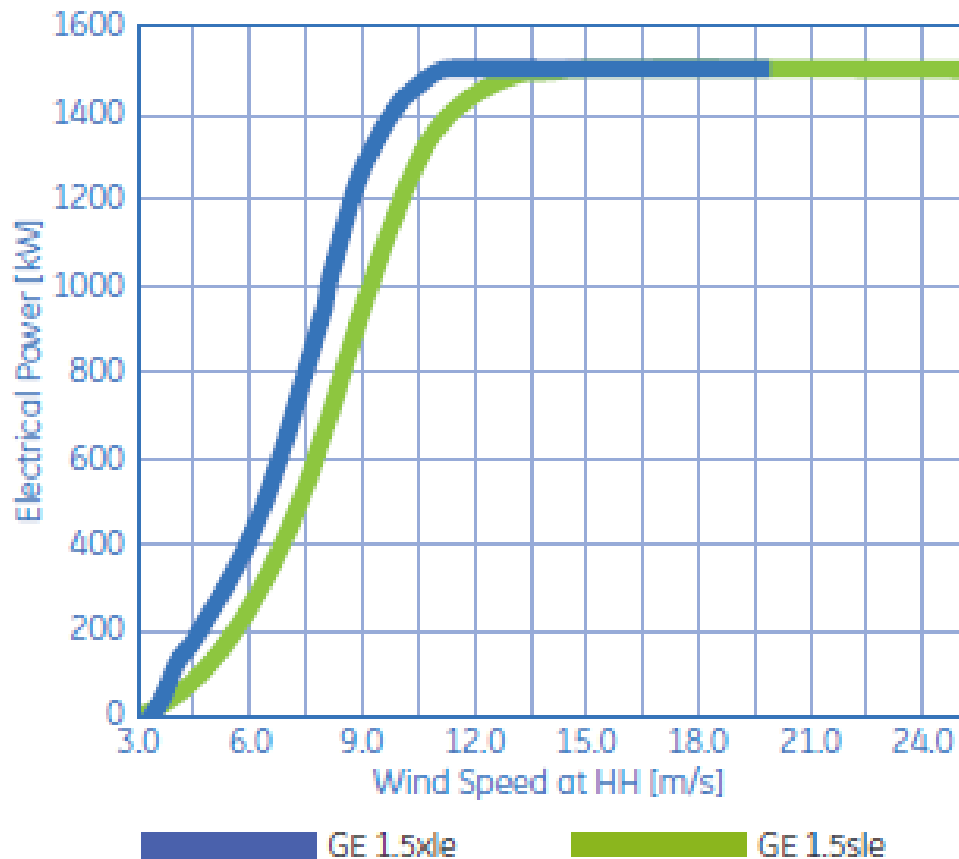


Figure 32. Power curve for GE 1.5 MW turbines.

5.3.2 Number of Turbines

Meneveau and Meyers (2010) reported, based on turbulence studies of the boundary layer and the wind turbines, that placing wind turbines 15 rotor diameters apart is most cost effective for power generation. For GE 1.5SLE, with a rotor diameter of 77 m, the separation needed is 1155 m and the land area needed for each wind turbine at this optimum configuration is 0.3335 km² or about three turbines per square kilometer. Considering other land uses and the constraints (i.e. legal, community-action, and/or environmental) for wind farm deployment, it is assumed that 10% of each grid cell area, on average, could be reasonably anticipated to be used to deploy wind farms. Each grid cell is $\sim 50 \text{ km} \times 66.7 \text{ km}$. Thus, the installed capacity in each grid cell is used to compute hourly capacity factors and also hourly power generation at each grid point.

5.4 Generation Duration Curves

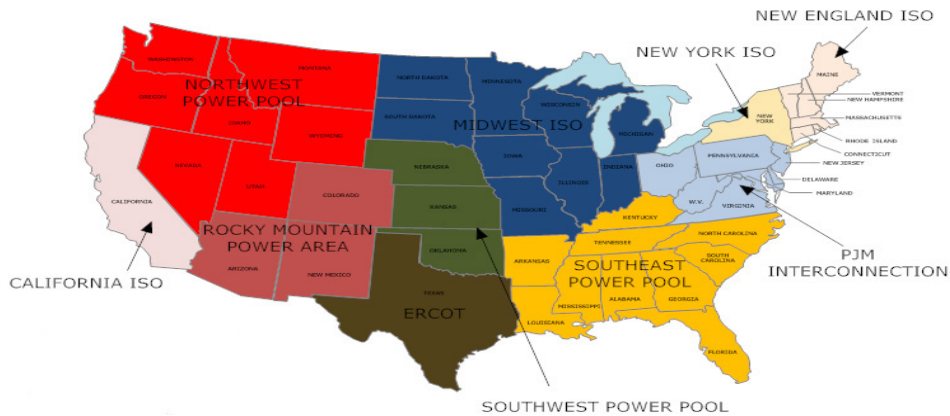


Figure 33. The map of the different ISOs in the U.S.

In a generation duration curve, the inverse cumulative probability distribution of the generated power is plotted as a function of the percentage of time in a year that the generation is greater than or equal to the ordinate generation. In the curves below, instead of absolute generation, the capacity factor is plotted against the percentage of time. **Figure 33** shows the different Independent System Operators (ISOs) considered for this part of the study. The grid points falling in each of these ISOs are aggregated and studied for their collective behavior. For each ISO, the generation as a fraction of the rated power (capacity factor) is plotted. The aggregated power of the whole ISO region is also plotted as the red curve.

Some observations that can be drawn from these duration curves are:

1. There is some period of time in each ISO for which no power is produced.
2. The regions that have less resource (California, New England, New York and PJM) have longer durations of no power whereas the regions in the central U.S. that have higher resource (MISO, ERCOT and SWPP) have no power for shorter durations.

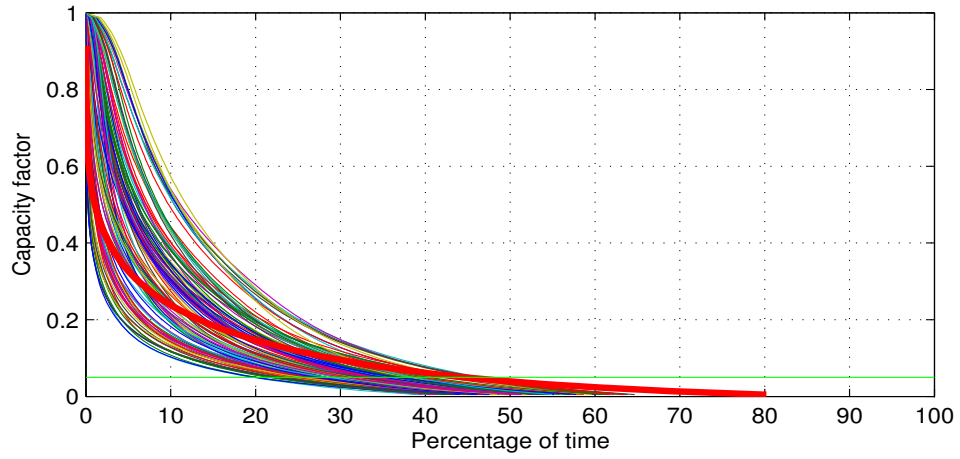


Figure 34. Duration curve for California ISO.

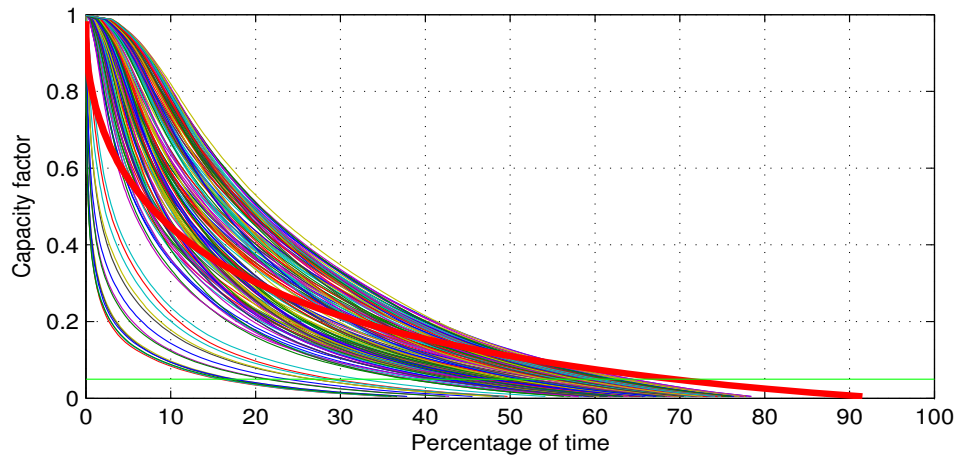


Figure 35. Duration curve for ERCOT.

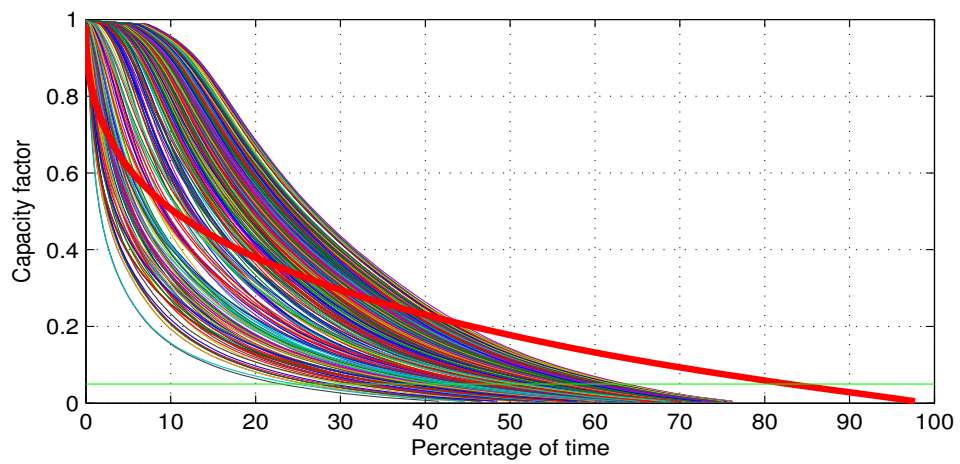


Figure 36. Duration curve for MISO.

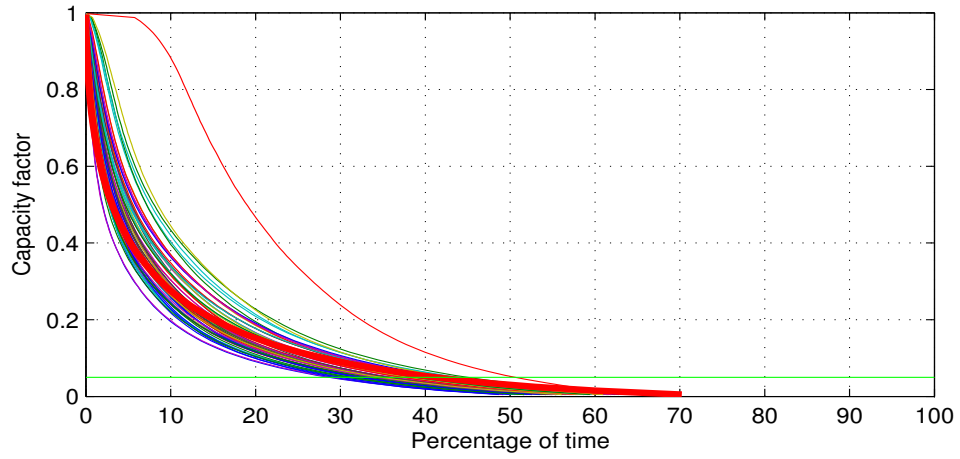


Figure 37. Duration curve for NEISO.

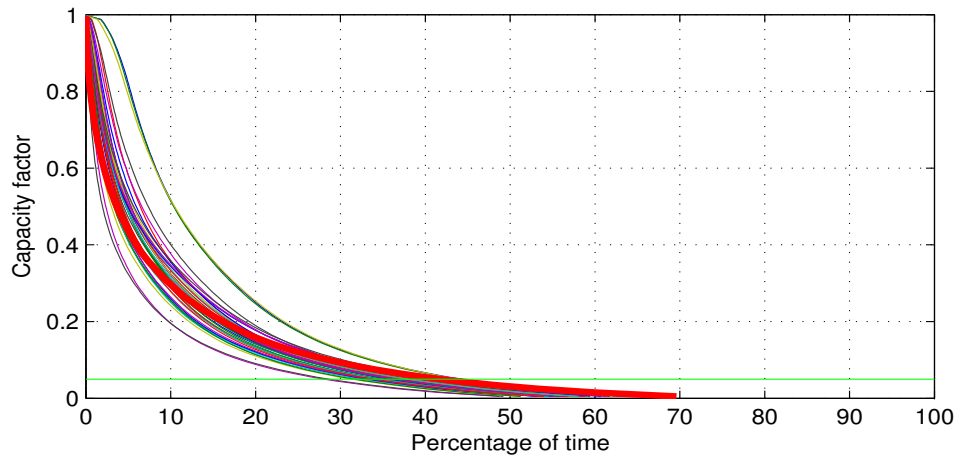


Figure 38. Duration curve for NYISO.

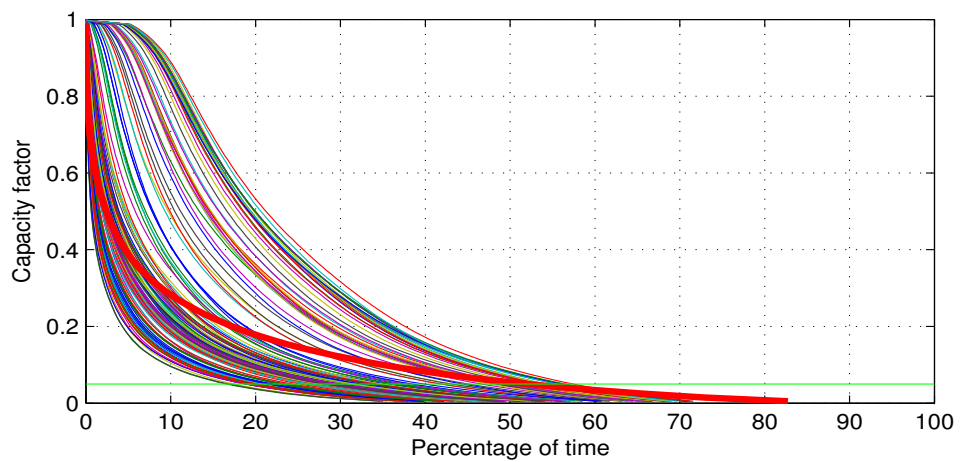


Figure 39. Duration curve for PJM.

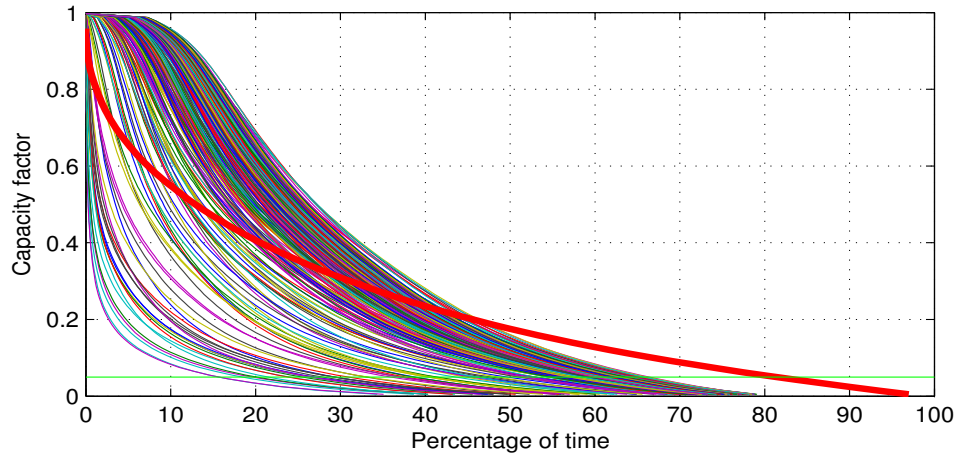


Figure 40. Duration curve for SWPP.

3. The green line in all of the duration curve plots corresponds to a capacity factor of 0.05 (5%). It is generally seen that as a result of aggregation of wind turbines in each ISO, the duration for which the capacity factor is above 5% is improved. But the improvement is very noticeable in the case of MISO and SWPP. As a result of aggregation, the duration for which the capacity factor is above 5% and also the duration for which there is at least 'some' usable power is enhanced compared to the durations for the individual grid points.
4. In a study of the advantages of aggregating wind farms in northeast Texas, Oklahoma and New Mexico (corresponding to the SWPP region), Archer and Jacobson (2007) report that an aggregation of 19 sites was seen to produce 21% of the rated power 79% of the time. From **Figure 40**, the aggregation of all the grid points produces 21% of the rated power only 45% of the time. One important reason for this difference is that Archer and Jacobson considered wind speed data for only the year 2000 and extrapolated it to 50 m whereas the present study considers a long record of 31 years. Incidentally, year 2000 was a La-Nina year and the wind speeds were larger than normal. Also, as seen in Figure 30, the number of grid points that had usable power density was greater.
5. In some of the ISOs (ERCOT, MISO, PJM and SWPP), there are some grid points which have a sharply falling duration curve. So, if these grid points are omitted, it is possible to enhance the performance of aggregation.
6. **Table 1** shows some of the critical statistics of the 31 years of data for the seven ISO regions. Because of the low wind resource, CalISO, NEISO, NYISO and PJM have very high number of hours for which the hourly capacity factors of these regions are less than 5% and 10% of their rated capacity. Since MISO and SWPP have very high wind power densities, they have lower number of critical hours ($\sim 15\%$ of the time of a year) and

level crossing rates for 5% and 10% of the rated capacity.

Table 1. Statistics of intermittency in different RTOs in the U.S.

ISO	Critical hours (%)		Level crossing rate		CoV of AP ¹	Median ACF ²
	< 5%	< 10%	5% level	10% level		
CalISO	53	70	298	263	1.26	0.04
ERCOT	28	45	239	262	1.02	0.12
MISO	15	30	150	212	0.82	0.18
NEISO	56	71	198	161	1.51	0.03
NYISO	56	70	198	160	1.52	0.04
PJM	45	63	213	189	1.22	0.06
SWPP	17	31	180	238	0.85	0.18

¹ AP: Aggregated power

² ACF: Aggregated capacity factor

5.5 Power Time Series

Figures 41 to 47 show illustrative time series of generated power from the wind turbines in the different ISOs. The abscissa is a sample interval of 100 hours, which is the same for all ISOs. Thus, all the curves are snapshots of generation for the same 100 hours. The thin lines show the power time series for the individual grid points whereas the thick red line shows that for the aggregate (normalized mean) of all the grid points in the ISO.

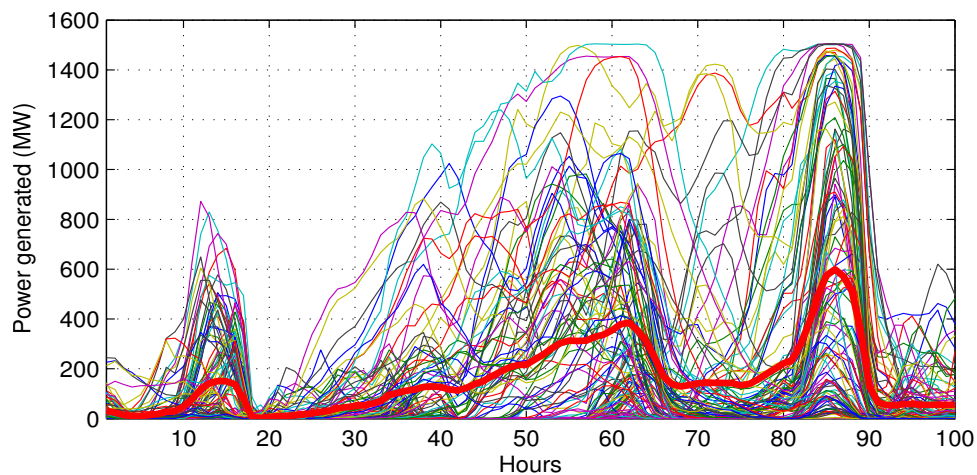


Figure 41. Time series of power in California ISO.

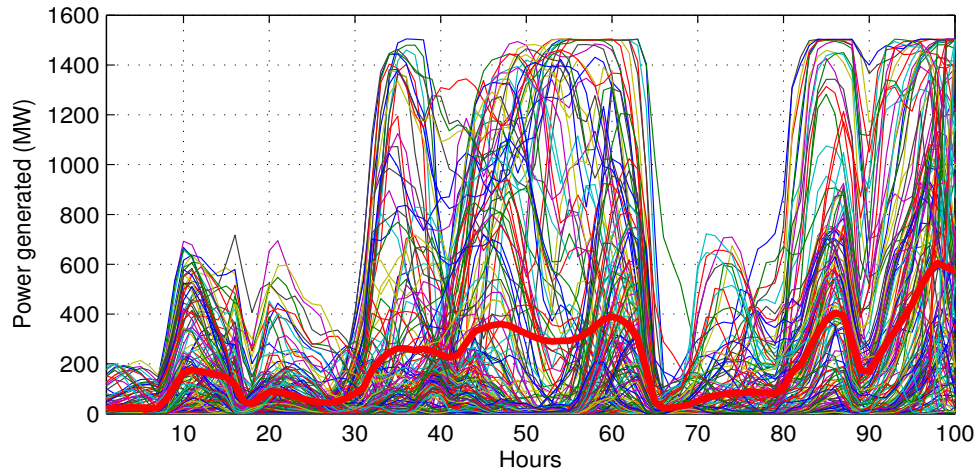


Figure 42. Time series of power in ERCOT.

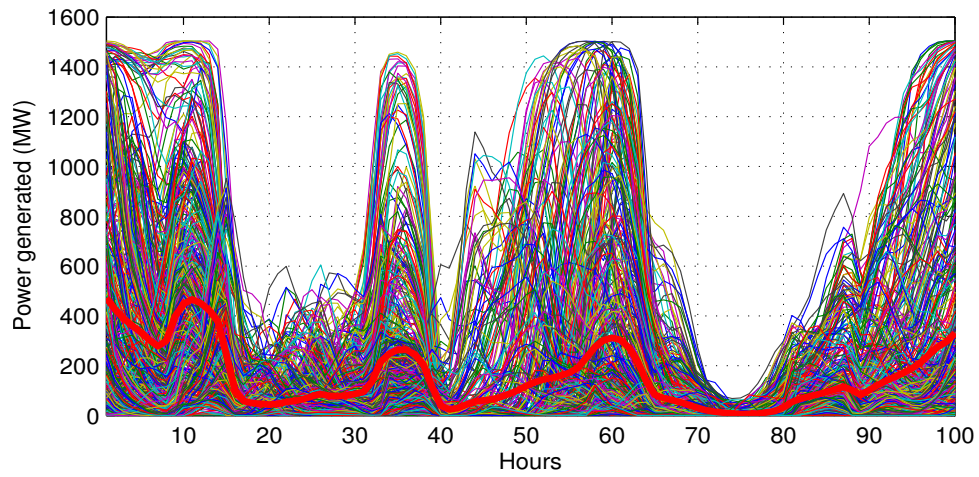


Figure 43. Time series of power in MISO.

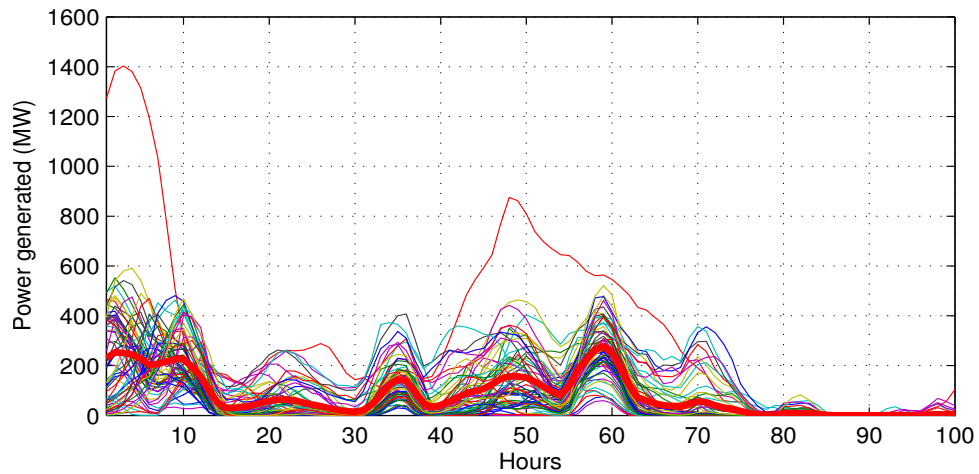


Figure 44. Time series of power in New England ISO.

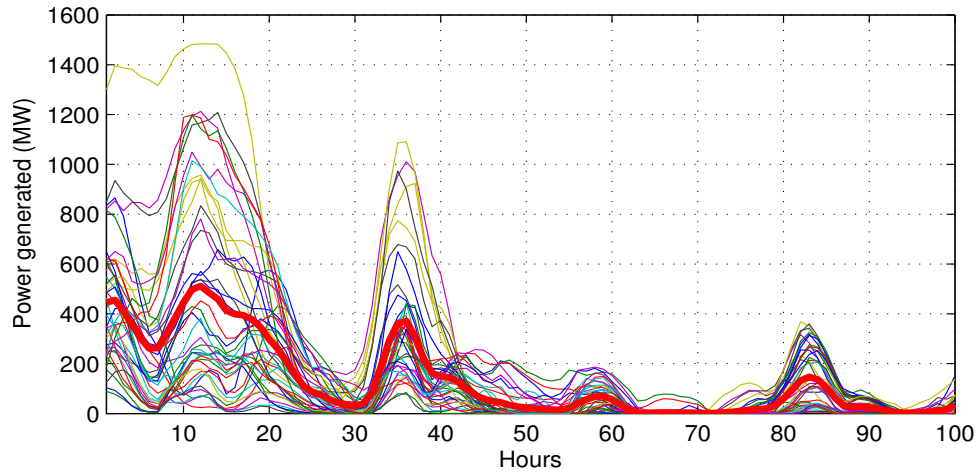


Figure 45. Time series of power in NY ISO.

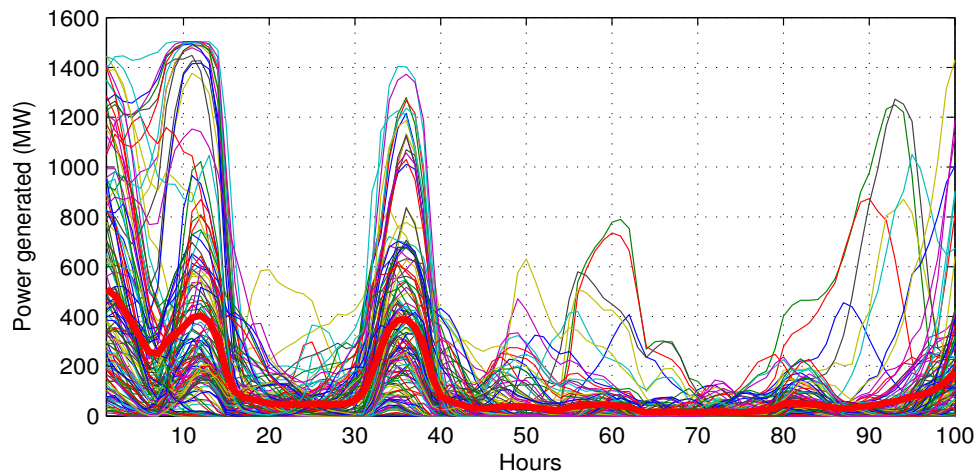


Figure 46. Time series of power in PJM ISO.

The following inferences can be drawn from these illustrative series plots.

1. As a result of the aggregation of wind turbines, during periods when there is no power at some grid points, there are grid points which have high wind power and hence there is compensation.
2. During the 100 hours considered, the high wind events at the different grid points are largely coincident.
3. There are instances when there is very little or practically no wind power. Most importantly, there are instances when there is no wind in the whole ISO.

Previous researchers have suggested that aggregation would level the wind power on the whole and as a result, reduce the instances when there is no power. These results and the lack of anti-coincidence discussed in an earlier section indicate that this is not a very

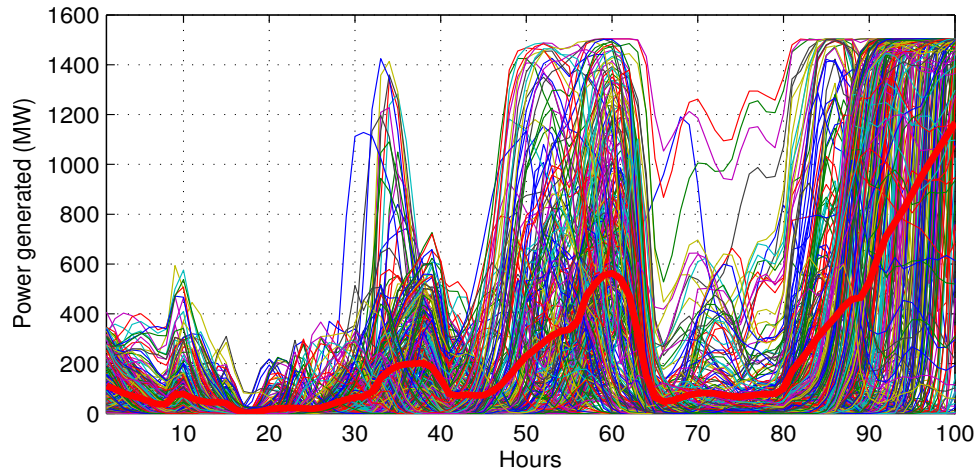


Figure 47. Time series of power in SWPP ISO.

robust strategy. With an effective aggregation (if the power at different grid points are anti-coincident), the aggregate power curve (thick red line) would be steady. However, large swings in the aggregate power generation are seen for all ISOs, and more importantly, the aggregate curve still falls to near zero for a number of instances. What is encouraging, however, is the aggregate curve exhibits substantially damped oscillations.

4. As noted by Sorensen *et al.* (2007), with higher penetration of wind power, aggregation of turbines makes the ramp rates very large. It may be noted that the aggregate curve in these time series plots is a mean of the power time series at the individual grid points. If that curve is multiplied by the number of grid points in the ISO region, the ramp rates may be sharp.
5. The power time series in California ISO indicate that the grid points in the west coast have a tendency to randomly change their power profile. This region, as shown by the anti-coincidence results above and also by Kahn (1979), is very amenable for aggregation to make the aggregate power steady, at least, to some extent.
6. A common question considered in wind integration is - 'will wind stop blowing everywhere at the same time?'. Between hours 60 and 80, in all these plots, (which correspond to 2000 Hrs on 11th Jan, 1979 and 1600 Hrs on 12th Jan, 1979), there is almost no wind in New England, New York, PJM, MISO, and very little wind blew in ERCOT and SWPP. **Figure 48** shows the average sea level pressure during those hours. This figure shows that there was a huge high pressure system over New England and New York and it extended westward and southward such that many ISOs did not have wind simultaneously. During these hours, California ISO has some variability across the grid points in wind. But, considering the fact that the wind resource in California is low compared to MISO, ERCOT and SWPP, the wind power from California is unlikely to

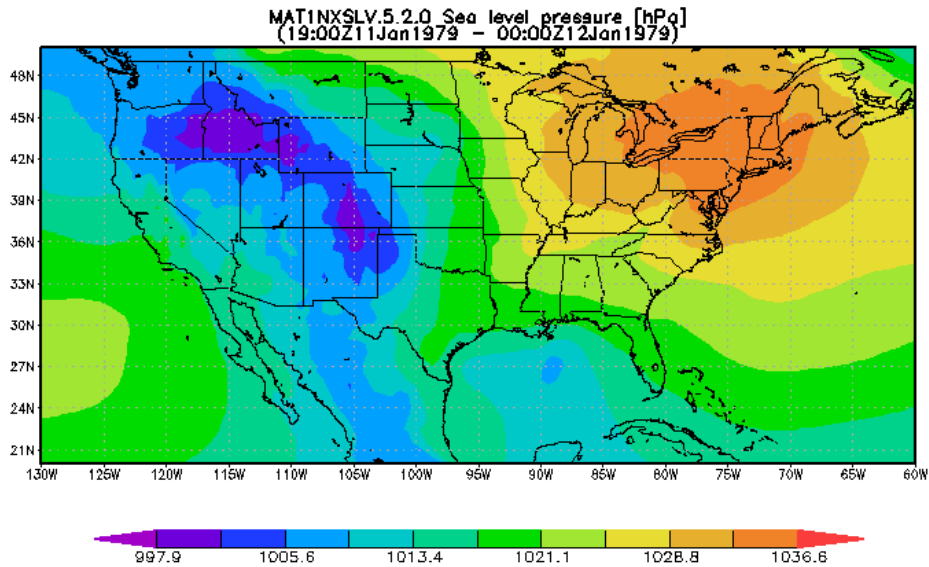


Figure 48. A high pressure system over a wide area in the U.S.

make up for the lull in the other ISOs.

We reiterate that one of the key assumptions of this study is the rather ubiquitous penetration of wind power across the U.S. (i.e. 10% of every grid cell contains wind farms). Thus, our results should be considered accordingly. Currently in the U.S., Texas has the largest aggregate wind power installation. **Figure 49** shows the installed wind capacity in each state in 2008. When the wind fraction of the installed capacity is small, the variability in wind generation is very small. Thus the ISOs consider it as a small variation in the load and try to match the net load (load - wind generation) with power generated from the other conventional generation. As wind penetration increases, this notion is no longer true. An illustrative instance is the emergency in ERCOT region of Texas on 26th February, 2008 when ~ 1800 MW of wind power was lost in three hours, and demand rose by ~ 1000 MW. **Figure 50** shows the averaged sea level pressure from 1200 Hrs on 26th February, 2008 to 0800 Hrs on 27th February, 2008.

As discussed earlier, because these high pressure systems, as shown in Figures 48 and 50, extend to very large areas, meteorologically these large regions are characterized by high correlation.

Thus, although the central U.S. region has very high wind resource, most of the grid points in this region are meteorologically homogeneous and are characterized by high correlation. The anti-coincidence experiments show that although steadiness of aggregated power occurs sometimes, more than 50% of the time, the grid points in the central U.S. are highly synchronized in their intermittent behavior.

Considering the statistical behavior of n number of grid points with equal mean power and equal fluctuation (Appendix on page 62), the ratio of coefficient of variation of power with and without

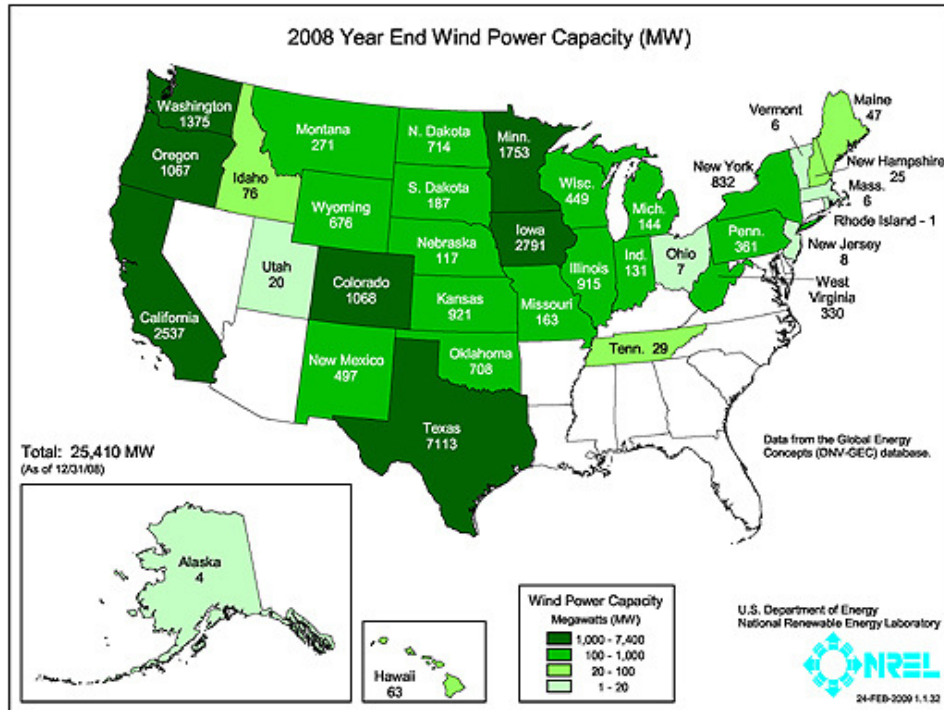


Figure 49. Installed wind capacity in the U.S. in December 2008.

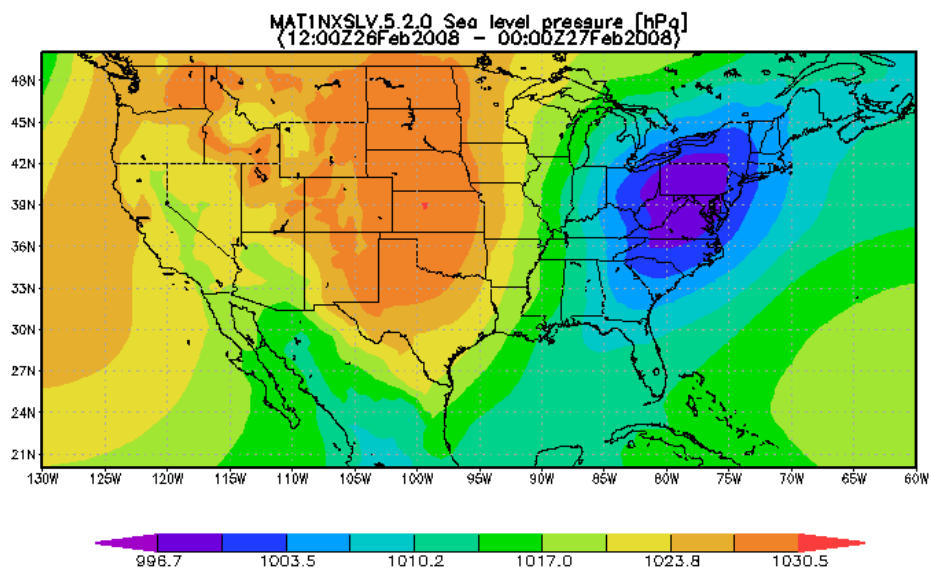


Figure 50. Sea level pressure on 26th Feb, 2008 showing the high pressure system spanning a wide area.

aggregation can be studied as a function of the number of grid points aggregated. An important parameter in this experiment is the mean correlation among the aggregated grid points. **Figure A1** shows the factor by which the CoV is reduced on the ordinate as a function of the number of grid points on the abscissa. The different curves correspond to different mean correlations as shown in the legend. This plot shows that with no mean correlation, the CoV is drastically reduced but with a non-zero mean correlation. The decay rate of reduction of CoV is dramatically reduced.

Another important inference from this plot is that the benefit of aggregation saturates beyond 10 grid points. It may be noted that Archer and Jacobson (2007) reported that the benefit of aggregation does not saturate with the number of points. But the asymptotic nature of the reduction factor results in a saturation. The fact that the benefit of aggregation saturates does not depend on the nature of the turbine or the wind resource at the individual locations.

The mean and standard deviation of power generated with and without aggregation presented in Archer and Jacobson (2007) have been used to compute the mean correlation coefficient in the aggregation considered in ERCOT in that work. The use of the analysis of the collective behavior of the wind power sites (Appendix-1) results in a mean correlation coefficient of 0.48. Thus, within the bounds of experimental error, the anti-coincidence plot 20 in which the number of points around every point that are anti-coincident at least 50% of the time are counted is vindicated.

Figures 51 to 57 show the annual distribution of frequency of wind power generation capacity factors. The red line shows the median capacity factor in each year. The red pluses represent the outliers (greater than 1.5 times the inter-quartile range). The following inferences can be drawn from these plots:

1. The median capacity factors are very low.
2. The lower capacity factors are more common and the higher capacity factors are outliers. That means that the distributions of capacity factors are longtailed.
3. It is also interesting that California, New England, New York and PJM have very long tails whereas MISO, ERCOT and SWPP have short tails. This implies that very high wind power occurs in the former ISOs rarely whereas in MISO, SWPP and ERCOT, very high wind power generation events occurs often.
4. The inter-annual variability in the median capacity factor is low in the ISOs with lower wind resource whereas MISO, ERCOT and SWPP medians have larger variation.
5. California, PJM, New England and New York ISOs have their 25th percentile very close to zero.

6. CONCLUSIONS

6.1 Limitations and Key Assumptions

Before summarizing the results and inferences of our study, we note the key assumptions and limitations of the study.

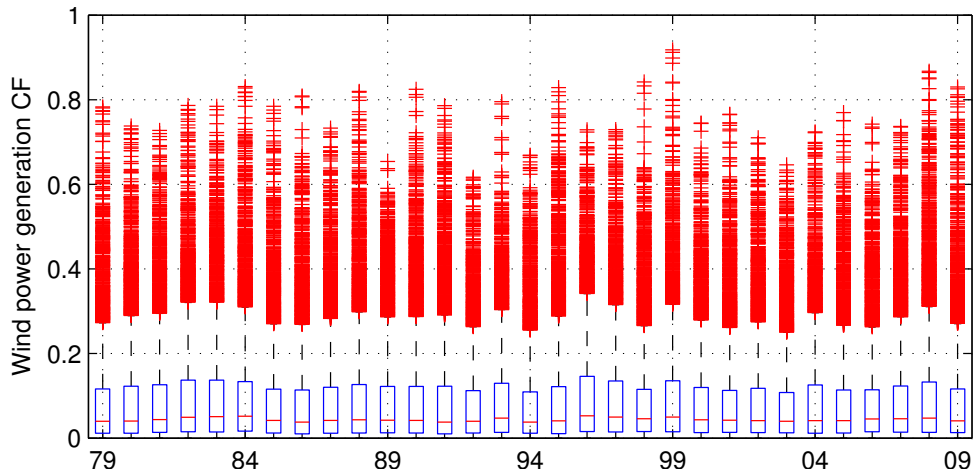


Figure 51. Annual distribution of wind generation capacity factor in California ISO.

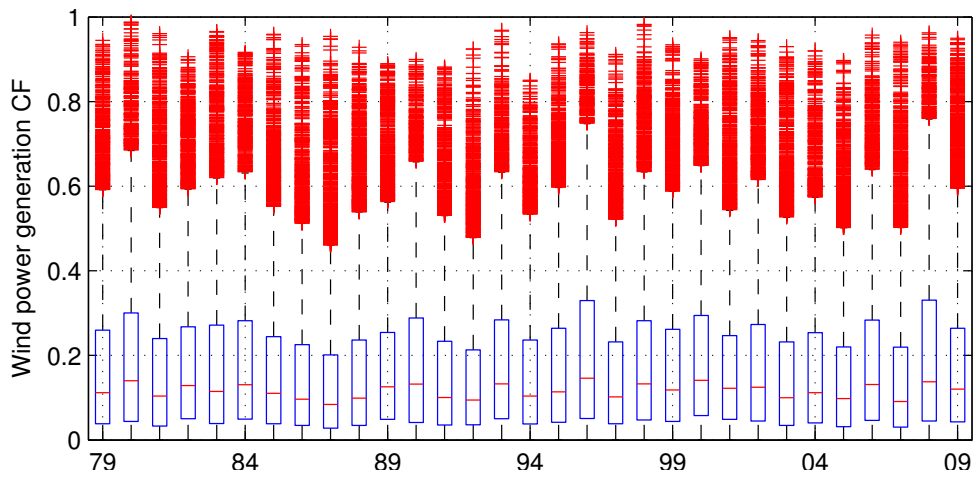


Figure 52. Annual distribution of wind generation capacity factor in ERCOT ISO.

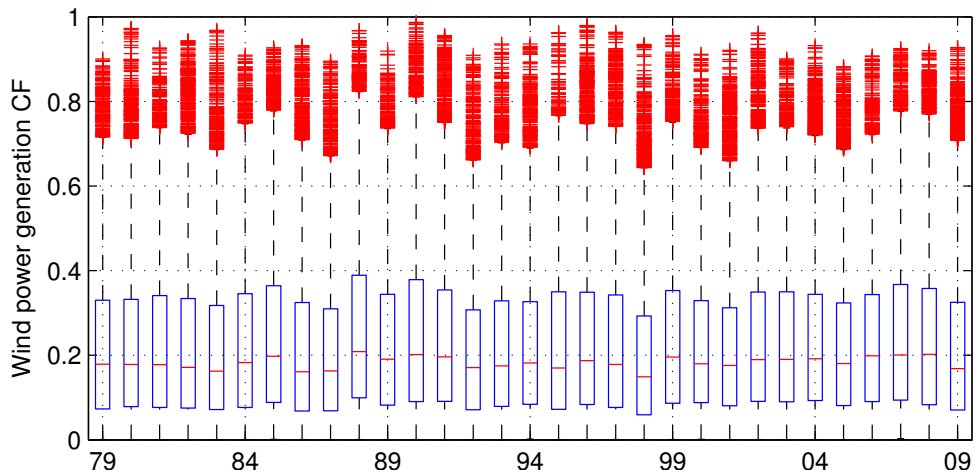


Figure 53. Annual distribution of wind generation capacity factor in MISO.

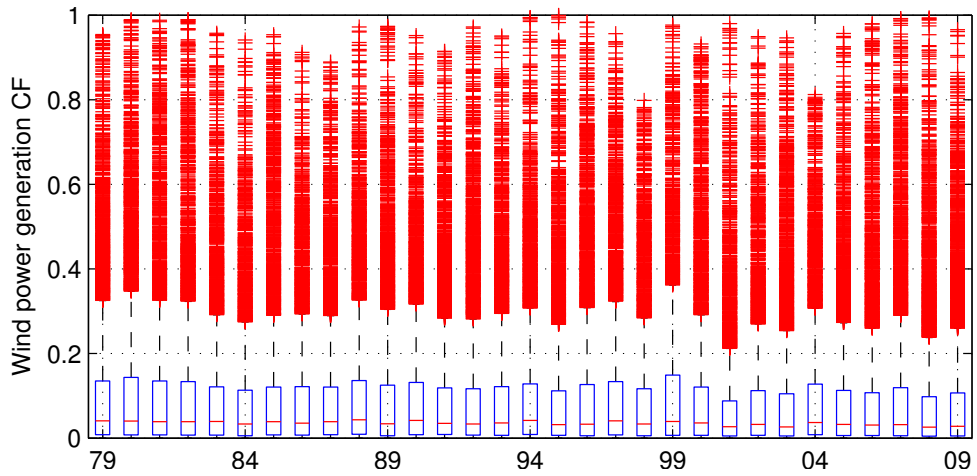


Figure 54. Annual distribution of wind generation capacity factor in NE ISO.

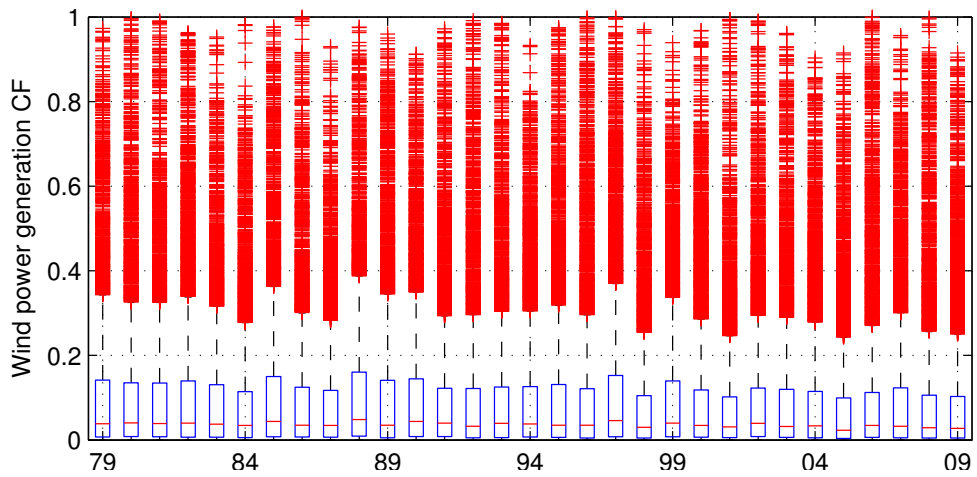


Figure 55. Annual distribution of wind generation capacity factor in NY ISO.

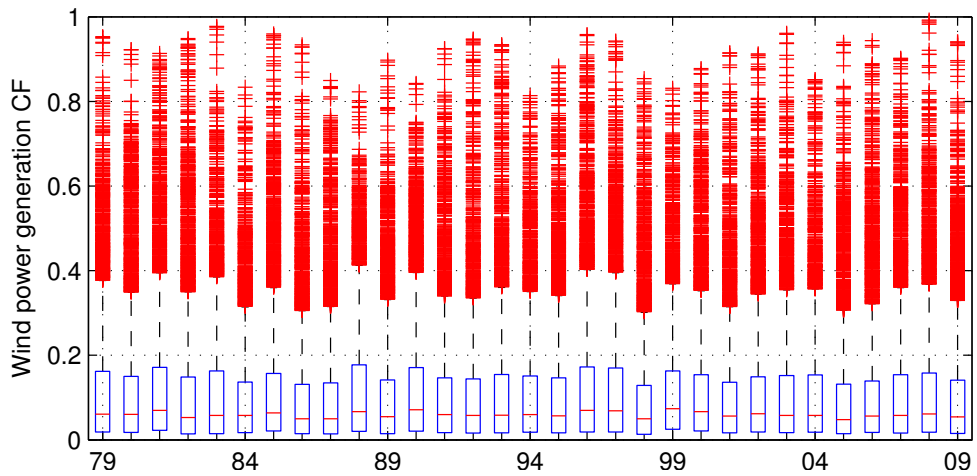


Figure 56. Annual distribution of wind generation capacity factor in PJM ISO.

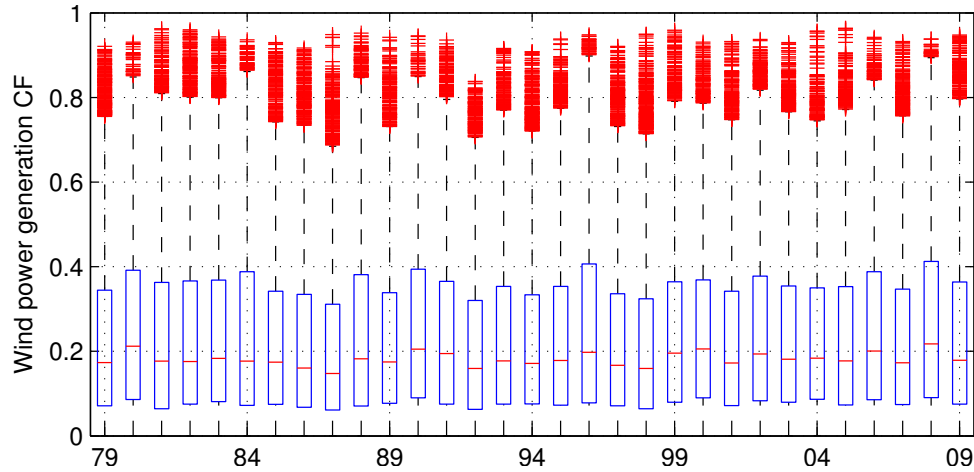


Figure 57. Annual distribution of wind generation capacity factor in SWPP ISO.

1. The data used for construction of the wind resource is a result of the assimilation of measurement and satellite remote sensed data into a global model. Thus the imperfections of the model and the assimilation schemes are bound to influence the computed output.
2. The spatial resolution of the data is $0.5^{\circ} \times 0.67^{\circ}$ and the temporal resolution is one hour. So, some local effects that change wind speeds like mountain passes and valleys are not represented in this study. Further, since the time resolution is an hour, intermittency and other phenomena of higher scale and their effects can only be studied.
3. It is assumed that all the wind resource that is available is harnessed.
4. While studying the variation of wind resource the demand or load and the economic feasibility are not taken into consideration.
5. Magnitudes of some of the results are dependent on the minimum wind power density threshold (200 W/m^2). But qualitatively, the results are very robust as a lower threshold (140 W/m^2) produced the same qualitative results.

6.2 Wind Power Density at the surface

We have undertaken an assessment of the wind power resource for the U.S. Wind power density time series at each grid point in the domain between 20° and 50°N , and 130° and 60°W has been constructed using the MERRA atmospheric reanalysis which has a spatial resolution of $0.5^{\circ} \times 0.67^{\circ}$ and hourly time resolution for the period 1979-2009. The effective wind speed at the center of the lowest model layer from the reanalysis has been used for this purpose. This dataset has been used to study and characterize the quality of onshore wind resource across the U.S. and our analysis has also considered offshore regions. The constructed mean wind power density map shows the established qualitative abundance of wind resource across the U.S. The median wind power

densities are approximately half of the mean values. Thus, for substantially more than 50% of the time, the wind power density at a place is less than half of the mean wind power density.

Conventionally, wind resource has been summarized in terms of the mean wind speed or the mean wind power density at a location. Since the mean wind speed does not include the effects of variations in density, the mean wind speed does not comprehensively represent the wind resource at a location. Also, the wind atlases produced by the energy agencies of many countries represent the wind resource in terms of the mean wind power density. Although wind power density is a good variable to encompass the effects of wind speed and air density simultaneously, our results indicated that the mean as a central tendency overestimates the resource as can be seen from the frequency distribution of wind power density which is a positively skewed and long tailed distribution. Thus, to more accurately represent this distribution, median should be used. The variability of the wind resource as measured by the coefficient of variation shows that, usually, the regions with higher wind resource have higher variability. But among those regions, the Atlantic offshore region has greater variability than the central U.S. region. Unavailability of wind resource, as a measure of the reliability of the system, has been mapped as the number of hours with no usable wind power density at a location. The map shows that the central U.S. has the lowest unavailability and the offshore regions have unavailability of 40% or lower.

Maps of statistics of the wind and no-wind episode lengths have been developed for the U.S. region. They help in understanding the persistence characteristics of wind power density and the lumped nature of intermittency. The maps of median and mean episode lengths show that for the central and non-central U.S., the distributions of wind episode lengths have distributions that are differently skewed. The wind episodes in the central U.S. are symmetrically distributed where as in the southeastern states, the wind power is very steady for some periods. Such knowledge of steadiness of wind power density is very helpful in planning the development of wind power harnessing.

6.3 Altitude Dependence of Wind Power Density

The boundary layer flux parameters friction velocity, surface aerodynamic roughness length and displacement height - and the similarity theory of boundary layer dynamics have been used to estimate the wind speed at different wind turbine hub heights - 50 m, 80 m, 100 m and 120 m - and the variation of the wind resource and its characteristics have been studied with respect to altitude. Since time varying parameters have been used in our estimation, they are likely to be more robust than those in the studies that used a logarithmic law or a power law with empirically determined exponents. Comparison of the wind power density at 50 m constructed in this study and that developed by NREL shows that the regions of appreciable wind source are similar in both the estimates. But there are some quantitative differences. Taking into account the uncertainty rating of the estimates in different regions in the NREL atlas, our estimates fall well within the bounds of the uncertainty estimates of the NREL atlas.

For the wind resource at 80 m, comparison of mean wind speed at 80 m estimated in this study and that estimated by NREL shows that both the estimates are very close qualitatively and also

quantitatively. There are a few patches of regions in the central U.S. where NREL estimates show wind speeds greater than 8.5 m s^{-1} which this estimate misses because of slightly lower resolution than the NREL study. To complete the picture, mean wind power density at 80 m has been examined (although a direct comparison with the NREL study was not possible). The central U.S. and offshore regions (especially off the coast of New England and central California) show the greatest potential. An interesting fact that this plot shows is that even though the mountainous regions on the west coast have high wind speeds, these regions have low wind power density because of the lower air density. This also shows that mean wind speed can not be a reliable measure of wind resource.

As the altitude is increased from 50 m to 80 m, there is a general increase in the wind resource while the increase is greater in the central U.S. region and in New England along the Appalachian region. The variation in wind resource with altitude is dependent on the wind resource at the lower height and the surface roughness length of the boundary layer. The wind resource increased rapidly in the central U.S. because of the higher wind speeds at lower altitudes and it increased in the New England due to the large roughness length. Another reason for the large increase in wind power density with altitude in the central U.S. is the presence of a strong nocturnal low level jet that has a maximum between 500 m and 800 m.

As the hub height is increased from 80 m to 100 m and 120 m, the mean wind power density increases fast initially and then the increase subsides. Although the change decreases, there does not seem to be a saturation even with reasonable increases beyond 120 m. The median wind power density also shows a similar change profile.

As the mean wind power density increases with altitude, it implies that the frequency distribution of the wind power density shifts to the right. Also, the frequency distribution is broadened. Thus, the wind resource and the variability of the resource increase with a rise in hub height from 80 m to 120 m. The increase in wind power density corresponds to almost more than one wind-power class.

The CoV of WPD with altitude shows different variation in different regions. Interestingly, while the CoV decreases over the land, it increases slightly over the oceans. It implies that the variance increases faster than the mean in the offshore regions. Further, the CoV decreases with altitude in the northeastern states. Interestingly, the largest increase in persistence of wind power density with altitude is in these northeastern states. The central U.S. and offshore regions have similar mean and median episode lengths whereas the non-central continental U.S. regions have longer mean episode lengths and shorter median episode lengths leading to the inference that the episode length distributions in the non-central U.S. are very skewed and are dominated by a few long episode lengths. With altitude, the mean episode length decreases less in the resource-rich regions but more so in the low-resource regions (e.g. northeast). Conversely, the median increases almost everywhere by about an hour or less. This leads to the important inference that as the turbine hub height is increased, a few very long episodes are replaced by a greater number of shorter episodes and hence more intermittent wind resource.

6.4 Intermittency

The most important part of this study is the characterization of intermittency of wind resource in the U.S. Unlike in previous studies, the fluctuations in wind power have been distinguished into two classes - fluctuating usable power density termed variability and lulls when the turbine does not produce usable power, which in this study is distinguished as intermittency. While acknowledging that intermittency of wind is a substantial impediment in increasing the penetration of wind power, many researchers suggested geographical diversification of wind generation as the most effective solution to mitigate the effect of intermittency in wind power. Central to this strategy is the assumption that the wind power density time series at different locations are less correlated or, according to some studies, even negatively correlated. Most of the studies showed that in the shorter timescales, the power time series or the power density time series were less correlated. Some studies with wind power time series in Germany, UK and Ireland found that the anti-correlation broke down in longer timescales - hours, days and longer timescales. It is interesting that all the studies that found the wind power time series anti-correlated or otherwise used shorter records of data - usually a year. Thus, to test this important assumption, the time series of wind power density constructed in this study has been used. To obviate the situation when the wind power density time series at two sites are below a minimum WPD and anti-correlated in the statistical sense, the wind and no-wind states as time series have been constructed with a cut-in WPD of 200 W/m^2 . The hourly wind states of two sites have been compared for their anti-coincidence.

Two metrics have been conceived to study the mutual anti-coincidence of intermittency states. A box of approximately $\sim 1000 \text{ km} \times 1000 \text{ km}$ has been constructed around every grid point in the U.S. domain, the points fulfilling a chosen anti-coincidence criterion with the center of the box are counted and the count is designated as the score of the center grid point. The first criterion chosen was if the number of X-OR logical states with the center of the box are at least 50% of the length of the record. The second criterion was if the number of hours for which a point has UWPD when the center does not, for at least 50% of the number of hours for which the center does not have UWPD. The most important conclusion from these experiments is that the west coast region of the U.S. has sufficient spatial inhomogeneity of wind resource intermittency, while the east coast has to a marginal extent. However, in the central U.S. which is very rich in wind resource, the number of points with UWPD around a point that has no UWPD is almost zero. It is interesting to note that with relaxed criterion, the geographical inhomogeneity of intermittency states increases on the east coast, west coast and the offshore regions, but the central U.S. shows no spatial inhomogeneity. A very important corollary of this inference is that the intermittency in the central U.S. is highly synchronized. As a result, vast areas in the central U.S. have UWPD at the same time or do not have UWPD. This coherence has important implications of power system stability and also to reliability of resource availability.

It is significant that with a lower value of UWPD, the collective behavior is very similar in the central U.S. This leads to the important and robust inference that the intermittency in the central U.S. is very highly synchronized. The collective behavior of the grid points with UWPD in the highly correlated central U.S. shows that the windy fraction of the grid points is less in the warmer

months than in the cooler/colder months, has large and frequent fluctuations in the colder months and is less than 0.5 for most of the time. When only the grid points that have appreciable wind resource (availability greater than 25%) have been considered, the synchronization of intermittency is exhibited to a greater extent. Assuming the ability to harness the wind power in the continental U.S. and 100 Km into the continental shelf, the fluctuation of the number of grid points with wind resource in the whole amenable area shows behavior that is very similar to the one of the central U.S., possibly because of the dominance of the central U.S. wind resource. For many hours in a year, the fraction of grid points that have UWPD is less than 10%. It is significant that the aggregated capacity factor in the EWITS shows similar behavior. Thus as the penetration of wind power increases, the large fluctuations in the longer time scales will have significant impact on the reliability of power resource.

The analyses also addressed the behavior of the hourly aggregated power in the seven regional transmission organization areas. A number of GE 1.5SLE turbines per unit area based on a condition for optimizing the extraction of wind power have been assumed at each grid point. Assuming that 10% of the area is used for wind farms, the hourly capacity factors and power generation at each grid point is estimated. The generation duration curves have been computed from the hourly capacity factor time series for the seven ISOs. They show that generally, there is no power for some fraction of time in each ISO. Also, as commonly agreed, aggregation of wind power in each ISO region mitigated intermittency to some extent and, as a result, the fraction of time for which the power is less than 5% has been reduced in each ISO. By removing the points for which the duration curves fall rapidly, the efficiency of aggregation can be improved. The results show that in spite of the improvement due to aggregation, each region has considerable fraction of time for which the capacity factor is less than 5%.

The time series of hourly wind power show instances of compensation because of aggregation. The high and low wind events are lumped in time in each ISO region. The time series of aggregated power are themselves intermittent. A random 100 hour plot of the time series for all seven ISOs shows that there are instances when there is no wind power in any ISO, which is corroborated by a meteorological chart of surface pressure which shows a high pressure system that supported low wind fields. Since the wind resource at each grid point is considered in this study, the conclusions in this study are expected to manifest with increasing penetration of wind power installations.

An analytical consideration of the behavior of coefficient of variation of aggregate power from several wind generation units shows that the benefit of aggregation saturates beyond ten units. Also, the benefit of aggregation falls rapidly with the correlation between the generating units.

The annual distributions of frequency of hourly capacity factors in the seven ISOs show that the median capacity factors are very low. The distributions of low-resource regions have very long tails whereas the regions in the central U.S., high wind events are more common.

6.5 Future Research

Since the ability of the U.S. and many other nations that are trying to harness wind power in large scale is critically dependent on the strategy to achieve near persistent wind resource and to

mitigate the impacts of intermittency, it is important that substantial research needs to be undertaken to understand the character of the variable nature of wind resource. The ability of the present study to utilize a long data record to understand the general structure of wind resource and its variability can be used to further address many issues in this area. Some that emanate immediately are given below.

1. Use of the different metrics suggested to reclassify the wind resource.
2. Taking into view the large differences in wind power resource over scales larger than a year, the interannual variability of wind resource need to be studied. This would also provide coarse predictive ability to foresee wind floods and wind droughts.
3. The variability of the wind power fluctuations due to the impact of different interannual atmospheric phenomena like El-Nino, La-Nina and North Atlantic Oscillation has discernible effect on the stability and behavior of power systems and also on the availability of wind resource. As inferred in the present study, the mean area with wind resource over the continental U.S. has a strong correlation with El-Nino. So, it is important to investigate the mechanisms by which the resource and variability are impacted in annual scale.
4. In view of the changing climate and the range of national and global policies to mitigate climate change, the patterns of the wind resource and its variability need to be assessed for ensuring the reliability of wind power systems.

Acknowledgements

The authors gratefully acknowledge support of the MIT Joint Program on the Science and Policy of Global Change by government, industry and foundation funding, MIT Energy Initiative and industrial sponsors. Comments from José Ignacio Perez Arriaga and Carlos Batlle, which prompted us to conduct further experiments to make the results in this study more robust, were very helpful.

7. REFERENCES

- Ackermann, T., 2005: *Wind Power in Power Systems*. John Wiley and Sons. ISBN 9780470855089.
- Apt, J., 2007: The Spectrum of Power from Wind Turbines. *Journal of Power Sources*, **169**(2): 369–374.
- Archer, C. L. and M. Z. Jacobson, 2003: Spatial and Temporal Distributions of US Winds and Wind Power at 80 M Derived from Measurements. *Journal of Geophysical Research*, **108**(D9): 42–89.
- Archer, C. L. and M. Z. Jacobson, 2007: Supplying Baseload Power and Reducing Transmission Requirements by Interconnecting Wind Farms. *Journal of Applied Meteorology and Climatology*, **46**(11): 1701–1717.
- Atkinson, N., K. Harman, M. Lynn, A. Schwarz and A. Tindal, 2006: Long-term Wind Speed Trends in Northwestern Europe. Garrad Hassan *Technical Report*.

- AWEA, 2005: The Economics of Wind Energy. Technical Report. American Wind Energy Association. Feb, 5 p. (<http://www.fishermensenergy.com/dms/showfile.php?id=44>).
- Boccard, N., 2009: Capacity Factor of Wind Power Realized Values vs. Estimates. *Energy Policy*, **37**(7): 2679–2688.
- Brower, M., 2008: Development of Eastern Regional Wind Resource and Wind Plant Output Datasets. *U.S. Department of Energy, National Renewable Energy Laboratory: Golden, CO*.
- Chang, T. J., Y. T. Wu, H. Y. Hsu, C. R. Chu and C. M. Liao, 2003: Assessment of Wind Characteristics and Wind Turbine Characteristics in Taiwan. *Renewable Energy*, **28**(6): 851–871.
- Corbus, D., M. Milligan, E. Ela, M. Schuerger and B. Zavadil, 2009: Eastern Wind Integration and Transmission Study–Preliminary Findings. *Proc. 8th International Workshop on Large Scale Integration of Wind Power and on Transmission Networks for Offshore Wind Farms*.
- Corbus, D., J. King, T. Mousseau, R. Zavadil, B. Heath, L. Hecker, J. Lawhorn, D. Osborn, J. Smith, R. Hunt and G. Moland, 2010: Eastern Wind Integration and Transmission Study. Prepared for NREL by EnerNex Corporation, Knoxville, Tennessee *Technical Report*, Jan (Revised Feb 2011), 242 p. (http://www.nrel.gov/wind/systemsintegration/pdfs/2010/ewits_final_report.pdf).
- Cox, J., 2009: Impact of Intermittency: How Wind Variability Could Change the Shape of the British and Irish Electricity Markets. *Pöyry Energy (Oxford) Ltd., Oxford, UK, Summary Report*.
- Degeilh, Y. and C. Singh, 2011: A Quantitative Approach to Wind Farm Diversification and Reliability. *International Journal of Electrical Power & Energy Systems*, **33**(2): 303–314. doi:[10.1016/j.ijepes.2010.08.027](https://doi.org/10.1016/j.ijepes.2010.08.027).
- Dorvlo, A. S., 2002: Estimating Wind Speed Distribution. *Energy Conversion and Management*, **43**(17): 2311–2318.
- Elliott, D. L., C. G. Holladay, W. R. Barchet, H. P. Foote and W. F. Sandusky, 1987: Wind Energy Resource Atlas of the United States. *NASA STI/Recon Technical Report N*, **87**: 24819.
- Elliott, D. L., L. L. Wendell and G. L. Gower, 1991: An Assessment of the Available Windy Land Area and Wind Energy Potential in the Contiguous United States. Pacific Northwest Lab., Richland, WA (United States), August.
- Eskin, N., H. Artar and S. Tolun, 2008: Wind Energy Potential of Gökçeada Island in Turkey. *Renewable and Sustainable Energy Reviews*, **12**(3): 839–851.
- Estanqueiro, A., 2008: Impact of Wind Generation Fluctuations in the Design and Operation of Power Systems. *7th International Workshop on Large Scale Integration of Wind Power and on Transmission Networks for Offshore Wind Farms, Madrid*, pp. 26–27.
- Gustavson, M. R., 1979: Limits to Wind Power Utilization. *Science*, **204**(4388): 13.
- He, Y., A. H. Monahan, C. G. Jones, A. Dai, S. Biner, D. Caya and K. Winger, 2010: Probability Distributions of Land Surface Wind Speeds over North America. *Journal of Geophysical Research*, **115**(D4): D04103.

- Hennessey, J., 1977: Some Aspects of Wind Power Statistics. *Journal of Applied Meteorology*, **16**: 119–128.
- Holttinen, H., 2005b: Hourly Wind Power Variations in the Nordic Countries. *Wind Energy*, **8**(2): 173–195. doi:[10.1002/we.144](https://doi.org/10.1002/we.144).
- Holttinen, H., 2005a: Impact of Hourly Wind Power Variations on the System Operation in the Nordic Countries. *Wind Energy*, **8**(2): 197–218.
- Holttinen, H., M. Milligan, B. Kirby, T. Acker, V. Neimane and T. Molinski, 2008: Using Standard Deviation As a Measure of Increased Operational Reserve Requirement for Wind Power. *Wind Engineering*, **32**(4): 355–377.
- Jaramillo, O. A. and M. A. Borja, 2004: Wind Speed Analysis in La Ventosa, Mexico: A Bimodal Probability Distribution Case. *Renewable Energy*, **29**(10): 1613–1630.
- Justus, C., W. Hargraves and A. Yalcin, 1976: Nationwide Assessment of Potential Output from Wind-Powered Generators. *Journal of Applied Meteorology*, **15**: 673–678.
- Kahn, E., 1979: The Reliability of Distributed Wind Generators. *Electric Power Systems Research*, **2**(1): 1–14.
- Katzenstein, W., E. Fertig and J. Apt, 2010: The Variability of Interconnected Wind Plants. *Energy Policy*, **38**(8): 4400–4410.
- Kempton, W., F. Pimenta, D. Veron and B. Colle, 2010: Electric Power from Offshore Wind Via Synoptic-Scale Interconnection. *Proceedings of the National Academy of Sciences*, **107**(16): 7240.
- Kiss, P. and I. M. Jánosi, 2008: Limitations of Wind Power Availability over Europe: A Conceptual Study. *Nonlin. Processes Geophys*, **15**: 803–813.
- Larsen, X. G. and J. Mann, 2009: Extreme Winds from the NCEP/NCAR Reanalysis Data. *Wind Energy*, **12**(6): 556–573.
- Lun, I. and J. Lam, 2000: A Study of Weibull Parameters Using Long-Term Wind Observations. *Renewable Energy*, **20**(2): 145–153.
- Lund, H., 2005: Large-Scale Integration of Wind Power into Different Energy Systems. *Energy*, **30**(13): 2402–2412.
- Makarov, Y., C. Loutan, J. Ma and P. de Mello, 2009: Operational Impacts of Wind Generation on California Power Systems. *Power Systems, IEEE Transactions on*, **24**(2): 1039–1050. doi:[10.1109/TPWRS.2009.2016364](https://doi.org/10.1109/TPWRS.2009.2016364).
- Meneveau, C. and J. Meyers, 2010: Optimization of Turbine Spacing in the Fully Developed Wind Turbine Array Boundary Layer. *Bulletin of the American Physical Society*, **55**.
- Morrissey, M., W. Cook and J. Greene, 2010: An Improved Method for Estimating the Wind Power Density Distribution Function. *Journal of Atmospheric and Oceanic Technology*, **27**(7): 1153–1164.
- NREL, 2010: Wind Powering America: 80-Meter Wind Maps and Wind Resource Potential.

- Parsons, B., M. Milligan, B. Zavadil, D. Brooks, B. Kirby, K. Dragoon and J. Caldwell, 2004: Grid Impacts of Wind Power: A Summary of Recent Studies in the United States. *Wind Energy*, **7**(2): 87–108.
- Parsons, B., M. Milligan, J. C. Smith, E. DeMeo, B. Oakleaf, K. Wolf, M. Schuerger, R. Zavadil, M. Ahlstrom and D. Y. Nakafuji, 2006: Grid Impacts of Wind Power Variability: Recent Assessments from a Variety of Utilities in the United States; Preprint. (<http://www.osti.gov/bridge/servlets/purl/888994-WBqulR>).
- Pavia, E. G. and J. J. O'Brien, 1986: Weibull Statistics of Wind Speed over the Ocean. *Journal of Applied Meteorology*, **25**: 1324–1332.
- Pryor, S. C. and R. J. Barthelmie, 2010: Climate Change Impacts on Wind Energy: A Review. *Renewable and Sustainable Energy Reviews*, **14**(1): 430–437.
- Rienecker, M. M., M. J. Suarez, R. Gelaro, R. Todling, J. Bacmeister, E. Liu, M. G. Bosilovich, S. D. Schubert, L. Takacs, G. Kim, S. Bloom, J. Chen, D. Collins, A. Conaty, A. da Silva, W. Gu, J. Joiner, R. D. Koster, R. Lucchesi, A. Molod, T. Owens, S. Pawson, P. Pegion, C. R. Redder, R. Reichle, F. R. Robertson, A. G. Ruddick, M. Sienkiewicz and J. Woollen, 2011: MERRA - NASA's Modern-Era Retrospective Analysis for Research and Applications. *Journal of Climate*. doi:[10.1175/JCLI-D-11-00015.1](https://doi.org/10.1175/JCLI-D-11-00015.1).
- Schwartz, M. and D. Elliot, 2001: Remapping of the Wind Energy Resource in the Midwestern United States. National Renewable Energy Lab., Golden, CO (U.S.) *Technical Report*.
- Schwartz, M. and D. Elliot, 2005: Towards a Wind Energy Climatology at Advanced Turbine Hub-Heights. *Preprint, 15th Conference on Applied Climatology, Savannah, GA, American Meteorological Society*.
- Sigl, A. B., R. B. Corotis and D. J. Won, 1979: Run Duration Analysis of Surface Wind Speeds for Wind Energy Application. *J. Appl. Meteorol.*, **18**(2).
- Sinden, G., 2007: Characteristics of the UK Wind Resource: Long-Term Patterns and Relationship to Electricity Demand. *Energy Policy*, **35**(1): 112–127.
- Smith, J., M. Milligan, E. DeMeo and B. Parsons, 2007: Utility Wind Integration and Operating Impact State of the Art. *IEEE Transactions on Power Systems*, **22**(3): 900–908.
- Sorensen, P., N. Cutululis, A. Viguera-Rodríguez, L. Jensen, J. Hjerrild, M. Donovan and H. Madsen, 2007: Power Fluctuations from Large Wind Farms. *IEEE Transactions on Power Systems*, **22**(3): 958–965.
- Stull, R. B., 1991: *An Introduction to Boundary Layer Meteorology*, volume 13. Kluwer Academic Publishers: Dordrecht, The Netherlands, first edition, 666 p.
- Tuller, S. E. and A. C. Brett, 1984: The Characteristics of Wind Velocity That Favor the Fitting of a Weibull Distribution in Wind Speed Analysis. *Journal of Applied Meteorology*, **23**: 124–134.
- Ucar, A. and F. Balo, 2009: Investigation of Wind Characteristics and Assessment of Wind-Generation Potentiality in Uludag-Bursa, Turkey. *Applied Energy*, **86**(3): 333–339.
- Zaharim, A., A. M. Razali, R. Z. Abidin and K. Sopian, 2009: Fitting of Statistical Distributions to Wind Speed Data in Malaysia. *European Journal of Scientific Research*, **26**(1): 6–12.

APPENDIX A: Statistics of Intermittency

Suppose there are n wind turbines with mean output power $\bar{p}_1, \bar{p}_2, \bar{p}_3 \dots \bar{p}_n$ and mean fluctuations $p'_1, p'_2, p'_3 \dots p'_n$. The aggregated power from these turbines is:

$$\bar{P} = (\bar{p}_1 + \bar{p}_2 + \bar{p}_3 \dots + \bar{p}_n) + (p'_1 + p'_2 + p'_3 \dots + p'_n) \quad (9)$$

at each hour and the mean squared deviation is:

$$\overline{P'^2} = (p_1'^2 + p_2'^2 + p_3'^2 + \dots + p_n'^2) + 2(\overline{p'_1 p'_2} + \overline{p'_2 p'_3} + \dots + \overline{p'_{n-1} p'_n}) \quad (10)$$

Now, to simplify the treatment, let us assume that:

1. each turbine has the same mean power p_m and
2. each turbine has the same fluctuation p_f .

Therefore,

$$\overline{P'^2} = np_f^2 + 2(\overline{p'_1 p'_2} + \overline{p'_2 p'_3} + \dots + \overline{p'_n p'_{n-1}}) = np_f^2 + n(n-1)\overline{C}p_f^2 \quad (11)$$

Letting $p' = \sqrt{\overline{P'^2}}$, the coefficient of variation of the aggregate power is given by:

$$CoV = \frac{p'}{\bar{P}} = \frac{\sqrt{np_f^2 + n(n-1)\overline{C}p_f^2}}{np_m} \quad (12)$$

Case 1: No correlation Let us assume there is no correlation between the turbines. Then, the second term in the square root above is zero. Therefore,

$$CoV_1 = \frac{\sqrt{n}p_f}{np_m} = \frac{1}{\sqrt{n}} \frac{p_f}{p_m} \quad (13)$$

Case 2: Positive correlation Now let us assume a common correlation coefficient of \overline{C} between every pair of turbines. Thus, the coefficient of variation becomes:

$$CoV_2 = \frac{p_f}{p_m} \frac{\sqrt{n + n(n-1)\overline{C}}}{n} \quad (14)$$

where p_f/m is the coefficient of variation of the individual turbines.

Figure A1 shows the variation of the coefficient of variation with the number of wind turbines or grid points that are aggregated and the coefficient of correlation \overline{C} is a parameter. This plot shows that for the initial 10 units, the reduction in CoV is drastic and for subsequent addition of each unit, the benefit of aggregation is marginal. More importantly, as the correlation between the units increases, the benefit of aggregation saturates faster, that is with fewer number of turbines. This plot also shows that with even a correlation of 0.3, the reduction in the coefficient of variation becomes almost half of that with no correlation.

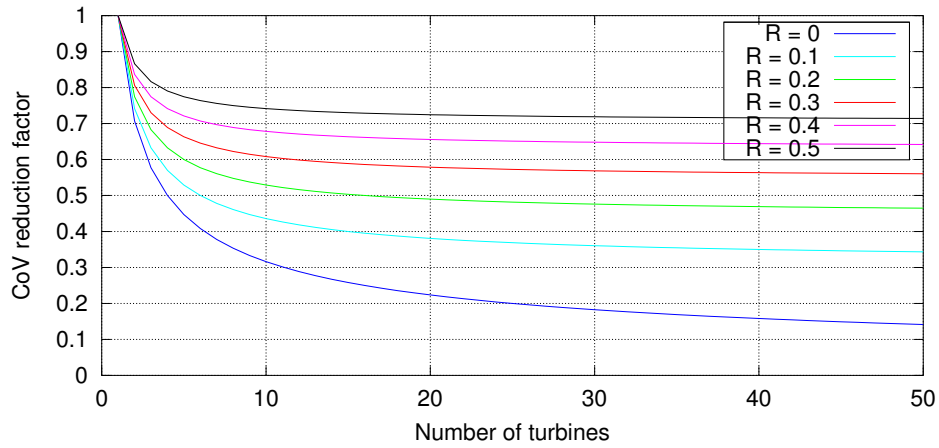


Figure A1. Variation of CoV with number of aggregated wind turbines.

APPENDIX B: WPD Distribution

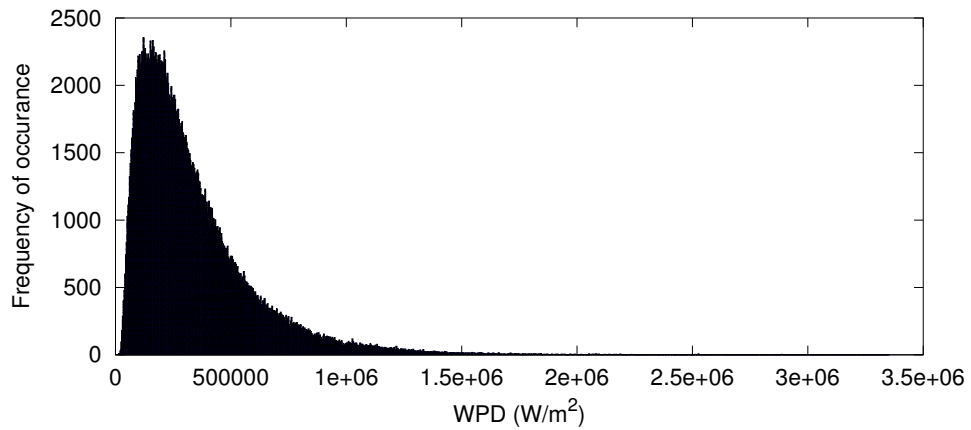


Figure B1. Illustrative distribution of the wind power density. The histogram corresponds to an example grid point in the central U.S.

APPENDIX C: Wind Power Classes

Table C1. Wind Power classes at 50 m height.

Class	Wind power density at 50 m (W/m ²)	Quality
1	0–200	Poor
2	200–300	Marginal
3	300–400	Fair
4	400–500	Good
5	500–600	Excellent
6	600–800	Outstanding
7	>800	Superb

Abbreviations

ACF	Aggregated Capacity Factor
AP	Aggregated Power
CalISO	California Independent Service Operator
CoV	Coefficient of Variation
ERCOT	Electricity Regulatory Commission Of Texas
GEOS	Global Earth Observing System
GMAO	Global Modeling and Assimilation Office
IQR	Inter-Quartile Range
ISO	Independent Service Operator
MASS	Mesoscale Atmospheric Simulation System
MERRA	Modern Era Retrospective-analysis for Research and Applications
MISO	Midwest Independent Service Operator
NCAR	National Center for Atmospheric Research
NCDC	National Climatic Data Center
NCEP	National Center for Environmental Prediction

NEISO	New England Independent Service Operator
NREL	National Renewable Energy Laboratory
NYISO	New York Independent Service Operator
SWPP	South West Power Pool
USWRA	US Wind Resource Atlas
UWPD	Useable Wind Power Density
WPD	Wind Power Density

REPORT SERIES of the MIT *Joint Program on the Science and Policy of Global Change*

1. **Uncertainty in Climate Change Policy Analysis**
Jacoby & Prinn December 1994
2. **Description and Validation of the MIT Version of the GISS 2D Model** *Sokolov & Stone* June 1995
3. **Responses of Primary Production and Carbon Storage to Changes in Climate and Atmospheric CO₂ Concentration** *Xiao et al.* October 1995
4. **Application of the Probabilistic Collocation Method for an Uncertainty Analysis** *Webster et al.* January 1996
5. **World Energy Consumption and CO₂ Emissions: 1950-2050** *Schmalensee et al.* April 1996
6. **The MIT Emission Prediction and Policy Analysis (EPPA) Model** *Yang et al.* May 1996 (*superseded* by No. 125)
7. **Integrated Global System Model for Climate Policy Analysis** *Prinn et al.* June 1996 (*superseded* by No. 124)
8. **Relative Roles of Changes in CO₂ and Climate to Equilibrium Responses of Net Primary Production and Carbon Storage** *Xiao et al.* June 1996
9. **CO₂ Emissions Limits: Economic Adjustments and the Distribution of Burdens** *Jacoby et al.* July 1997
10. **Modeling the Emissions of N₂O and CH₄ from the Terrestrial Biosphere to the Atmosphere** *Liu* Aug. 1996
11. **Global Warming Projections: Sensitivity to Deep Ocean Mixing** *Sokolov & Stone* September 1996
12. **Net Primary Production of Ecosystems in China and its Equilibrium Responses to Climate Changes**
Xiao et al. November 1996
13. **Greenhouse Policy Architectures and Institutions**
Schmalensee November 1996
14. **What Does Stabilizing Greenhouse Gas Concentrations Mean?** *Jacoby et al.* November 1996
15. **Economic Assessment of CO₂ Capture and Disposal**
Eckaus et al. December 1996
16. **What Drives Deforestation in the Brazilian Amazon?**
Pfaff December 1996
17. **A Flexible Climate Model For Use In Integrated Assessments** *Sokolov & Stone* March 1997
18. **Transient Climate Change and Potential Croplands of the World in the 21st Century** *Xiao et al.* May 1997
19. **Joint Implementation: Lessons from Title IV's Voluntary Compliance Programs** *Atkeson* June 1997
20. **Parameterization of Urban Subgrid Scale Processes in Global Atm. Chemistry Models** *Calbo et al.* July 1997
21. **Needed: A Realistic Strategy for Global Warming**
Jacoby, Prinn & Schmalensee August 1997
22. **Same Science, Differing Policies; The Saga of Global Climate Change** *Skolnikoff* August 1997
23. **Uncertainty in the Oceanic Heat and Carbon Uptake and their Impact on Climate Projections**
Sokolov et al. September 1997
24. **A Global Interactive Chemistry and Climate Model**
Wang, Prinn & Sokolov September 1997
25. **Interactions Among Emissions, Atmospheric Chemistry & Climate Change** *Wang & Prinn* Sept. 1997
26. **Necessary Conditions for Stabilization Agreements**
Yang & Jacoby October 1997
27. **Annex I Differentiation Proposals: Implications for Welfare, Equity and Policy** *Reiner & Jacoby* Oct. 1997
28. **Transient Climate Change and Net Ecosystem Production of the Terrestrial Biosphere**
Xiao et al. November 1997
29. **Analysis of CO₂ Emissions from Fossil Fuel in Korea: 1961-1994** *Choi* November 1997
30. **Uncertainty in Future Carbon Emissions: A Preliminary Exploration** *Webster* November 1997
31. **Beyond Emissions Paths: Rethinking the Climate Impacts of Emissions Protocols** *Webster & Reiner* November 1997
32. **Kyoto's Unfinished Business** *Jacoby et al.* June 1998
33. **Economic Development and the Structure of the Demand for Commercial Energy** *Judson et al.* April 1998
34. **Combined Effects of Anthropogenic Emissions and Resultant Climatic Changes on Atmospheric OH**
Wang & Prinn April 1998
35. **Impact of Emissions, Chemistry, and Climate on Atmospheric Carbon Monoxide** *Wang & Prinn* April 1998
36. **Integrated Global System Model for Climate Policy Assessment: Feedbacks and Sensitivity Studies**
Prinn et al. June 1998
37. **Quantifying the Uncertainty in Climate Predictions**
Webster & Sokolov July 1998
38. **Sequential Climate Decisions Under Uncertainty: An Integrated Framework** *Valverde et al.* September 1998
39. **Uncertainty in Atmospheric CO₂ (Ocean Carbon Cycle Model Analysis)** *Holian* Oct. 1998 (*superseded* by No. 80)
40. **Analysis of Post-Kyoto CO₂ Emissions Trading Using Marginal Abatement Curves** *Ellerman & Decaux* Oct. 1998
41. **The Effects on Developing Countries of the Kyoto Protocol and CO₂ Emissions Trading**
Ellerman et al. November 1998
42. **Obstacles to Global CO₂ Trading: A Familiar Problem**
Ellerman November 1998
43. **The Uses and Misuses of Technology Development as a Component of Climate Policy** *Jacoby* November 1998
44. **Primary Aluminum Production: Climate Policy, Emissions and Costs** *Harnisch et al.* December 1998
45. **Multi-Gas Assessment of the Kyoto Protocol**
Reilly et al. January 1999
46. **From Science to Policy: The Science-Related Politics of Climate Change Policy in the U.S.** *Skolnikoff* January 1999
47. **Constraining Uncertainties in Climate Models Using Climate Change Detection Techniques**
Forest et al. April 1999
48. **Adjusting to Policy Expectations in Climate Change Modeling** *Shackley et al.* May 1999
49. **Toward a Useful Architecture for Climate Change Negotiations** *Jacoby et al.* May 1999
50. **A Study of the Effects of Natural Fertility, Weather and Productive Inputs in Chinese Agriculture**
Eckaus & Tso July 1999
51. **Japanese Nuclear Power and the Kyoto Agreement**
Babiker, Reilly & Ellerman August 1999
52. **Interactive Chemistry and Climate Models in Global Change Studies** *Wang & Prinn* September 1999

Contact the Joint Program Office to request a copy. The Report Series is distributed at no charge.

REPORT SERIES of the MIT *Joint Program on the Science and Policy of Global Change*

53. **Developing Country Effects of Kyoto-Type Emissions Restrictions** Babiker & Jacoby October 1999
54. **Model Estimates of the Mass Balance of the Greenland and Antarctic Ice Sheets** Bugnion Oct 1999
55. **Changes in Sea-Level Associated with Modifications of Ice Sheets over 21st Century** Bugnion October 1999
56. **The Kyoto Protocol and Developing Countries** Babiker et al. October 1999
57. **Can EPA Regulate Greenhouse Gases Before the Senate Ratifies the Kyoto Protocol?** Bugnion & Reiner November 1999
58. **Multiple Gas Control Under the Kyoto Agreement** Reilly, Mayer & Harnisch March 2000
59. **Supplementarity: An Invitation for Monopsony?** Ellerman & Sue Wing April 2000
60. **A Coupled Atmosphere-Ocean Model of Intermediate Complexity** Kamenkovich et al. May 2000
61. **Effects of Differentiating Climate Policy by Sector: A U.S. Example** Babiker et al. May 2000
62. **Constraining Climate Model Properties Using Optimal Fingerprint Detection Methods** Forest et al. May 2000
63. **Linking Local Air Pollution to Global Chemistry and Climate** Mayer et al. June 2000
64. **The Effects of Changing Consumption Patterns on the Costs of Emission Restrictions** Lahiri et al. Aug 2000
65. **Rethinking the Kyoto Emissions Targets** Babiker & Eckaus August 2000
66. **Fair Trade and Harmonization of Climate Change Policies in Europe** Viguier September 2000
67. **The Curious Role of "Learning" in Climate Policy: Should We Wait for More Data?** Webster October 2000
68. **How to Think About Human Influence on Climate** Forest, Stone & Jacoby October 2000
69. **Tradable Permits for Greenhouse Gas Emissions: A primer with reference to Europe** Ellerman Nov 2000
70. **Carbon Emissions and The Kyoto Commitment in the European Union** Viguier et al. February 2001
71. **The MIT Emissions Prediction and Policy Analysis Model: Revisions, Sensitivities and Results** Babiker et al. February 2001 (*superseded* by No. 125)
72. **Cap and Trade Policies in the Presence of Monopoly and Distortionary Taxation** Fullerton & Metcalf March '01
73. **Uncertainty Analysis of Global Climate Change Projections** Webster et al. Mar. '01 (*superseded* by No. 95)
74. **The Welfare Costs of Hybrid Carbon Policies in the European Union** Babiker et al. June 2001
75. **Feedbacks Affecting the Response of the Thermohaline Circulation to Increasing CO₂** Kamenkovich et al. July 2001
76. **CO₂ Abatement by Multi-fueled Electric Utilities: An Analysis Based on Japanese Data** Ellerman & Tsukada July 2001
77. **Comparing Greenhouse Gases** Reilly et al. July 2001
78. **Quantifying Uncertainties in Climate System Properties using Recent Climate Observations** Forest et al. July 2001
79. **Uncertainty in Emissions Projections for Climate Models** Webster et al. August 2001
80. **Uncertainty in Atmospheric CO₂ Predictions from a Global Ocean Carbon Cycle Model** Holian et al. September 2001
81. **A Comparison of the Behavior of AO GCMs in Transient Climate Change Experiments** Sokolov et al. December 2001
82. **The Evolution of a Climate Regime: Kyoto to Marrakech** Babiker, Jacoby & Reiner February 2002
83. **The "Safety Valve" and Climate Policy** Jacoby & Ellerman February 2002
84. **A Modeling Study on the Climate Impacts of Black Carbon Aerosols** Wang March 2002
85. **Tax Distortions and Global Climate Policy** Babiker et al. May 2002
86. **Incentive-based Approaches for Mitigating Greenhouse Gas Emissions: Issues and Prospects for India** Gupta June 2002
87. **Deep-Ocean Heat Uptake in an Ocean GCM with Idealized Geometry** Huang, Stone & Hill September 2002
88. **The Deep-Ocean Heat Uptake in Transient Climate Change** Huang et al. September 2002
89. **Representing Energy Technologies in Top-down Economic Models using Bottom-up Information** McFarland et al. October 2002
90. **Ozone Effects on Net Primary Production and Carbon Sequestration in the U.S. Using a Biogeochemistry Model** Felzer et al. November 2002
91. **Exclusionary Manipulation of Carbon Permit Markets: A Laboratory Test** Carlén November 2002
92. **An Issue of Permanence: Assessing the Effectiveness of Temporary Carbon Storage** Herzog et al. December 2002
93. **Is International Emissions Trading Always Beneficial?** Babiker et al. December 2002
94. **Modeling Non-CO₂ Greenhouse Gas Abatement** Hyman et al. December 2002
95. **Uncertainty Analysis of Climate Change and Policy Response** Webster et al. December 2002
96. **Market Power in International Carbon Emissions Trading: A Laboratory Test** Carlén January 2003
97. **Emissions Trading to Reduce Greenhouse Gas Emissions in the United States: The McCain-Lieberman Proposal** Paltsev et al. June 2003
98. **Russia's Role in the Kyoto Protocol** Bernard et al. Jun '03
99. **Thermohaline Circulation Stability: A Box Model Study** Lucarini & Stone June 2003
100. **Absolute vs. Intensity-Based Emissions Caps** Ellerman & Sue Wing July 2003
101. **Technology Detail in a Multi-Sector CGE Model: Transport Under Climate Policy** Schafer & Jacoby July 2003
102. **Induced Technical Change and the Cost of Climate Policy** Sue Wing September 2003
103. **Past and Future Effects of Ozone on Net Primary Production and Carbon Sequestration Using a Global Biogeochemical Model** Felzer et al. (revised) January 2004

Contact the Joint Program Office to request a copy. The Report Series is distributed at no charge.

REPORT SERIES of the MIT *Joint Program on the Science and Policy of Global Change*

104. **A Modeling Analysis of Methane Exchanges Between Alaskan Ecosystems and the Atmosphere** Zhuang *et al.* November 2003
105. **Analysis of Strategies of Companies under Carbon Constraint** Hashimoto January 2004
106. **Climate Prediction: *The Limits of Ocean Models*** Stone February 2004
107. **Informing Climate Policy Given Incommensurable Benefits Estimates** Jacoby February 2004
108. **Methane Fluxes Between Terrestrial Ecosystems and the Atmosphere at High Latitudes During the Past Century** Zhuang *et al.* March 2004
109. **Sensitivity of Climate to Diapycnal Diffusivity in the Ocean** Dalan *et al.* May 2004
110. **Stabilization and Global Climate Policy** Sarofim *et al.* July 2004
111. **Technology and Technical Change in the MIT EPPA Model** Jacoby *et al.* July 2004
112. **The Cost of Kyoto Protocol Targets: *The Case of Japan*** Paltsev *et al.* July 2004
113. **Economic Benefits of Air Pollution Regulation in the USA: *An Integrated Approach*** Yang *et al.* (revised) Jan. 2005
114. **The Role of Non-CO₂ Greenhouse Gases in Climate Policy: *Analysis Using the MIT IGSM*** Reilly *et al.* Aug. '04
115. **Future U.S. Energy Security Concerns** Deutch Sep. '04
116. **Explaining Long-Run Changes in the Energy Intensity of the U.S. Economy** Sue Wing Sept. 2004
117. **Modeling the Transport Sector: *The Role of Existing Fuel Taxes in Climate Policy*** Paltsev *et al.* November 2004
118. **Effects of Air Pollution Control on Climate** Prinn *et al.* January 2005
119. **Does Model Sensitivity to Changes in CO₂ Provide a Measure of Sensitivity to the Forcing of Different Nature?** Sokolov March 2005
120. **What Should the Government Do To Encourage Technical Change in the Energy Sector?** Deutch May '05
121. **Climate Change Taxes and Energy Efficiency in Japan** Kasahara *et al.* May 2005
122. **A 3D Ocean-Seaice-Carbon Cycle Model and its Coupling to a 2D Atmospheric Model: *Uses in Climate Change Studies*** Dutkiewicz *et al.* (revised) November 2005
123. **Simulating the Spatial Distribution of Population and Emissions to 2100** Asadoorian May 2005
124. **MIT Integrated Global System Model (IGSM) Version 2: *Model Description and Baseline Evaluation*** Sokolov *et al.* July 2005
125. **The MIT Emissions Prediction and Policy Analysis (EPPA) Model: *Version 4*** Paltsev *et al.* August 2005
126. **Estimated PDFs of Climate System Properties Including Natural and Anthropogenic Forcings** Forest *et al.* September 2005
127. **An Analysis of the European Emission Trading Scheme** Reilly & Paltsev October 2005
128. **Evaluating the Use of Ocean Models of Different Complexity in Climate Change Studies** Sokolov *et al.* November 2005
129. **Future Carbon Regulations and Current Investments in Alternative Coal-Fired Power Plant Designs** Sekar *et al.* December 2005
130. **Absolute vs. Intensity Limits for CO₂ Emission Control: *Performance Under Uncertainty*** Sue Wing *et al.* January 2006
131. **The Economic Impacts of Climate Change: *Evidence from Agricultural Profits and Random Fluctuations in Weather*** Deschenes & Greenstone January 2006
132. **The Value of Emissions Trading** Webster *et al.* Feb. 2006
133. **Estimating Probability Distributions from Complex Models with Bifurcations: *The Case of Ocean Circulation Collapse*** Webster *et al.* March 2006
134. **Directed Technical Change and Climate Policy** Otto *et al.* April 2006
135. **Modeling Climate Feedbacks to Energy Demand: *The Case of China*** Asadoorian *et al.* June 2006
136. **Bringing Transportation into a Cap-and-Trade Regime** Ellerman, Jacoby & Zimmerman June 2006
137. **Unemployment Effects of Climate Policy** Babiker & Eckaus July 2006
138. **Energy Conservation in the United States: *Understanding its Role in Climate Policy*** Metcalf Aug. '06
139. **Directed Technical Change and the Adoption of CO₂ Abatement Technology: *The Case of CO₂ Capture and Storage*** Otto & Reilly August 2006
140. **The Allocation of European Union Allowances: *Lessons, Unifying Themes and General Principles*** Buchner *et al.* October 2006
141. **Over-Allocation or Abatement? *A preliminary analysis of the EU ETS based on the 2006 emissions data*** Ellerman & Buchner December 2006
142. **Federal Tax Policy Towards Energy** Metcalf Jan. 2007
143. **Technical Change, Investment and Energy Intensity** Kratena March 2007
144. **Heavier Crude, Changing Demand for Petroleum Fuels, Regional Climate Policy, and the Location of Upgrading Capacity** Reilly *et al.* April 2007
145. **Biomass Energy and Competition for Land** Reilly & Paltsev April 2007
146. **Assessment of U.S. Cap-and-Trade Proposals** Paltsev *et al.* April 2007
147. **A Global Land System Framework for Integrated Climate-Change Assessments** Schlosser *et al.* May 2007
148. **Relative Roles of Climate Sensitivity and Forcing in Defining the Ocean Circulation Response to Climate Change** Scott *et al.* May 2007
149. **Global Economic Effects of Changes in Crops, Pasture, and Forests due to Changing Climate, CO₂ and Ozone** Reilly *et al.* May 2007
150. **U.S. GHG Cap-and-Trade Proposals: *Application of a Forward-Looking Computable General Equilibrium Model*** Gurgel *et al.* June 2007
151. **Consequences of Considering Carbon/Nitrogen Interactions on the Feedbacks between Climate and the Terrestrial Carbon Cycle** Sokolov *et al.* June 2007

REPORT SERIES of the MIT *Joint Program on the Science and Policy of Global Change*

- 152. Energy Scenarios for East Asia: 2005-2025** *Paltsev & Reilly* July 2007
- 153. Climate Change, Mortality, and Adaptation: Evidence from Annual Fluctuations in Weather in the U.S.** *Deschênes & Greenstone* August 2007
- 154. Modeling the Prospects for Hydrogen Powered Transportation Through 2100** *Sandoval et al.* February 2008
- 155. Potential Land Use Implications of a Global Biofuels Industry** *Gurgel et al.* March 2008
- 156. Estimating the Economic Cost of Sea-Level Rise** *Sugiyama et al.* April 2008
- 157. Constraining Climate Model Parameters from Observed 20th Century Changes** *Forest et al.* April 2008
- 158. Analysis of the Coal Sector under Carbon Constraints** *McFarland et al.* April 2008
- 159. Impact of Sulfur and Carbonaceous Emissions from International Shipping on Aerosol Distributions and Direct Radiative Forcing** *Wang & Kim* April 2008
- 160. Analysis of U.S. Greenhouse Gas Tax Proposals** *Metcalf et al.* April 2008
- 161. A Forward Looking Version of the MIT Emissions Prediction and Policy Analysis (EPPA) Model** *Babiker et al.* May 2008
- 162. The European Carbon Market in Action: Lessons from the first trading period** Interim Report *Convery, Ellerman, & de Perthuis* June 2008
- 163. The Influence on Climate Change of Differing Scenarios for Future Development Analyzed Using the MIT Integrated Global System Model** *Prinn et al.* September 2008
- 164. Marginal Abatement Costs and Marginal Welfare Costs for Greenhouse Gas Emissions Reductions: Results from the EPPA Model** *Holak et al.* November 2008
- 165. Uncertainty in Greenhouse Emissions and Costs of Atmospheric Stabilization** *Webster et al.* November 2008
- 166. Sensitivity of Climate Change Projections to Uncertainties in the Estimates of Observed Changes in Deep-Ocean Heat Content** *Sokolov et al.* November 2008
- 167. Sharing the Burden of GHG Reductions** *Jacoby et al.* November 2008
- 168. Unintended Environmental Consequences of a Global Biofuels Program** *Melillo et al.* January 2009
- 169. Probabilistic Forecast for 21st Century Climate Based on Uncertainties in Emissions (without Policy) and Climate Parameters** *Sokolov et al.* January 2009
- 170. The EU's Emissions Trading Scheme: A Proto-type Global System?** *Ellerman* February 2009
- 171. Designing a U.S. Market for CO₂** *Parsons et al.* February 2009
- 172. Prospects for Plug-in Hybrid Electric Vehicles in the United States & Japan: A General Equilibrium Analysis** *Karplus et al.* April 2009
- 173. The Cost of Climate Policy in the United States** *Paltsev et al.* April 2009
- 174. A Semi-Empirical Representation of the Temporal Variation of Total Greenhouse Gas Levels Expressed as Equivalent Levels of Carbon Dioxide** *Huang et al.* June 2009
- 175. Potential Climatic Impacts and Reliability of Very Large Scale Wind Farms** *Wang & Prinn* June 2009
- 176. Biofuels, Climate Policy and the European Vehicle Fleet** *Gitiaux et al.* August 2009
- 177. Global Health and Economic Impacts of Future Ozone Pollution** *Selin et al.* August 2009
- 178. Measuring Welfare Loss Caused by Air Pollution in Europe: A CGE Analysis** *Nam et al.* August 2009
- 179. Assessing Evapotranspiration Estimates from the Global Soil Wetness Project Phase 2 (GSWP-2) Simulations** *Schlosser and Gao* September 2009
- 180. Analysis of Climate Policy Targets under Uncertainty** *Webster et al.* September 2009
- 181. Development of a Fast and Detailed Model of Urban-Scale Chemical and Physical Processing** *Cohen & Prinn* October 2009
- 182. Distributional Impacts of a U.S. Greenhouse Gas Policy: A General Equilibrium Analysis of Carbon Pricing** *Rausch et al.* November 2009
- 183. Canada's Bitumen Industry Under CO₂ Constraints** *Chan et al.* January 2010
- 184. Will Border Carbon Adjustments Work?** *Winchester et al.* February 2010
- 185. Distributional Implications of Alternative U.S. Greenhouse Gas Control Measures** *Rausch et al.* June 2010
- 186. The Future of U.S. Natural Gas Production, Use, and Trade** *Paltsev et al.* June 2010
- 187. Combining a Renewable Portfolio Standard with a Cap-and-Trade Policy: A General Equilibrium Analysis** *Morris et al.* July 2010
- 188. On the Correlation between Forcing and Climate Sensitivity** *Sokolov* August 2010
- 189. Modeling the Global Water Resource System in an Integrated Assessment Modeling Framework: IGSM-WRS** *Strzepek et al.* September 2010
- 190. Climatology and Trends in the Forcing of the Stratospheric Zonal-Mean Flow** *Monier and Weare* January 2011
- 191. Climatology and Trends in the Forcing of the Stratospheric Ozone Transport** *Monier and Weare* January 2011
- 192. The Impact of Border Carbon Adjustments under Alternative Producer Responses** *Winchester* February 2011
- 193. What to Expect from Sectoral Trading: A U.S.-China Example** *Gavard et al.* February 2011
- 194. General Equilibrium, Electricity Generation Technologies and the Cost of Carbon Abatement** *Lanz and Rausch* February 2011
- 195. A Method for Calculating Reference Evapotranspiration on Daily Time Scales** *Farmer et al.* February 2011

Contact the Joint Program Office to request a copy. The Report Series is distributed at no charge.

REPORT SERIES of the MIT *Joint Program on the Science and Policy of Global Change*

- 196. Health Damages from Air Pollution in China** *Matus et al.* March 2011
- 197. The Prospects for Coal-to-Liquid Conversion: A General Equilibrium Analysis** *Chen et al.* May 2011
- 198. The Impact of Climate Policy on U.S. Aviation** *Winchester et al.* May 2011
- 199. Future Yield Growth: What Evidence from Historical Data** *Gitiaux et al.* May 2011
- 200. A Strategy for a Global Observing System for Verification of National Greenhouse Gas Emissions** *Prinn et al.* June 2011
- 201. Russia's Natural Gas Export Potential up to 2050** *Paltsev* July 2011
- 202. Distributional Impacts of Carbon Pricing: A General Equilibrium Approach with Micro-Data for Households** *Rausch et al.* July 2011
- 203. Global Aerosol Health Impacts: Quantifying Uncertainties** *Selin et al.* August 2011
- 204. Implementation of a Cloud Radiative Adjustment Method to Change the Climate Sensitivity of CAM3** *Sokolov and Monier* September 2011
- 205. Quantifying the Likelihood of Regional Climate Change: A Hybridized Approach** *Schlosser et al.* Oct 2011
- 206. Process Modeling of Global Soil Nitrous Oxide Emissions** *Saikawa et al.* October 2011
- 207. The Influence of Shale Gas on U.S. Energy and Environmental Policy** *Jacoby et al.* November 2011
- 208. Influence of Air Quality Model Resolution on Uncertainty Associated with Health Impacts** *Thompson and Selin* December 2011
- 209. Characterization of Wind Power Resource in the United States and its Intermittency** *Gunturu and Schlosser* December 2011